Julius-Maximilians-Universität Würzburg

Fakultät für Biologie

Evaluating the combination of oncolytic vaccinia virus and ionizing radiation in therapy of preclinical glioma models

Dissertation

Zur Erlangung des naturwissenschaftlichen Doktorgrades der

Julius-Maximilians-Universität Würzburg

vorgelegt von Lisa Buckel

aus Rothenburg ob der Tauber

Würzburg, Oktober 2012

Eingereicht am: _____

Mitglieder der Promotionskommission:

Vorsitzender: _____

     Prof. J. Schultz

Erstgutachter: _____

     Prof. A. A. Szalay

Zweitgutachter: _____

     Prof. G. Krohne

Tag des Promotionskolloquiums: _____

Doktorurkunde ausgehändigt am: _____

Erklärung gemäß § 4 Absatz 3 der Promotionsordnung der Fakultät für Biologie der Bayerischen Julius-Maximilians-Universität Würzburg

Hiermit erkläre ich, die vorgelegte Dissertation selbständig angefertigt zu haben und keine anderen als die von mir angegebenen Quellen und Hilfsmittel verwendet zu haben.

Des Weiteren erkläre ich, dass die vorliegende Arbeit weder in gleicher noch in ähnlicher Form bereits in einem anderen Prüfungsverfahren vorgelegt wurde.

Zuvor habe ich neben dem akademischen Grad "Master of Science" keine weiteren akademischen Grade erworben.

 Die vorliegende Arbeit wurde von Prof. A. A. Szalay betreut.

Würzburg, den 25.10.2012

Lisa Buckel

Table of Contents

TABLE OF CONTENTS

TABLE OF CONTENTS

TABLE OF CONTENTS

Summary

Glioblastoma multiforme (GBM) represents the most aggressive form of malignant brain tumors and remains a therapeutically challenge. The overall prognosis for patients diagnosed with GBM has not significantly improved in the last 20-30 years and with concurrent chemo-radiotherapy the median survival is 12-14 months. Intense research in the field has lead to the testing of oncolytic viruses to improve tumor control. Oncolytic viruses represent a class of viruses that selectively target the tumor while sparing surounding normal tissue. Currently, a variety of different oncolytic viruses are being evaluated for their ability to be used in anti-cancer therapy and a few have entered clinical trials. Vaccinia virus, a member of the family of orthopox viruses, is one of the viruses being studied. GLV-1h68, an oncolytic vaccinia virus engineered by Genelux Corporation, was constructed by insertion of three gene cassettes, RUC-GFP fusion, β-galactosidase and β-glucuronidase into the genome of the LIVP strain. In preclinical tumor models, it has been successfully used for therapy of a variety of tumor xenografts, where it was shown to specifically target and replicate in tumors and resulting in tumor shrinkage with minimal toxicity to normal tissue. Recently, a phase I trial was completed at the Royal Marsden Hospital in London which demonstrated that administration of GL-ONC1, clinical grade GLV-1h68, is well tolerated by patients with no observed dose limiting toxicities and preliminary evidence of anticancer activity. Since focal tumor radiotherapy is a mainstay for cancer treatment, including glioma therapy, it is of clinical relevance to assess how systemically administered oncolytic vaccinia virus could be combined with targeted ionizing radiation for therapeutic gain.

In this work we show how focal ionizing radiation (IR) can be combined with multiple systemically delivered oncolytic vaccinia virus strains in murine models of human U-87 glioma. After initial experiments which confirmed that ionizing radiation does not damage viral DNA or alter viral tropism, animal studies were carried out to analyze the interaction of vaccinia virus and ionizing radiation in the *in vivo* setting. We found that irradiation of the tumor target, prior to systemic administration of oncolytic vaccinia virus GLV-1h68, increased viral replication within the U-87 xenografts as measured by viral reporter gene expression and viral titers. Importantly, while GLV-1h68 alone had minimal effect on U-87 tumor growth delay, IR enhanced GLV-1h68 replication, which translated to increased tumor growth delay and mouse survival in subcutaneous and orthotopic U-87 glioma murine models compared to monotherapy with IR or GLV-1h68. The ability of IR to enhance vaccinia replication was not restricted to the multi-mutated GLV-1h68, but was also seen with the less attenuated

SUMMARY

oncolytic vaccinia, LIVP 1.1.1.   We have demonstrated that in animals treated with combination of ionizing radiation and LIVP 1.1.1 a strong pro-inflammatory tissue response was induced.   When IR was given in a more clinically relevant fractionated scheme, we found oncolytic vaccinia virus replication also increased.   This indicates that vaccinia virus could be incorporated into either larger hypo-fraction or more conventionally fractionated radiotherapy schemes.   The ability of focal IR to mediate selective replication of systemically injected oncolytic vaccinia was demonstrated in a bilateral glioma model.   In mice with bilateral U-87 tumors in both hindlimbs, systemically administered oncolytic vaccinia replicated preferentially in the focally irradiated tumor compared to the shielded non-irradiated tumor in the same mouse.   We showed that preferential replication of oncolytic vaccinia virus in irradiated xenografts was not due to increased viral particles initially reaching the tumor by alterations of the tumor vessel permeability due to irradiation.   Cell culture experiments analyzing the interaction of GLV-1h68 and ionizing radiation demonstrated that increased viral replication upon focal irradiation of tumors is not due to a radiation induced upregulation of cytosolic thymidine kinase 1 (TK-1) which is needed for viral replication since all vaccinia strains used within this work are TK-negative.   Also combination of vaccinia virus and ionizing radiation had no influence on cell cycle or induction of DNA double-strand breaks.

We demonstrated that tumor control could be further improved when fractionated focal ionizing radiation was combined with a vaccinia virus caring an anti-angiogenic payload targeting vascular endothelial growth factor (VEGF).   In addition to its involvement in angiogenesis, VEGF is reported to mediate radioresistance of endothelial cells to irradiation by inhibiting radiation induced cell killing.   Our studies showed that following ionizing radiation expression of VEGF is upregulated in U-87 glioma cells in culture.   We further showed a concentration dependent increase in radioresistance of human endothelial cells in presence of VEGF.   Interestingly, we found effects of vascular endothelial growth factor on endothelial cells were reversible by adding purified GLAF-1 to the cells.   GLAF-1 is a single-chain antibody targeting human and murine VEGF and is expressed by oncolytic vaccinia virus GLV-109.   In U-87 glioma xenograft murine models the combination of fractionated ionizing radiation with GLV-1h164, a vaccinia virus also targeting VEGF by expression of a single-chain antibody similar to GLAF-1, which is called GLAF-2, resulted in the best volumetric tumor response and a drastic decrease in vascular endothelial growth factor as early as three days post viral injection. Histological analysis of embedded tumor sections 14 days after viral administration confirmed that blocking VEGF translated into a decrease in vessel number to 30% of vessel number found in control tumors in animals treated with GLV-164 and fractionated IR which was lower than for all other treatment groups.

SUMMARY

Our experiments with GLV-1h164 and fractionated radiotherapy have shown that in addition to ionizing radiation and viral induced tumor cell destruction we were able to effectively target the tumor vasculature. This was achieved by enhanced viral replication translating in increased levels of GLAF-2 disrupting tumor vessels as well as the radiosensitization of tumor vasculature to IR by blocking VEGF.

Our preclinical results have important clinical implications of how focal radiotherapy can be combined with systemic oncolytic viral administration for highly aggressive, locally advanced tumors with the potential, by using a vaccinia virus targeting human vascular endothelial growth factor, to further increase tumor radiation sensitivity by engaging the vascular component in addition to cancer cells.

Zusammenfassung

Glioblastoma multiforme (GBM) verkörpert die aggressivste Form von bösartigen Gehirntumoren und seine Therapie gestaltet sich nach wie vor schwierig. Die Prognose für Patienten, die an einem Glioblastom erkranken, hat sich in den letzten 20-30 Jahren nicht statistisch verbessert und die mittlere Überlebenszeit bei gleichzeitiger Chemo- und Bestrahlunstherapie beträgt 12-14 Monate. Weitläufige Forschung in diesem Bereich hat dazu geführt, dass onkolytische Viren zur Verbesserung der Tumorbehandlung untersucht wurden. Onkolytische Viren stellen eine Art der selektiven Krebsbehandlung dar, bei der das Virus gezielt den Tumor angreift während gleichzeitig umgebendes gesundes Gewebe verschont bleibt. Gegenwärtig wird eine Vielzahl an verschiedenen onkolytischen Viren hinsichtlich ihrer Eignung in der Krebstherapie untersucht und einige wenige befinden sich bereits in klinischen Studien. Eines der Viren die untersucht werden, ist das Vaccinia-Virus, ein Angehöriger der Gattung der Orthopox-Viren. GLV-1h68, ein onkolytisches Vaccinia-Virus, hergestelllt von der Genelux Corporation, wurde durch die Einfügung von drei Genkasseten, RUC-GFP Fusion, β- Galaktosidase und β- Glucuronidase in das Genom des LIVP Stammes hergestellt. In vorklinischen Mausmodellen wurde dieses erfolgreich zur Therapie von verschiedenen Tumorxenograften benutzt, wo es sich spezifisch im Tumor replizierte und Tumorregression herbeiführte, wobei es gleichzeitig eine geringe Toxizität für gesundes Gewebe aufwies. Kürzlich wurde am Royal Marsden Hospital in London eine klinische Studie der Phase 1 abgeschlossen, die zeigte, dass die Verabreichung von GL-ONC1, was für die Klinik hergestelltes GLV-1h68 darstellt, von Patienten gut toleriert wurde, keine Dosis limitierende Toxizität erreicht wurde und ebenfalls Anzeichen einer anti-tumoralen Wirkung vorhanden waren. Da fokale Bestrahlungstherapie aus der Behandlung von Krebs, nicht nur im Falle von Glioblastomen, nicht wegzudenken ist, ist es klinisch relevant, zu untersuchen, wie ein systemisch verabreichtes Vaccinia-Virus mit gezielter ionisierender Strahlung (IR) kombiniert werden könnte, um Therapiechancen zu verbesseren.

In dieser Arbeit konnte gezeigt werden, wie gezielte IR mit verschiedenen sytemisch injizierten Vaccinia-Virus Stämmen in einem Mausmodell für humane U-87-Glioma kombiniert wurde. Nachdem einleitende Versuche bestätigten, dass IR die virale Erbinformation nicht beschädigt und auch nicht den viralen Tropismus verändert, wurden Tierstudien durchgeführt, die die Interaktion des Vaccinia-Virus mit Bestrahlungtherapie *in vivo* untersuchten. Wir konnten zeigen, dass eine vorherige Bestrahlung des Tumors, bevor das GLV-1h68-Virus systemisch injiziert wurde, eine erhöhte viraler Replikation im Tumor

zur Folge hatte, wie wir durch gesteigerte virale Titer und Markergenexpression belegen konnten. Von wesentlicher Bedeutung ist, dass eine Verabreichung von ausschliesslich GLV-1h68 einen minimalen Einfluss auf das U-87 Tumorwachstum hatte, während die durch die Bestrahlung ausgelöste erhöhte Vermehrung von Virus im Tumor eine Verzögerung des Tumorwachstums sowie ein verlängertes Überleben von Mäusen mit subkutanen oder orthotopischen U-87-Xenografts zur Folge hatte. Die Fähigkeit von IR virale Vermehrung zu erhöhen, war nicht nur auf das mutierte GLV-1h68 Virus beschränkt, sondern wurde auch für das weniger attenuierte LIVP 1.1.1-Virus gezeigt. Zudem wurde demonstriert, dass in Mäusen, die mit der Kombination aus Bestrahlung und LIVP 1.1.1 behandelt wurden eine deutliche Entzündungsreaktion des Tumorgewebes ausgelöst wurde. Wenn die Bestrahlung in einem staerker klinisch relevanten fraktionierten Bestrahlungsschema verabreicht wurde, war virale Replikation ebenfalls erhöht. Dies verdeutlicht, dass das Vaccinia-Virus klinisch entweder in eine Bestrahlung mit einer einzelnen Dosis oder in eine konventionelle fraktionierte Bestrahlung integriert werden kann. Die Fähigkeit von fokaler IR, eine selektive Vermehrung von systemisch injizierten onkolytischen Vaccinia-Viren zu ermöglichen, wurde in einem bilateralen Gliomamausmodell bestätigt. In Mausen mit Tumoren an beiden Hinterbeinen, vermehrte sich das systemisch gespritzte Vaccinia-Virus bevorzugt im bestrahlten Tumor und nicht im unbestrahlten Tumor derselben Maus. Wir konnten zeigen, dass die bevorzugte Vermehrung des onkolytischen Vaccinia-Virus im bestrahlten Tumor, nicht eine Folge einer erhöhten Viruspartikelzahl war, die durch eine Veränderung der Permeabilität der Tumorblutgefäße durch die Bestrahlung den Tumor erreichte. In Zellkulturversuchen, in denen die Interaktion von GLV-1h68 und IR untersucht wurde, konnte gezeigt werden, dass vermehrte virale Replikation als Resultat der fokalen Bestrahlung, keine Folge einer Bestrahlung-abhängigen Hochregulation von cytosolischer Thymindinkinase war. Cytosolische Thymindinkinase wird von allen in dieser Arbeit untersuchten Viren für die Vermehrung benötigt, da sie einen TK-negativen Genotyp aufweisen. Die Kombination von IR und Vaccinia-Virus hatte ebenfalls keinen Einfluss auf den Zellzyklus oder auf die Anzahl an DNA-Doppelstrangbrüchen, die durch IR induziert wurden.

Wir konnten zeigen, wie die Tumorkontrolle darüber hinaus weiter verbessert werden kann, wenn fraktionierte fokale Bestrahlung mit einem Vaccinia-Virus kombiniert wird, das eine anti-angiogenetische Ladung, die den vaskulaeren endothelialen Wachstumsfaktor (VEGF) inhibiert, exprimiert. Zusaetzlich zu der Rolle von VEGF in der Angiogenese, wird angenommen, dass dieser eine Rolle für die Entstehung von Radioresistenz in Endothelzellen spielt, da er eine Blockade des durch die Bestrahlung erfolgenden Zelltodes auslöst. Unsere Studien konnten zeigen, dass durch die Bestrahlung von U-87-

ZUSAMMENFASSUNG

Gliomazellen in Kultur eine Hochregulation von VEGF-Expression ausgelöst wurde. Darüber hinaus konnten wir bestätigen, dass die Radioresistenz von Endothelzellen konzentrationsabhängig ansteigt, wenn VEGF vorhanden ist. Interessanterweise konnten wir zeigen, dass die durch VEGF verursache Radioresistenz umkehrbar ist, wenn zusätzlich aufgereinigtes GLAF-1 zu den Zellen gegeben wurde. Bei GLAF-1 handelt es sich um einen einzelkettigen Antikörper, der sich gegen humanes und murine VEGF richtet und der vom onkolytischen Vaccinia-Virus GLV-1h109 produziert wird. In einem Mausmodell für humane U-87 Gliomas, zeigte die Kombination aus fraktionierter Bestrahlung und GLV-1h164, ein Vaccinia-Virus, das ebenfalls einen einzelkettigen Antikörper mit Ähnlichkeit zu GLAF-1, namens GLAF-2, exprimiert, resultierte in der stärksten volumetrischen Tumorantwort. Es wurde ebenfalls eine drastische Abnahme an VEGF im Tumor bereits 3 Tagen nach Virus-Injektion nachgewiesen. Histologische Analyse von eingebetteten Tumorschnitten bestätigte, dass die Blockade von VEGF eine Erniedrigung der Anzahl von Tumorblutgefäßen, zu 30% von Kontrolltumoren, zur Folge hatte. Dieser Wert war niedriger als in allen anderen Behandlungsgruppen.

Unsere Versuche mit fraktionierter Bestrahlung und GLV-1h164 konnten zeigen, dass zusaetzlich zu der durch Virus und Bestrahlung ausgelösten Tumorzellzerstörung, eine effiziente Degeneration der Tumorblutgefäße möglich war. Dies wurde durch eine erhöhte Virus-Vermehrung als Folge der Bestrahlung, die in eine erhöhte Menge an GLAF-2 übersetzt wurde, sowie durch Sensitiveren der tumoralen Endothelzellen durch Blockierung von VEGF-A erreicht.

Die Ergebnisse, die in dieser Arbeit vorgelegt werden, haben wichtige Konsequenzen für die klinische Anwendung, da sie zeigen, wie fokale Bestrahlungstherapie mit systemisch verabreichten onkolytische Vaccinia-Viren für aggressive, fortgeschrittene Tumore kombiniert werden kann. Es ist denkbar, dass die Tumortherapie weiter verbessert werden kann, wenn ein Vaccinia-Virus benutzt wird, das sich zusätzlich gegen VEGF richtet, so werden zu den Krebszellen zusätzlich Tumorblutgefäße in die Therapie miteinbezogen, um die Sensitivität von Endothelzellen gegen Bestrahlung weiter zu erhöhen.

1   Introduction

1.1   Vaccinia virus

1.1.1 Vaccinia virus and smallpox

Vaccinia virus (VACV) is a member of the family of Poxviridae which is composed of a large number of different viruses. More precisely VACV belongs to the orthopoxvirus genus and is historically recognized as an immunizing agent against the most famous member of the same genus variola virus, the cause of smallpox. Smallpox is a fatal infectious disease claiming vast numbers of lives over the past centuries. There were two different forms of the disease known which were clearly distinguishable in severity and etiopathology yet similar on a genomic level caused by two different variola viruses, variola major and variola minor. Upon infection with the variola major subtype, the smallpox fatality rate was 30-40% [1]. Interestingly, a prior exposure to variola minor, inducing a less severe form of smallpox, as well as other members of the orthopoxviruses, protected against infection with variola major. This crucial discovery was made by Edward Jenner who set a milestone for disease control in 1776 when he successfully immunized humans against smallpox by infection with cowpox virus which results in considerable milder etiopathology [2]. This immunologic cross-reaction opened the doors for a worldwide immunization campaign starting in 1878 which stopped the spread of smallpox almost four decades ago and resulted in declaration of disease eradication by the World Health Organization (WHO) in 1980 [3, 4]. However, it was recognized in the 1930s that the smallpox vaccines being used in the 20th century were not the cowpox virus but a distinct species of the orthopoxviruses which was named vaccinia virus. It is thinkable that the VACV strain represents a virus extinct in nature which yet has survived in the laboratory or that it resembles a derivative originated from the cowpox virus but mutated due to serial passages under laboratory conditions [5].

1.1.2 Morphology and life cycle of vaccinia virus

Poxviruses are brick-like shape particles with dimensions of 300 by 200 by 100 nm and have a large linear double-stranded DNA genome which a range in size between 130 and 300 kb and encodes for approximately 200 genes [6]. A unique characteristic of poxviruses is their ability to replicate in the cytoplasm of the host cell instead of the nucleus. This ability makes them ideal candidates for oncolytic viral vectors since there is minimal chance of cell transformation due to lack of integration into the host genome. On the other hand this

INTRODUCTION

replicating in the cytoplasm necessitates VACV to encode for their own multi-subunit RNA polymerase as well as most of the enzymes needed to produce a correctly capped, methylated and polyadenylated mRNA instead of using the host's transcription machinery. Proteins needed for initiating replication are packaged in the virion core and are activated even before host cell infection [7]. Different forms of infectious particles exist for VACV: an intracellular form called intracellular mature virus (IMV) which is the first form to be produced, is surrounded by one single membrane and remains inside of the cell until cell lysis as well as two extracellular forms. The latter are generated from the IMV by adding one additional lipid bilayer from the host's trans-Golgi or from the early endosomal compartment. The extracellular forms which are important for virus dissemination are called cell-associated enveloped virus (CEV) when still membrane-associated or extracellular enveloped virus (EEV) when released from the host cell. The outer membrane of CEV and EEV exhibits a different viral protein composition than the IMV membrane making CEV and EEV antigenetically, structurally and functionally distinct form IMV particles [8]. Distant dissemination of VACV within the host is suggested to be carried out primarily by the EEV since it is more resistant to neutralizing antibodies than the IMV particle. While the process through which VACV attaches and enters the host cell is not fully understood it is proposed that at least for the IMV particle two different entry ways exist, Fig. 1A.
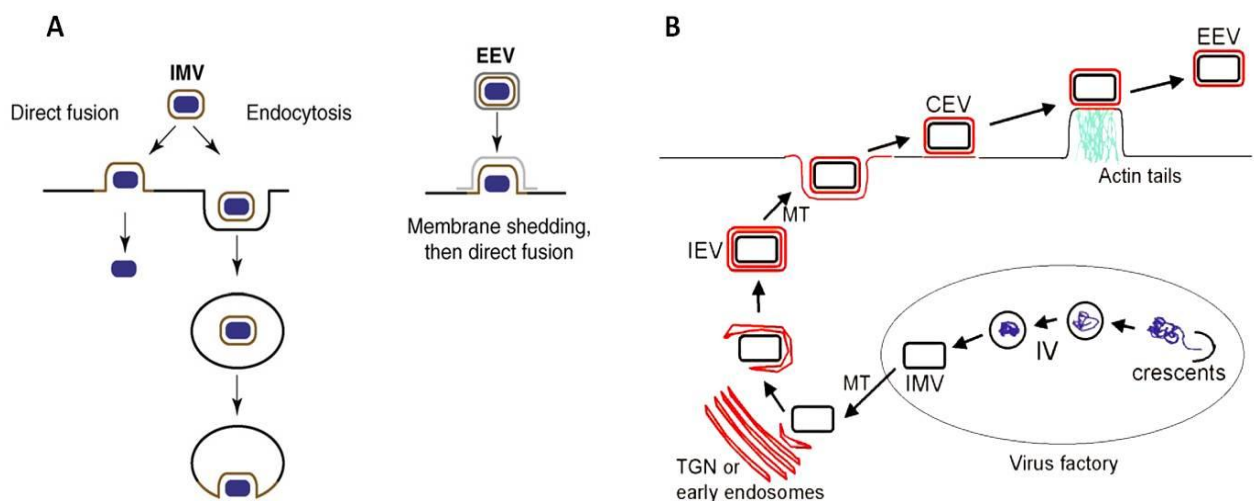
Fig. 1 Entry of vaccinia virus into host cells and morphology (modified from [8, 9]
   A) Vaccinia virus IMV particle can enter host cells either via direct fusion where the naked core is released into to cytoplasm or by endocytosis where the viral particle membrane fuses with the membrane of the vesicle while already inside of the host cell. The EEV particle which carries an extra membrane sheds the outer membrane first followed by a direct fusion with the host membrane. **B)** IMV assembly occurs in so called virus factories. The particles are transported by microtubule to the trans-Golgi apparatus or early endosomes where they acquire two more membranes and form IEV. The IEV are transported again via microtubule to the cell surface where they remain as CEV or are released in form of EEV.

INTRODUCTION

After the surrounding membranes are shed, the core is transported through the cytoplasm via microtubules. Like for most viruses, virus replication and assembly is regulated by temporal gene expression, where proteins required early (e.g. DNA replication or nucleotide biosynthesis) are transcribed first, whereas proteins for morphogenesis and virus assembly are generated during later stages of the viral replication cycle. Early gene transcription is initiated shortly after host cell entry and since replication is carried out in the cytoplasm all proteins as well as enzymes needed for mRNA synthesis need to be present in the core together with viral DNA. Moreover, viral replication initiates a reprogramming of the host cell to support viral replication as well as the release of growth factor-like molecules to facilitate infection of neighboring cells. During later stages of infection when the viral genome is amplified and structural proteins are synthesized, viral core assembly takes place in distinct virus "factories". Immature virions only consisting of lipid and proteins mature by incorporating DNA into IMV, Fig. 1B. A smaller percentage of IMV acquire additional membranes from the trans-Golgi or endosomal compartment before they are transported via microtubules to the cell membrane where they are retained as CEV and move to neighboring cells by induction of actin polymerization or are released as EEV [1, 10].

1.2 Cancer

In spite of tremendous efforts and resources put into cancer research, cancer remains one of the major health problems of our time. The therapeutic limitations become clearly evident in the context of metastases, the spread of a primary tumor to distant locations in the body. Currently, metastatic disease carries a grim prognosis and largely remains incurable. In 2012, cancer is accountable for one in four deaths in the United States making it the second leading cause of death following cardiovascular disease. According to the American Cancer Society roughly 1.6 million people are going to be diagnosed with cancer in 2012 and almost 600,000 people are going to die a cancer-related death the same year (see Fig. 2 for detailed estimates).

Estimated New Cases*

			Males	Females			
Prostate	241,740	29%			Breast	226,870	29%
Lung & bronchus	116,470	14%			Lung & bronchus	109,690	14%
Colon & rectum	73,420	9%			Colon & rectum	70,040	9%
Urinary bladder	55,600	7%			Uterine corpus	47,130	6%
Melanoma of the skin	44,250	5%			Thyroid	43,210	5%
Kidney & renal pelvis	40,250	5%			Melanoma of the skin	32,000	4%
Non-Hodgkin lymphoma	38,160	4%			Non-Hodgkin lymphoma	31,970	4%
Oral cavity & pharynx	28,540	3%			Kidney & renal pelvis	24,520	3%
Leukemia	26,830	3%			Ovary	22,280	3%
Pancreas	22,090	3%			Pancreas	21,830	3%
All Sites	**848,170**	**100%**			**All Sites**	**790,740**	**100%**

Estimated Deaths

			Males	Females			
Lung & bronchus	87,750	29%			Lung & bronchus	72,590	26%
Prostate	28,170	9%			Breast	39,510	14%
Colon & rectum	26,470	9%			Colon & rectum	25,220	9%
Pancreas	18,850	6%			Pancreas	18,540	7%
Liver & intrahepatic bile duct	13,980	5%			Ovary	15,500	6%
Leukemia	13,500	4%			Leukemia	10,040	4%
Esophagus	12,040	4%			Non-Hodgkin lymphoma	8,620	3%
Urinary bladder	10,510	3%			Uterine Corpus	8,010	3%
Non-Hodgkin lymphoma	10,320	3%			Liver & intrahepatic bile duct	6,570	2%
Kidney & renal pelvis	8,650	3%			Brain & other nervous system	5,980	2%
All Sites	**301,820**	**100%**			**All Sites**	**275,370**	**100%**

Fig. 2 Estimated cancer new cases and deaths for 2012 (from American Society of Cancer, Facts and Figures 2012)
The upper part of the figure shows for 2012 estimated numbers of newly diagnosed cancers in men and women ranked by their incidence. The lower part shows estimated cancer-related deaths in 2012 ranked by numbers in men and woman.

While cancer strikes people of all ages, the risk of being diagnosed increases with advancing age. In addition, numerous external factors such as life style, tobacco use or exposure to mutagens as well as genetic predispositions can be correlated with the chance of developing the disease. Cancer comprises a large group of illnesses all characterized by uncontrolled invasive cell growth with possible spread to distant body parts. The presence of invasive cell growth distinguishes malignant from benign tumors, which refer to a condition which is locally contained without invasion of neighboring tissue or further spread and therefore not (yet) cancerous. Extensive preclinical research suggests that tumor development and progression is a multistep process in which normal cells acquire mutations in cell growth regulation which enables them to transform into highly malignant derivatives. Underlying mechanisms of transformation are genomic instability as well as inflammation. Douglas Hanahan and Robert A. Weinberg propose the manifestation of eight different cellular alterations present in the vast majority of cancer types which drive tumorgenesis: sustaining

proliferative signaling, evading growth suppressors, resisting cell death, enabling replicative immortality, inducing angiogenesis, activating invasion and metastasis, reprogramming of energy metabolism and evading immune destruction [11, 12].

1.3 Angiogenesis in cancer

The complex network of blood vessels ensures transport of oxygenated blood and nutrients throughout the body. Angiogenesis, which is the progress of growing new blood vessels, is a tightly regulated and fundamental biological process necessary for embryonic development as well as wound healing in the adult. Regulation of angiogenesis is dependent on a complex interaction of growth factors and inhibitors. Therefore, it comes as no surprise that dysfunctional angiogenesis due to imbalance in the regulation machinery contributes to the pathogenesis of various medical conditions. Cancer is one of the best known diseases where angiogenesis is deregulated. As tumors grow they are in need of increasing amounts of oxygen and nutrients to sustain their exponential growth. Over a century ago, researchers began to recognize that tumor progression is accompanied by a dramatic increase in vascularity [13]. Fig. 3 shows the first in vivo image of tumor angiogenesis which was photographed in 1939 showing the vascular network in transplanted rabbit epithelioma. It was suggested that tumors are capable of recruiting new blood vessels by secretion of a variety of tumor derived pro-angiogenic factors [14].
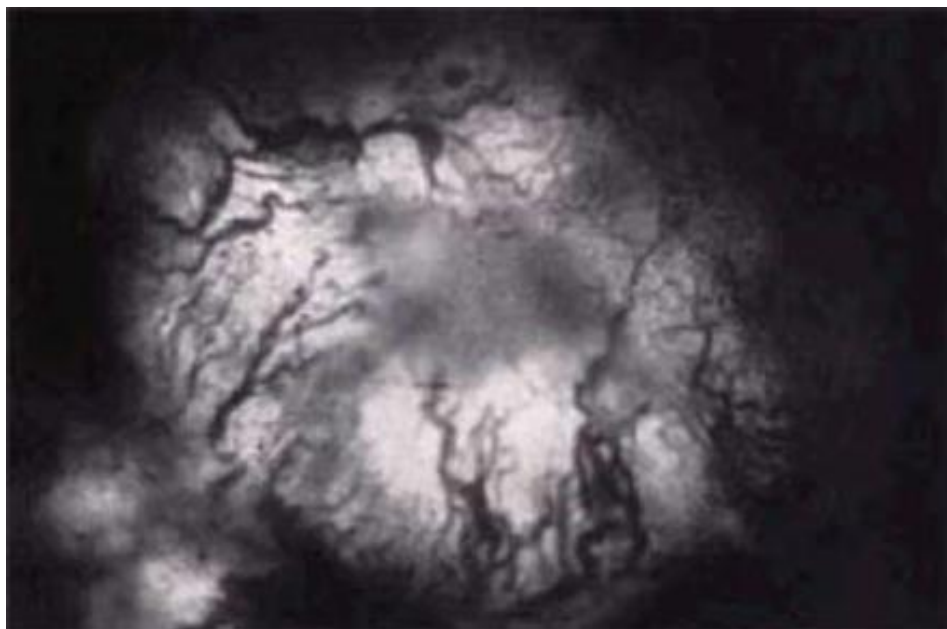
Fig. 3 First *in vivo* image of tumor angiogenesis from 1939 (from [14])
The image shows the drastic vascularization of the Brown-Pearce rabbit epithelioma transplant as seen in with a transparent ear chamber.

INTRODUCTION

By realizing tumors are dependent on initiating their own neovascularization, researchers hypnotized in the early 1970's that inhibiting tumor associated-angiogenesis could be potentially utilized as an effective anti-cancer therapy. This resulted in studies aimed to elucidate angiogenesis inducing molecules as well as potential therapeutic anti-angiogenic factors [15]. While there are numerous molecular players involved in the process to stimulate proliferation of endothelial cells, one of the most critical factors secreted by tumors to induce angiogenesis is vascular endothelial growth factor A (VEGF-A). VEGF was discovered in the 1980 by multiple laboratories working on different projects in the field of angiogenesis and it is believed to be a fundamental molecule for physiological as well as pathological angiogenesis [16-18]. The loss of a single VEGF-A allele results in embryonic lethality. Studies have demonstrated that VEGF-A is upregulated in many human tumors [19]. One very well-established stimulus for VEGF gene expression in tumors is hypoxia [20]. Hypoxia results in the stabilization of hypoxia inducible factor (HIF) which is degraded under normoxia by the tumor suppressor protein von Hippel-Lindau (VHL). VHL is often found to be mutated in certain cancers. VEGF binds to two different receptor tyrosine kinases, VEGFR1 and VEGFR2, while binding of VEGF to the latter is known to initiate the angiogenic and permeability enhancing effects in endothelial cells of VEGF [21]. Currently, a variety of angiogenesis inhibitors are under evaluation in clinical trials that mainly target the VEGF pathway. An overview of the various strategies employed to inhibit the VEGF signaling pathway is shown in Fig. 4.
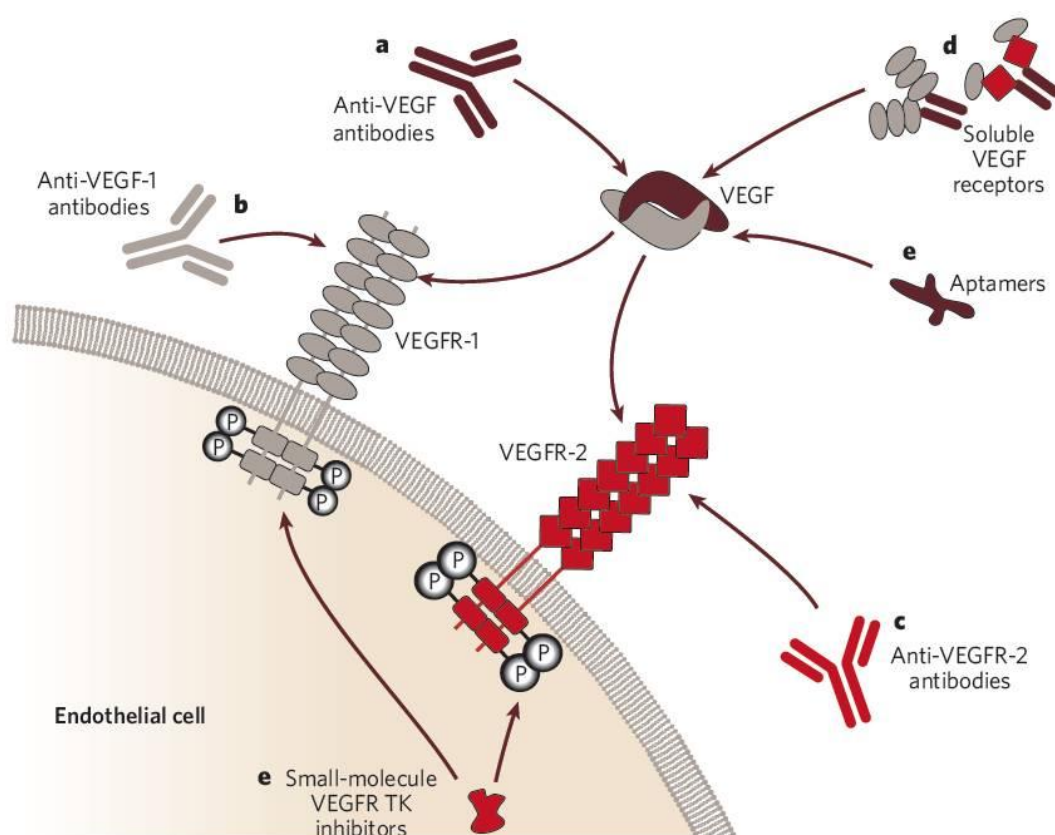
Fig. 4 Strategies to inhibit VEGF signaling for cancer treatment (from [21]).
Strategies to interfere with the VEGF signaling pathway include monoclonal antibodies directed against VEGF (a) or VEGFR (b,c) as well as chimeric soluble receptors, so-called VEGF traps (d), extracellular inhibitor aptamers to bind VEGF or small molecules to inhibit VEGFR autophosphorylation (e).

Bevacizumab (trade name: Avastin) is the most prominent anti-angiogenic agent and also represents the first clinically approved angiogenesis inhibitor. Bevacizumab is a humanized monoclonal antibody directed against VEGF-A. Initial approval of bevacizumab was granted by the FDA in 2004 which was based on a large, double-blind, randomized phase III clinical study of bevacizumab in combination with chemotherapy for metastatic colorectal cancer [22].

Most tumors appear highly vascularized and tumor vessels are structurally as well as functionally abnormal when compared to vessels of normal tissue. The tumor vasculature is characterized by heterogeneous, tortuous and leaky vessels, leading to areas of severe hypoxia within tumors. This results in a vicious circle, hypoxia induces upregulation of various angiogenic factors creating ultimately more abnormal vessels which further increases hypoxia due to dysfunctional composition of vessels [23]. Most tumors are characterized by a high interstitial pressure and inadequate blood flow into tumors making it extremely difficult to deliver anti-cancer drugs. An emerging concept in anti-angiogenic

therapy is "vessel normalization". The idea behind this is somewhat conflictive to the original anti-angiogenic paradigm to starve tumors by depletion of nutrition by destroying the feeding vasculature [15]. Pro- and anti-angiogenic factors are severely imbalanced within the tumor with resultant abnormal tumor vasculature. Restoring the balance of angiogenic modulators by decreasing pro-angiogenic factors such as VEGF may aid in the reorganization of vessels to a more normal state. This concept of "vessel normalization" established by Jain *et al.* proposes that by decreasing VEGF signaling a transient normalized tumor vasculature is created which is typified by less tortuous and leaky vessels that appear more like mature vessels [24, 25]. Correcting the abnormal vasculature to a more physiological functional state is characterized by a decrease in edema and interstitial pressure in the tumor as well as increased oxygenation status and drug delivery. There are indications from clinical trials evaluating efficacy of anti-VEGF therapy that such normalization of otherwise dysfunctional tumor vessels can be induced in patients as well [26].

1.4 Radiotherapy

1.4.1 Principles of ionizing radiation

More than 100 years ago, the German physicist Wilhelm Röntgen discovered laconically "eine neue Art von Strahlen" - a new kind of rays which he named x-rays (x to indicate the unknown). One year later, in 1896, Antonie-Henri Becquerel found that uranium compounds emit radioactivity followed by Pierre and Marie Curie who shortly after discovered radium and polonium to be radioactive as well. These historic events which would revolutionize medicine and lead to intense research in the field of radiobiology guiding the way to its crucial and worldwide applications in medicine for diagnosis and therapy.

The term ionizing radiation (IR) comprises all types of radiation that exhibit enough energy to detach electrons from molecules leaving them charged or ionized. Ionization is characterized by the release of energy. For simplicity, IR can be subdivided into particulate (alpha or beta radiation) or electromagnetic (gamma or x-rays) radiation. Electromagnetic radiation is indirectly ionizing, meaning they do not cause biological damage themselves but rather through the production of high energized charged particles as they pass through biological material. These charged particles subsequently cause damage resulting in biologic phenotypes. The damage induced by IR mainly results from DNA damage. Fig. 5 shows the two routes of how DNA is damaged.

INTRODUCTION
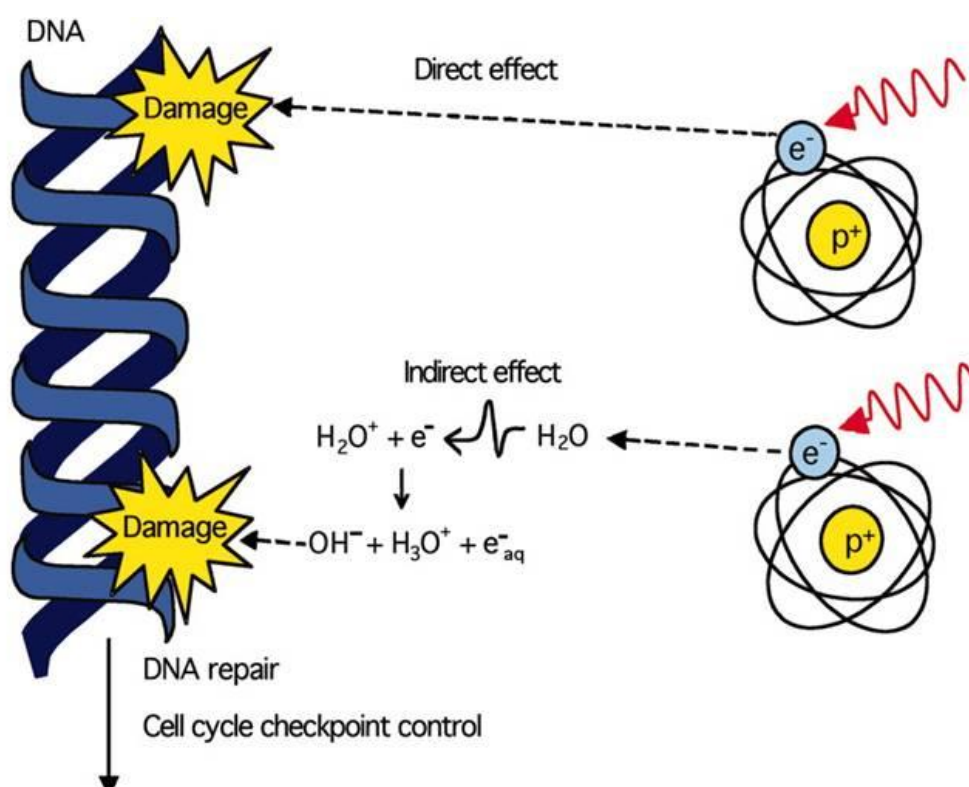
Fig. 5 Direct and indirect effects of ionizing radiation on DNA [27]
A secondary electron generated by IR has two mechanisms of damaging DNA: The upper part of the figure shows the direct damage of DNA by the electron itself. In the lower part the secondary electron indirectly damages DNA by generating a highly reactive ion radicals through collision with other molecules, in this case water, in the cell which then damage DNA.

The upper part of figure shows the direct action of IR. Here, a secondary electron generated by for example x- or gamma rays directly interacts with its target DNA. In the lower part of the figure the secondary electron interacts with another target in the cell first. For simplicity, the process in this figure is shown for a water molecule since it is the most abundant molecule in the cell. This interaction generates a highly unstable ion radical (H_2O^+) as well as an electron. Due to the unpaired electron in the outer shell the H_2O^+ ion radical is highly reactive and quickly reacts with another water molecule generating a hydroxyl radical (OH^-) which is a highly reactive species. This chain reaction induced by absorption of IR ultimately results in damage of cellular targets including DNA, proteins, and lipid membranes. The critically lethal target for IR-induced radical is DNA. Interestingly, while damage of DNA occurs rather quickly after exposure to IR, the manifestation of induced damage can range from hours to years after exposure. This depends, of course, on the extent and location of damage to the DNA, possibly resulting in cell death or DNA mutation. DNA mutation, when occurring in the germ line, can be passed on to progeny or when occurring in the somatic line may transform cells and ultimately lead to cancer.

INTRODUCTION

The DNA damage induced by IR ranges from base damage to single or double strand breaks as well as DNA-protein cross links. The cell possesses distinct intrinsic mechanisms to sense and react to those different types of DNA damage, and the cellular stress response to IR will be summarized in the next paragraph. Induction of DNA repair is accompanied by an arrest in cell cycle progression to enable DNA repair before cells divide. If DNA damage persists the cell may undergo apoptosis or senescence to avoid propagation of defective DNA to daughter cells (summarized from [28]).

One important factor influencing the extent of damage induced by IR to DNA is the level of molecular oxygen O_2 present in the irradiated cell. Fig. 6B shows the differences of survival in well oxygenated as well as hypoxic cells. Aerated cells are more sensitive to IR. In hypoxic cells the radiation dose that is required to achieve comparable biologic effect has to be 2.5 to 3.5 fold higher [29].
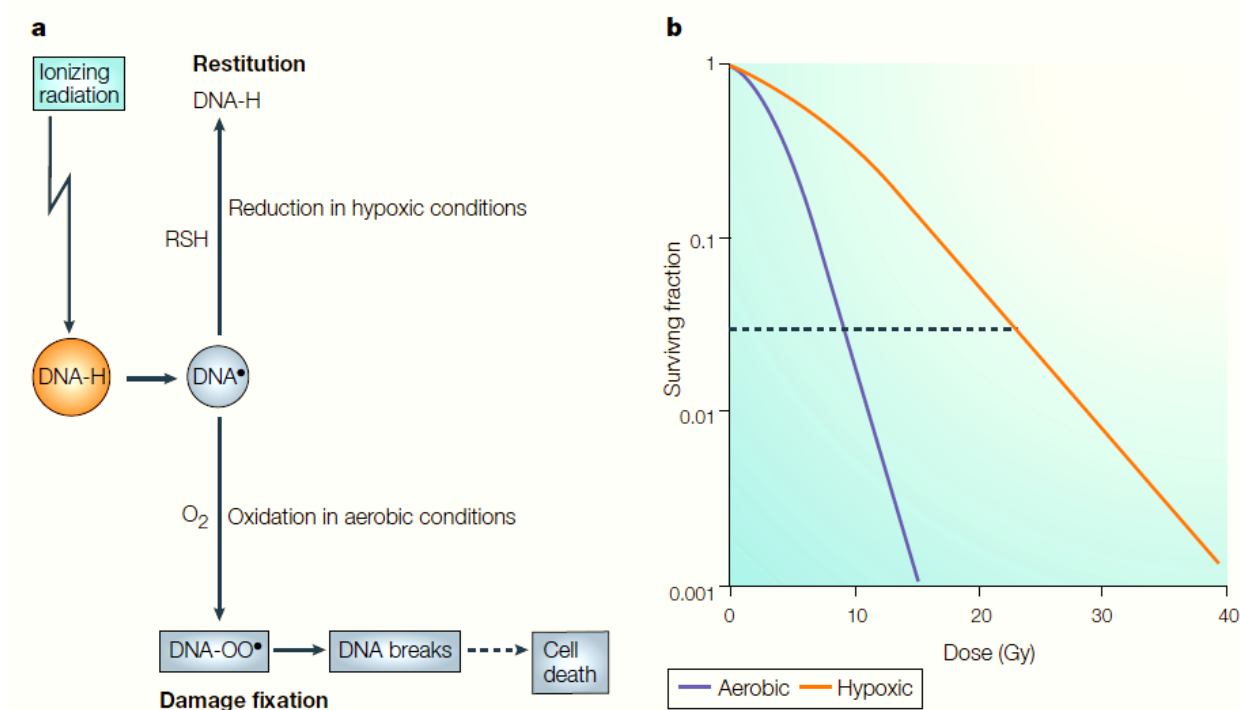
Fig. 6 Resistance of hypoxic cells to radiation [29]
A) DNA damage induced by IR is "fixed" in well-aerated cells. Lesions in form of free radicals in the DNA can be restituted during hypoxic conditions while remain permanent in the presence of oxygen. B) Well-aerated cells are more radiosensitive than hypoxic cells. In hypoxic conditions the IR dose has to be 2.5 to 3.5 fold higher to achieve comparable cell death.

The reason for this is explained by the "oxygen fixation hypothesis", see Fig. 6A. Here, DNA damage is fixed in the presence of O_2 but reversible under hypoxic conditions. Direct or indirect DNA damage produces DNA radicals which can react with any molecule containing a sulfhydryl (SH) group which leads to chemical restitution of the DNA. In the presence of

16

molecular oxygen however, the DNA radical reacts with O_2 and forms an organic peroxide (OO•) which is chemically impossible to restore and therefore makes the lesion permanent [28].

1.4.2 IR induced stress signaling and repair of radiation induced DNA damage

Following exposure to IR, a multi-faceted stress response is induced which includes activation of several early response genes. Upon irradiation several molecular stress signaling pathways are initiated, Fig. 7, which determine the fate of the cell. Complex signaling cascades decide if the cell will survive and further proliferate, in which case IR induced DNA damage must be resolved. In situations where cellular damage is beyond repair, signaling events result in the induction of cell death. One of the major responses to DNA damage is coordinated through the phosphatidyl- inositol-3-OH kinase-like kinases (PIKK) family. The PIKK family compromises of many proteins involved in cellular stress responses and DNA repair. Key DNA sensing proteins include Ataxia Telangiectasia Mutated (ATM) and ATM Rad3 related (ATR) which both act as surveillance and signaling proteins that once activated, phosphorylate several downstream effector components of the cellular stress response to DNA damage. Effector proteins include p53, checkpoint proteins chk1, chk2, and DNA repair proteins BRCA1, NBS1 [30]. Another downstream target for ATM is the chromatin protein H2AX which become phosphorylated shortly after DNA damage and accumulates at DNA damage sites where it orchestrates assembly of other DNA repair factors [31]. Staining for γH2AX serves as a surrogate marker for DNA breaks and is commonly used in the laboratory. Another pathway that is induced upon irradiation of cells is the acid sphingomyelinase (ASMase) pathway for the generation of ceramide. This pathway plays an important role in the induction of apoptosis in irradiated cells. Fig. 7 summarizes events on molecular level induced by IR.

INTRODUCTION
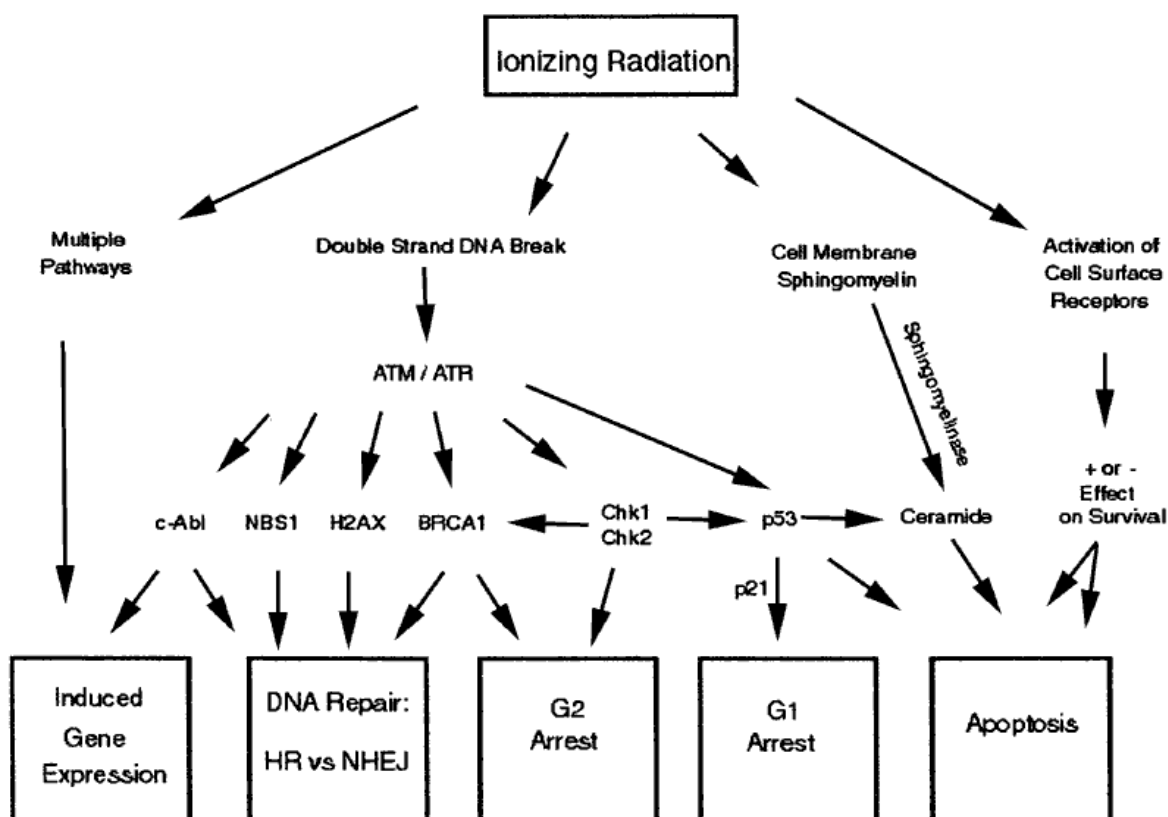
Fig. 7 Molecular events occurring upon irradiation of cells (simplified) [30]
There are various signaling pathways induced by ionizing radiation. Major events include the induction of gene expression, initiation of DNA repair mechanisms due to IR-induced DNA damage, cell cycle arrest and possible induction of apoptosis mainly related to activation of p53 and ceramide production.

Double-strand breaks represent the most lethal form of DNA damage and cells have two major DNA double-strand break repair mechanisms that are activated through ATM/ATR: non-homologues end joining (NHEJ), which occurs throughout the cell cycle and homologous recombination (HR), which predominates in late S or G_2 phase of the cell cycle since it requires the presence of homologous sister chromatids for repair [32]. In addition to those two pathways, mammalian cells are in possession of other evolutionary conserved mechanisms to sense and act on different types of DNA damage. It is of importance to know that cells exhibit a different sensitivity to irradiation depending on which stage of the cell cycle they are in, with late S phase being the most radio resistant and the G_2/M phase being most radiosensitive [33]. Resistance in S phase is thought to be based on facilitated and effective DNA repair by HR due to proximity of sister chromatids. Taken together, the fate of the cell exposed IR is tightly regulated and involves numerous proteins as well as regulation mechanisms which is beyond the scope of the present work.

IR mediated damage and subsequent repair can be phenotypically distinguished in distinct processes. Experiments conducted with irradiated cells have shown that based on the

severity the damage can be subdivided into three types: Lethal damage, potentially lethal damage (PLD) and sublethal damage (SLD). Lethal damage to cells is irreparable and always leads to cell death, whereas cells that undergo PLD can potentially be rescued depending on environmental conditions of the cells before and after irradiation. At low doses of irradiation, SLD can be repaired with the aid of various DNA repair mechanisms unless more sublethal damage is induced by additional irradiation given in close temporal proximity [28].

1.4.3 Radiation therapy in cancer treatment

Radiation therapy is a mainstay of cancer treatment with approximately 50 percent of all cancer patients receiving some form of radiotherapy during their course of treatment. Since radiation itself does not discriminate between normal and cancerous cells it is of crucial importance to enable adequate targeting of IR to tumorous tissue. Radiation therapy can be delivered to a patient's tumor in a variety of ways. In teletherapy or external beam radiation therapy, radiation is given from outside of the patient's body by a machine capable of delivering IR. In contrast, brachytherapy places radioactive sources into the patient adjacent to the tumor site. A third possibility is the systemic delivery of a radioactive substance, such as ^{131}I for thyroid tumors. The treatment that is chosen depends on the cancer's characteristics such as type, stage, location and size as well as patient specific circumstances like health, age, medical history and additional treatment that is performed. The machines that are most commonly used in clinic for external beam radiation are linear accelerators (Linacs) which produce high energy megavoltage x-rays. Therapeutic x-rays are characterized by short wavelengths with high frequencies which makes them highly energetic and therefore suitable for penetration and deposition of dose in matter. In a linear accelerator electrons are accelerated to a high speed exploiting their intrinsic negative charge towards the positive anode and then abruptly stopped on a metallic target. Upon hitting the metal target, the kinetic energy of the electrons is converted into a spectrum of x-rays through bremsstrahlung process which is then used to irradiate to the tumor target [28].

Clinically, radiation therapy is mostly delivered in a fractionated scheme. Each fraction consists of a relatively small dose (1.2-3.0 Gy) and numerous fractions are delivered over a period of weeks. Fractionation of radiation goes back to experiments conducted in the 1920's and 1930's where researchers found that a ram could not be sterilized with a high dose of radiation without extensive skin damage. In this model system the highly reproductive tissue of the testes was supposed to mimic the proliferating tumor while

surrounding skin represents normal tissue. The seminal finding at the time was that the researchers found that when the radiation dose was split into multiple smaller daily fractions, sterilization was possible with significantly less skin damage. The conclusion drawn from those experiments was that fractionation of radiation yields equivalent tumor control but with decreased toxicity to surrounding normal tissue. The basis of this observation in part has resulted in a paradigm of fractionated radiotherapy based on the "four Rs" of radiobiology: repair, redistribution, repopulation and reoxygenation.

As described earlier, damage to cells from IR ranges from sub-lethal to lethal. Delivering smaller doses of IR allows for repair of sublethal damage in normal tissue with resultant less long term damage. In the case of the tumor, all cells that are in sensitive phases of the cell cycle are potentially damaged beyond repair while those in resistant phase remain only partially damaged. Those cells might continue progression through the cell cycle meaning that cell population is reassorted or redistributed within the cell cycle. Moving into more radio-sensitive G_2/M phases of the cell cycle allows for IR to kill more cells in the next delivered fraction of IR. Radiation is also known to stimulate cell proliferation in response to tissue damage which occurs in both normal as well as tumor tissue. This repopulation effect ultimately has a profound impact in the overall tumor response to treatment. When fractions of radiation are longer apart then the length of the cell cycle, tumor regrowth may outbalance tumor killing. Hyperfractionation of radiation, delivering multiple IR doses per day is one way radiation oncologists mitigate the effects of tumor cell repopulation. The final "R" of radiobiology is reoxygenation: As discussed previously, O_2 status in the tumor has a direct correlation with radio-sensitivity. Since hypoxic tumor regions are radioresistant, splitting of IR doses allows killing of oxygenated cells which is followed by reoxygenation of hypoxic tumor cells which can then be killed with follow-up doses of IR, Fig. 8, summarized from [28].

INTRODUCTION
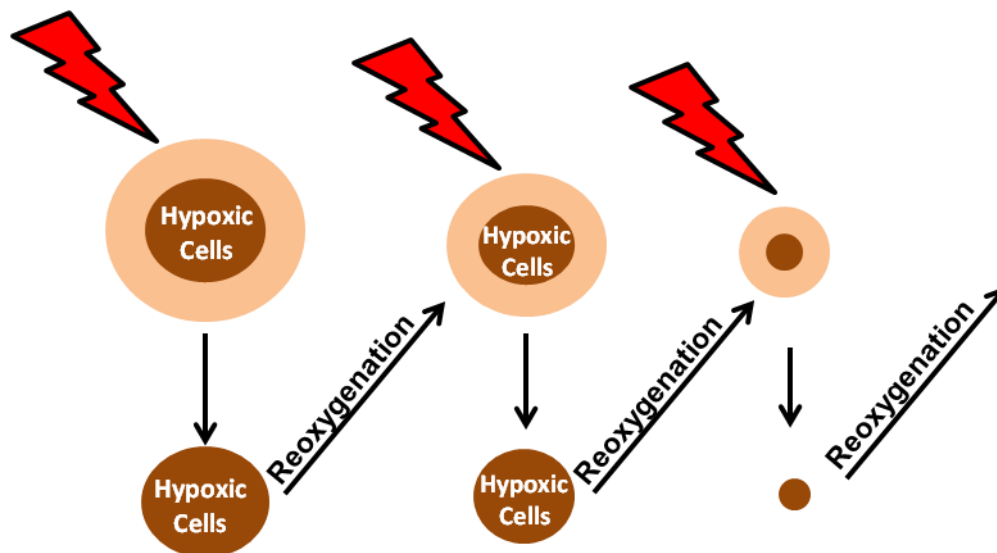
Fig. 8 Principles of reoxygenation of hypoxic tumor regions in fractionated radiotherapy
IR damages only well-aerated cells while the hypoxic part of the tumor remains relatively unaffected. Reoxygenation of previous hypoxic tumor regions allows a following IR dose to induce cell death in now radio-sensitive tumor cells increasing overall tumor control.

While various types of cancer are treated with radiation therapy and a large percentage of those successfully, radiation therapy still has its limitations especially in the context of metastatic disease, locally aggressive tumors or those tumors in locations adjacent to vital critical structures that are not treatable without unacceptable damage to surrounding normal tissue. As often is the case, increased tumor control with higher radiation doses unfortunately comes with increased toxicity to adjacent normal tissue. The course of radiotherapy therefore has to be planned precisely to choose a treatment strategy that exhibits a high percentage of tumor control while minimizing risk of complication for the patient.

1.4.4 Combination radiation therapy with anti-angiogenic therapy

Amassing preclinical data suggests that outcomes of radiation therapy can be improved when combined with anti-angiogenic agents. When vessels become normalized due to anti-angiogenic treatment, interstitial pressure and hypoxia in tumors decrease and delivery of drugs is facilitated, at least transiently. This means, when IR is delivered to the tumor within that "normalization window" cytotoxic effects should be increased due to higher oxygen levels present in target tissue. As described earlier, molecular oxygen is a critical determinant for cell death induced by radiation and the reason why hypoxic tumors respond relatively poorly to IR. Various preclinical studies have found improved tumor control when

INTRODUCTION

IR was delivered to normalized tumor vessels [34, 35]. But the relationship of anti-angiogenic therapy and IR goes deeper and exhibits a direct interaction as well. Studies have shown that radiation itself can initiate the angiogenic process and tumor cells were shown to upregulate VEGF expression after being irradiated [36, 37]. This upregulation is part of the overall stress response induced by IR through various cellular stress kinases as discussed earlier. Enhanced angiogenesis ultimately drives the tumor to a multi-mutated, genomically unstable phenotype characterized by resistance to chemo- and radiation therapy. There is also evidence that fractionation of radiation into multiple small doses can activate Hif-1-inducing pleotropic effects in tumor versus endothelium. Moeller *et al.* reported that Hif-1 expression helps to radiosensitize tumor cells by allowing reoxygenization of tumor cells but simultaneously increasing radioresistance in endothelial cells [23]. In different studies it was shown that blocking the VEGF-induced stress response in tumor cells by inhibition the VEGF signaling cascade increases the effects of adjuvant radiation. In these sets of experiments the presence of VEGF was shown to increase radioresistance of endothelial cells while leaving tumor cells unaffected [36, 38]. Given these observations, a large research focus has been put on engaging the vascular component of the tumor response to ionizing radiation. In a landmark study scientists led by Zvi Fuks at Memorial Sloan Kettering Cancer Center reported that the tumor response to higher doses of IR is dependent on endothelial cell apoptosis induced via the ASMase pathway and not on tumor cell death as widely believed [39]. The doses used in these sets of experiments were relatively high but still clinically relevant. There is growing interest in targeting the vascular network by anti-tumor therapies since tumor vessels are easier to assess than the tumor itself and in theory less resistant to cytotoxic agents since they appear less transformed. In addition angiogenesis only occurs in limited situations such as wound healing, making anti-tumor vascular therapy a promising avenue of research and also a potentially non-toxic therapy to normal tissue [40].

It becomes evident that combining radiation with anti-angiogenic therapy holds big potential but since both treatment regimens are mutually influencing each other and outcomes for tumor as well as the vascular component are strongly dependent on radiation dose as well as treatment scheduling, further research is necessary to unravel the complicated interplay between the tumor microenvironment, endothelium, angiogenesis, hypoxia and tumor cells themselves. Currently, clinical trials are ongoing evaluation the overall benefit of combining radiation and anti-angiogenic treatment.

1.5   Glioma

In general, there are two different forms of brain tumors, those which originate in the brain parenchyma (primary tumors) and those which metastasize to the brain from non-CNS tumor sites in the body (secondary brain tumors). The vast majority of tumors originating in the brain are malignant. The most common form of *de novo* brain cancers are gliomas, which include all types of tumors originating from glial cells located in the central or peripheral nervous system. Malignant glioma comprises glioblastoma (GBM), anaplastic astrocytoma, mixed anaplastic oligoastrocytoma and anaplastic oligodendroglioma. Close histological examination of patient biopsies is necessary to distinguish between different tumor types and diagnosis is carried out according to WHO guidelines. The prognosis depends on tumor histology as well as location within the brain. Pure oligodendroglioma carries the best outcome with better responses rates to treatment compared to other malignant gliomas [41, 42]. Glioblastoma which is a WHO grade IV tumor carries the worst prognosis and represents the most common type of malignant gliomas. GBM remains largely incurable and is considered one of the deadliest cancers [43] with a median survival of 12-14 months with conventional therapies. Malignant gliomas are highly neuro-destructive and treatment remains for the large part insufficient due to the intrinsic aggressive nature of the tumor. A common feature of all gliomas is their infiltrative nature with deep invasion into the cerebral parenchyma. These brain tumors are highly vascularized and with increasing histological grade often exhibit areas of hypoxia and necrosis. Complete surgical resection is hindered by the invasive nature of the tumor infiltrating deeply into brain tissue. In addition, GBMs are considered one of the most radio-resistant tumors with the vast majority of patients having tumor failures following radiotherapy. The poor prognosis of GBM along with other malignant gliomas is mainly based on high rates of local tumor recurrance. It has been reported that 90% of glioma patients have tumor recurrence at the original tumor site and in 5% of patients multiple lesion sites were detectable after treatment [44]. Surgically non removable as well as radio-resistant cancer cells result in high tumor recurrence rates and treatment failure. Although extensive preclinical research has been done, patient survival has not significantly improved over the last years. Treatment of malignant gliomas should be carried out by a multidisciplinary team and involves handling of related clinical symptoms like possible steroid therapy to reduce tumor-associated edema as well as anti-epileptica to control seizures. Standard of care up to today is a multi-modality approach of surgical resection followed by radiotherapy with concomitant and adjuvant temozolomide [45]. Surgery is the initial therapy to reduce tumor mass, alleviate intracranial pressure and to obtain biopise material for histological examination. After maximal safe resection patients receive fractionated radiotherapy with a total dose of 60 Gy (30-33 fractions of 1.8- 2 Gy or

INTRODUCTION

equivalent) in combination with chemotherapy. Temozolomide (TMZ) is given daily during radiotherapy and continued six cycles of 5 days every 4 weeks for six cycles [42]. Temozolomide is an oral alkylating agent which undergoes spontanious converstion under physiological conditions into its reactive form monomethyl triazeno imidazole carboxamide (MTIC). The cytotoxic effect of MTIC is based on its capacity to methylate guanine at the O^6 position. Identical to signaling events caused by ionizing radiation, TMZ induced DNA methylation leads to DNA damage response as well as activation of DNA repair mechanisms. In more detail, a process called mismatch repair is activated which induces G_2/M cell cycle arrest and eventually induction of apoptosis [46].

Taken together, glioma is rarely curable and treatment options are primarily palliative in intent. This grim prognosis clearly demonstrates the need for new effective therapy alternatives.

1.5.1 Angiogenesis in brain tumors

GBM represents one example of a highly vascularized tumor and neoangiogenesis, present in and around the tumor, is a crucial step in its pathogenesis. The level of angiogenesis in GBM is correlated with prognosis meaning patients with increased amounts of dysfunctional vessel exhibit a poorer prognosis [47]. It is believed that the formation of the dysfunctional tumor vessels along with the deeply infiltrating nature into the white matter is the key reasons for treatment failure and treatment resistance. In glioma, the formation of new tumor blood vessels results from either angiogenesis, vasculogenesis (*de novo* vessel formation from circulation bone marrow derived endothelial progenitors) or arteriogenesis [48], with angiogenesis being the primary formation progress. Glioma vessels exhibit all classical characteristics of abnormal tumor vasculature such as increased vessel diameter, high permeability inducing areas of severe hypoxia. The balance of pro- and anti-angiogenic leans towards neoangiogenesis triggering the "angiogenic switch" inducing blood vessel and extracellular matrix breakdown, migration of endothelial cells with ultimately new vessel formation [49]. Similar to other solid tumors the VEGF/VEGFR pathway exhibits a key role in GBM angiogenesis, and VEGF-A is found to be highly upregulated in malignant gliomas [50].

1.5.2 Targeting VEGF-induced angiogenesis in GBM

The therapeutic approach of correcting dysfuntional glioma vessel architecture to improve cytotoxic chemotherapy delivery as well as efficacy of anti-tumor agents is appealing especially for highly vascularized gliomas. Similar to other tumor types a major focus lies on targeting the VEGF signaling pathway. Preclinically, the treatment of glioma cells with anti-angiogenic agents by VEGFR-2 blockage had no direct influence on tumor cells but created a "normalization window" as described earlier where effects of IR or chemotherapy were increased indicating that anti-angiogenic therapy could be combined into a multimodality-treatment regimen [51]. Bevacizumab, the monoclonal antibody targeting VEGF, is approved for use in recurrent GBM either as a single agent or in combination with chemotherapy [52, 53]. Ideally, different anti-angiogenic treatments could be combined since tumors are known to develop resistance when only one part of a pathway is blocked. Ongoing preclinical evaluation and clinical trials will guide the way in what context best to integrate an anti-angiogenic treatment regiment into conventional GBM therapy.

1.6 Principles of oncolytic virotherapy

Several cancers have limited effective therapeutic options, especially in the context of metastases. As described for glioma, multiple tumors are routinely treated with a combination of different treatment regimens such as chemotherapy concomitant or adjuvant to radiotherapy. The rationale of combination therapy over monotherapy is that by combining different anti-cancer modalities the disease is targeted through different modes of action reducing the chances of tumor resistance arising to one particular drug. In addition to standard therapies, new cancer therapies exploiting different modes of action are urgently needed to improve therapeutic success and patient outcomes. Ideally, such novel agents should work well on their own or even better, synergize with established cancer therapies. Over the last years tremendous progress in the field of novel and experimental new cancer therapies, such as small molecule drugs or monoclonal antibodies targeting different cencer-related pathways, has been made in laboratories worldwide. Multiple novel agents exploring unique models of action are moving from the bench to clinic trials. In the last decade, the field of oncolytic virotherapy has gained importance as novel anti-cancer treatment that harnesses the viruses' inherent capacity to infect and kill cells and re-target such viruses to preferentially replicate and kill tumor cells. Fig. 9 illustrates the principle of oncolytic virotherapy.
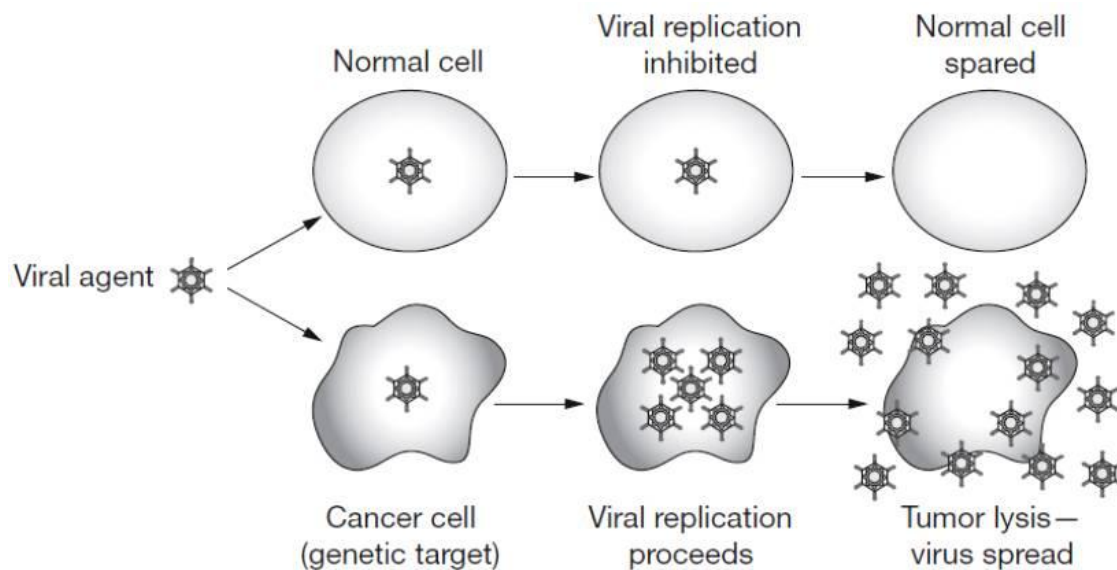
Fig. 9 Principle of oncolytic virotherapy [54]
In oncolytic virotherapy the viral agents selectively targets abnormal tumor cells while replication in normal cells is inhibited. Ultimately, this leads to the lysis of cancer cells accompanied by viral release to restart the cycle with minimal toxicity to normal tissue.

The knowledge that some viruses exhibit an oncolytic capacity dates back almost a hundred years where single-case reports indicated that concomitant severe infections with wild-type viruses were at least temporally beneficial for cancer control [54].

Oncolytic viruses (OV) specifically target and replicate in cancer cells while normal tissue is spared. Upon tumor cell lysis amplified viral progeny is released and able to infect surrounding tumor cells to initiate another cycle of tumor destruction. This unique model of action is aided by additional virus related effects on the tumor microenvironment such as modulation of the immune system or the nutrients delivering tumor vasculature. From a safety standpoint most oncolytic viruses used for tumor therapy are attenuated to minimize toxicity to normal tissue or even genetically altered to enhance tumor selective specificity. Moreover, to improve cancer therapy oncolytic viruses are often times genetically engineered to express various therapeutic genes. A key question in oncolytic virus research is why the viruses are specific to cancer cells while sparing normal cells. The selectivity of oncolytic viruses is most likely based on their ability to utilize the very same cellular alterations that are responsible for cancer growth to selectively allow for viral infection and replication. Some OV are genetically altered to redirect viral attachment from normal to receptors on cancerous cells by either targeting them to the tumor microenvironment or by engineering them to bind tumor antigens. A more common phenomenon is the restriction of viral replication to tumor cells by exploiting altered gene expression inherent to tumor cells. In most cases, this implies the OV is only able to replicate when certain tumor-specific genes

are upregulated, which locally restricts OV to transformed cancerous cells [55, 56]. By the extensive progress that has been made in the field of genetic engineering in the last decades, genetic manipulation OV to increase tumor cell selectivity became feasible and overcame initial concerns of possible viral toxicity. One way to achieve tumor selective viral replication is by cloning a promoter sequence into the viral genome which allows viral replication only when a certain transcription factor is over expressed in tumorous cells as compared to normal cells. Another well documented example for creating OV is through dependence on host gene expression, such as thymidine kinase (TK)-dependent replication of several OV. In this paradigm, the viruses are constructed with a disrupted viral TK gene locus making viral replication dependent on hosts TK expression. TK is amongst a group of genes strongly upregulated in cancer cells when compared to normal cells due to the proliferating nature of cancer cells restricting replication to tumor.

As of today, a multitude of different viruses, either wild-type, engineered or engineered and armed, have entered clinical trials. Virus species tested in clinical applications include adeno-, herpes, reo-, paramyxo-, such as mumps or measles, or vaccinia virus [54]. So far, most of the studies carried out suggest that the viruses which are administered intratumoral or intravenously are safe and in some cases there are early indications of anti-tumoral effects. Still, further intensive research is required to understand the inherent biology of this new line of anti-tumor virotherapeutics and to develop techniques to optimize its therapeutic potential. Efficacy of virotherapy might be strongly dependent on tumor type and characteristics, as well as patient immune status which could drive the field into an individual patient tailored therapy direction [57]. However, randomized phase III trials, partially ongoing (see clinicaltrials.gov for details), need be carried out in order to guide the way of how these novel anti-cancer therapeutics can be used or be combined with other targeting modalities to improve tumor control in patients.

1.6.1 Vaccinia virus in cancer therapy

Vaccinia virus along with other poxviruses exhibit unique features making them very suitable as anti-tumoral agents when compared to other oncolytic viruses as reviewed by D.H. Kirn and S.H. Thorne [58]. From a safety standpoint, VACV is in the unique possession of a multiple decade's long clean track record in man due to being extensively studied during its natural use in the worldwide immunization against smallpox clearly demonstrating safety and tolerability in people. Moreover, possible complication after exposure to VACV have been studied and documented in detail and anti-viral treatments are at hand. This broad knowledge minimizes the chances of rare events endangering the patient to almost zero. Another important characteristic making VACV a safe OV is its cytoplasmic replicative

lifestyle. As mentioned earlier, VACV replication is restricted to the cytoplasm of infected host cells therefore no integration of viral DNA into the host's genome with resultant cell transformation is possible. Besides its safety in patients, VACV also shows a broad tumor tropism because viral attachment is not dependent to specific receptors and in addition tumor lysis occurs rapidly when compared to other oncolytic agents. One promising feature of oncolytic VACV is its potential to be administered systemically. The broad majority of clinical trials conducted with OV so far focuses on local or regional viral delivery such as intra-tumoral (i.t.) or intracavitary. However, to target the metastatic disease it is necessary for an oncolytic agent to travel and survive in the bloodstream to reach distant tumor sites [59]. After initial replication, when viral progeny is released the composition of EEV with an outer membrane derived from the host facilitates dissemination in the patient's body by evading the immune system to travel to possible distant tumor as well as metastasis sites. Furthermore, VACV displays a large cloning capacity with possible insertion of up to 25 kB which enables the expression of various genes to enhance tumor destruction, target the tumor microenvironment or to detect and image the virus itself within the tumor or host [58, 60, 61]. One promising oncolytic VACV, JX-594 (Jennerex Biotherapeutics, Inc. USA) with extensive preclinical evaluation has accomplished the step form laboratory bench to clinic and demonstrated safety and efficacy in initial trials. JX-594 was engineered from the Wyeth vaccine strain and is attenuated by TK disruption. In addition JX-594 expresses an immune-stimulatory factor (human granulocyte-macrophage colony-stimulating factor, GM-CSF) as well as β-galactosidase as a marker gene [62-64]. Another promising candidate, used within this work, is GLV-1h68 engineered by Genelux Corporation, San Diego, USA. The virus was constructed by insertion of three expression cassettes *Renilla* luciferase-Aequorea green fluorescent protein (RUC-GFP) fusion, β-galactosidase (LacZ), and β-glucuronidase (GusA) into the F14.5L, J2R (thymidine kinase) and A56R (hemagglutinin) loci of the viral genome of the Lister (LIVP) strain, respectively [65]. Fig. 10 shows a schematic representation of GLV-1h68. It has been shown to selectively replicate in cancer cells compared to non-transformed cells [66].
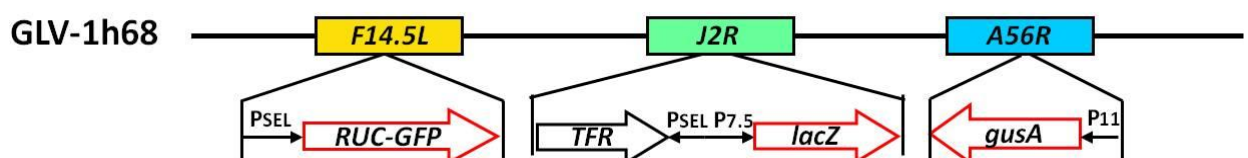

Fig. 10 Oncolytic VACV GLV-1h68

Schematic representation shows the insertion of the three gene cassettes Renilla RUC-GFP fusion, LacZ and GusA into the F14.5L, J2R and A56R loci of the viral genome of the LIVP strain.

In preclinical animal models systemically administered GLV-1h68 was shown to specifically target, colonize and replicate in tumor tissue with resultant tumor regression. This has been demonstrated for a variety of different cancer types, including breast, melanoma, pancreas, prostate, squamous cell carcinoma, brain and others [65, 67-71]. Another VACV, used within this work, is LIVP 1.1.1 which is a plaque purified isolate of the non- attenuated LIVP strain of VACV. Although less attenuated than GLV-1h68, sequencing of LIVP 1.1.1 demonstrates it has a deletion in VACV thymidine kinase gene as well.

One initial phase one clinical study in patients with solid tumors focusing on safety with GL-ONC1 (clinical grade GLV-1h68) has been completed recently indicating that intravenous administration of the virus is well tolerated at therapeutic dose levels. Further clinical evaluation in phase I/II studies is on-going (clinical trials identifier NCT01443260, NCT01584284 and NCT00794131).

1.6.2 Oncolytic viruses in glioma therapy

As mentioned earlier, the use of OV for cancer therapy dates back over a century. One of the initial setbacks in using different OV, especially for brain tumors, was their lack of neurotropism. As the field of OV developed and mechanisms to engineer viruses to alter their tissue tropism were established, the idea of curing brain malignancies with oncolytic viruses was met with renewed interest again. Initial clinical studies were carried out in the 1990 using attenuated Herpes simplex and adenovirus [72]. Zemp *et al.* summarized the obstacles that have to be overcome for the use of OV in glioma therapy as followed: Overcoming/recruiting the antiviral/antitumoral immune response, minimizing neurotropism while maintain OV efficacy, optimizing modes of administration in order to overcome the glioma microenvironment, and targeting brain tumor- initiating cells [73]. Preclinical, different oncolytic viruses are being evaluated for their potential use for glioma therapy. By the end of 2011, 20 clinical trials have been completed or are on-going in GBM assessing safety and efficacy of seven different attenuated oncolytic viruses. Importantly, completed trials so far all show general safety for patients, without any severe adverse effects induced upon virus administration into the brain. However, a significant benefit in terms of efficacy that was suggested in preclinical studies has not been achieved as of yet [74, 75]. Recent data in different tumor types indicate promising result of OV by inducing anti-tumor immunity as well as combination with chemotherapeutics [76-79]. Future trials should be headed in the direction of trying to incorporate establishes treatments in combination with OV. Virus therapy together with radio- or chemotherapy might exhibit strong interaction, resulting in

increased tumor control, which could tip the balance in favor for the patient and make an impact on GBM clinical outcomes.

1.6.3 Combination of oncolytic viruses with radiation therapy

One of the major clinical challenges in the development of clinically safe viral oncolytics is the trade-off of efficacy for safety. OV are genetically attenuated to restrict replication to tumor tissue and minimize the toxicity to normal tissue. This of course comes to a certain extent at the expense of efficacy. One mechanism to augment oncolytic virotherapy is to combine it with standard therapies such as radio- or chemotherapy, which can increase viral replication by upregulation of cellular stress pathways resulting in enhanced tumor control [55, 80]. From a clinical perspective it makes sense to incorporate oncolytic viruses into a treatment regimen where it is combined with established modalities that are part of standard of care. Radiotherapy, despite its limitations, is a mainstay in cancer therapy and novel agents which can possibly enhance radiation induced anti-tumor effects or decrease toxicity to surrounding normal tissue are likely to succeed in clinical trials. Initial evidence that radiotherapy interacts with an oncolytic virus was given by Advani *et al.* in 1998, where an intra tumoral delivered oncolytic herpes simplex virus 1 (HSV-1) was combined with focal radiation resulting in increased viral replication within the tumor followed by enhance tumor regression [81]. Follow up studies confirmed a survival increase in mice bearing orthotopically implanted glioma cells treated with the combination of HSV-1 and IR [82]. Since then, it was demonstrated that besides HSV, multiple intra-tumoral delivered viruses such as adeno-, measles or reovirus can be combined with IR to increase tumor control in animal models [83-88]. When thinking about combining oncolytic virotherapy with ionizing radiation two possible mechanisms exist of how both regiments might interact. First, viral replication within the tumor could induce cellular changes making tumors more sensitive to radiation or in contrast, ionizing radiation might function as a "viral sensitizer" by inducing cellular changes in the tumor that support viral replication or spread [80]. Since most viruses studied to date were delivered by intra-tumoral inoculation which has at least initially limited spread within the tumor the second scenario is more likely to explain interaction of various OV with IR as seen in preclinical models. As demonstrated in Fig. 11 the combination of IR with intratumoral oncolytic virotherapy is attractive because of its local-regional manner, meaning replication of an oncolytic virus is ideally locally restricted to tumor tissue which is precisely the target for IR as well.
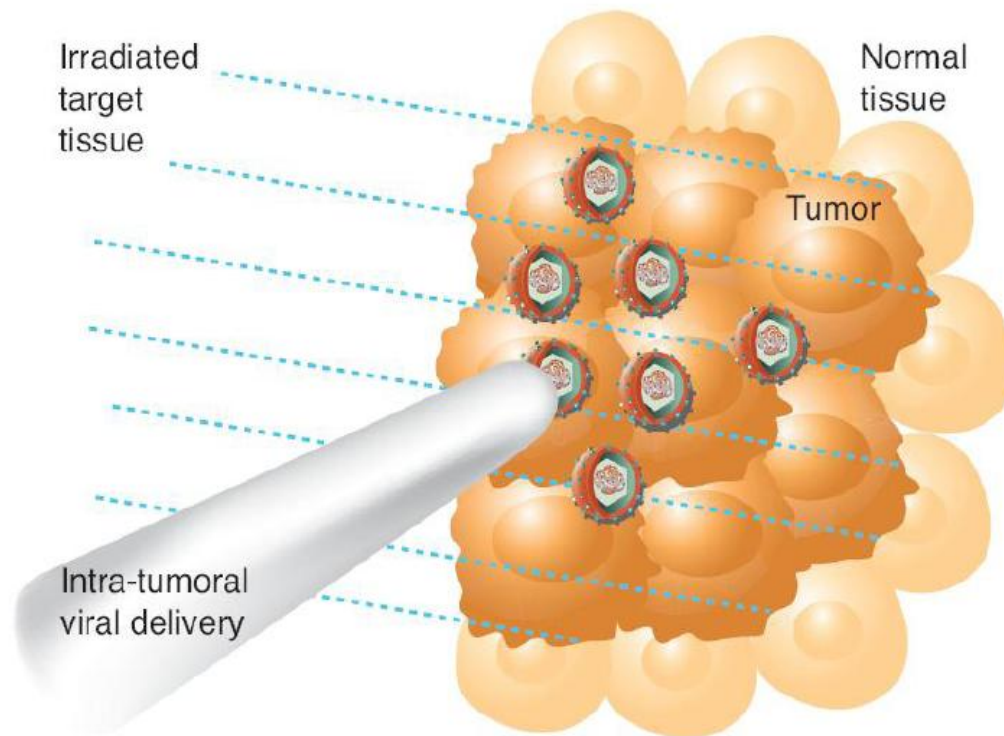
Fig. 11 Spatial interaction of oncolytic virotherapy and IR [80]
  IR and the intra-tumoral delivered OV interact in a loco-regional manner while leaving surrounding normal tissue unaffected. IR targets the tumor tissue and creates a potentially more conducive environment for the OV to replicate.

That spatial interaction between virus and IR should at least induce a local benefit simply of the additive effects of both modalities numerous times demonstrated for combination therapy including less risk for resistant clones to emerge. In the best case scenario IR and oncolytic virus might interact in a way that is beyond additive creating an environment more favorable for tumor destruction resulting in synergistic tumor control [80].

There is evidence that VACV and radiation interact as well [89, 90]. Studies conducted in the late 1990's showed that treatment of C6 rat glioma was improved when on oncolytic VACV, also derived from the Lister strain, was combined with radiation. In these sets of experiments, C6 tumors were subcutaneously implanted and radiation as well as oncolytic VACV was delivered in multiple doses locally to the tumor. Furthermore the authors analyzed a VACV construct expressing p53 since the C6 rat glioma has low detectable amounts of p53. Both viruses interacted well with radiation and tumor control was enhanced in combination groups when compared to animals treated with single modalities. However, here, as well as in the other studies analyzing oncolytic virotherapy in combination with radiation, the oncolytic virus was delivered by intra-tumoral injection.

1.7 Aims of this work

Glioblastoma multiforme represents the most aggressive form of malignant brain tumors and remains a therapeutically challenge. With concurrent chemo-radiotherapy the median survival for patients diagnosed with GBM is 12-14 months. Intense research in the field has lead to the testing of oncolytic viruses to improve tumor control and systemically delivered oncolytic vaccinia viruses have currently entered clinical trials.

The main goal of this work was to analyze how systemically administered oncolytic vaccinia virus could be combined with targeted ionizing radiation for therapeutic gain.

For this purpose animal models exhibiting subcutaneous (s.c.) or orthotopically implanted U-87 human glioma xenografts are generated to analyze interaction of systemically delivered oncolytic vaccinia viruses GLV-1h68 or LIVP 1.1.1. and ionizing radiation delivered focally to the tumor. Following systemic injection of VACV viral-encoded marker gene expression as well as viral colonization and distribution within tumors should be analyzed and compared for irradiated and non-irradiated xenografts. To further characterize the interaction a bilateral tumor model will be established where oncolytic vaccinia should be injected systemically and radiation is delivered specifically to the right flank tumor, while the left flank tumor remains shielded. Viral replication and tumor regression, after systemic injection, will be analyzed.

To further improve tumor control a different VACV construct, GLV-1h164, which expresses a single-chain antibody (scAB) to target VEGF will be analyzed in combination with fractionated IR to involve the tumor microenvironment and target angiogenesis. Since GBM was shown to be highly vascularized with intrinsic high levels of VEGF-A, targeting of this molecule by VACV should increase therapeutic efficacy. Effects of VEGF and VEGF inhibition on radio-response of endothelial cells will be analyzed. Volumetric tumor response to combination treatment will be determined in an s.c. U-87 glioma xenograft model. Furthermore, intra-tumoral levels of VEGF will be quantitated and effects of VEGF inhibition on vessel number in tumors will be established.

2   Material

2.1   Chemicals and enzymes

Chemical	Manufacturer
1 kb DNA Ladder	NEB
1,4-Diazabicyclo[2,2,2]octane (DABCO)	Sigma
3,3',5,5'-Tetramethylbenzidine (TMB) Liquid	Sigma
3M Vetbound Skin Adhesive	Centric Pets
4, 6-diamidino-2-phenylindole (DAPI)	Sigma
45% Glucose solution	Cellgro
Acetic acid ($C_2H_4O_2$)	Fisher
Agarose	BioRad
Agarose Low Melt	Fisher
Ampicillin	Sigma
Antibiotic-Antimycotic Solution	Cellgro
Antisedan (Altipamezole)	Pfitzer
Benzonase	Merck
Benzyl-coelenterazine	Nanolight
Blocker™ Casein in PBS	Pierce
Bovine serum albumin (BSA)	Sigma
Bovine plasma gamma globuline	BioRad
Burphrenophine	Butler
Carboxymethylcellulose (CMC)	MP
Coomassie brilliant blue G-250	Sigma
Crystal violet	Sigma
Dexmedetomidine	Pfitzer
Diaminoethanetetraacetic acid (EDTA)	Sigma

MATERIAL

Dulbecco's Modification of Eagle's Medium (DMEM)	Cellgro
Dimethyl sulfoxide (DMSO)	VWR
Dulbecco's Phosphate Buffered Saline (DPBS) 1x	Cellgro
EBM basal media	Lonza
EDTA-Trypsin	Cellgro
EGM SingleQuot Kit Suppl. & Growth Factors	Lonza
Eagles Minimum Essential Medium (EMEM)	Cellgro
Ethanol (p.a.)	Sigma
Ethidium bromide	Sigma
Evans Blue Dye	Sigma
Fetal bovine serum (FBS)	Cellgro
Formaldehyde	Fisher
Formalin	Fisher
G418 sulfate	Cellgro
Gelatine from porcine skin, type A	Sigma
Glycerol	Fisher
Glycine	BioRad
Goat serum	Sigma
Hematoxylin QS	Vector
HEPES buffer	Cellgro
Hoechst	Sigma
HyClone HyPure cell culture water	Fisher
Hydrochloric acid (HCl) 12M	VWR
Hydrogen peroxide (H_2O_2)	Sigma
Hypoxanthine	Sigma
Isoflorane	Explora

MATERIAL

Isopropyl alcohol	EMD
Kanamycin	Sigma
Ketamine (Kethesia)	Butler
Laemmli sample buffer 4x	BioRad
Magnesium chloride hexaanhydride (MgCl$_2$·6H$_2$O)	Sigma
Methanol	Sigma
Modified Eagle's medium (MEM)	Cellgro
Mowiol 4-88	Sigma
Mycophenolic acid (MPA)	Sigma
N-,N-Dimethylformamide ((CH$_3$)$_2$N(O)H)	Sigma
Non-essential amino acids (NEAA)	Cellgro
Nonidet P-40	Sigma
Nocodazole	Sigma
NuPAGE 10% Bis-Tris Gel	Invitrogen
NuPAGE 12% Bis-Tris Gel	Invitrogen
NuPAGE LDS sample buffer 4x	Invitrogen
NuPAGE MOPS running buffer 20x	Invitrogene
NuPAGE sample reducing agent 10x	Invitrogene
NuPAGE transfer buffer 20x	Invitrogene
Modified Mayer's Hematoxylin	R.-A. Scientific
Paraformaldehyde 16% solution (PFA)	EMS
Paraplast Tissue Embedding Medium	McCormick Scientific
Phalloidin-TRITC	Sigma
Phenylmethylsulfonyl fluoride (PMSF)	Sigma
Phosphate buffered saline tablets (PBS)	Sigma
Potassium chloride (KCl)	Fisher
Potassium ferricyanide (K$_3$Fe(CN)$_6$)	Sigma

MATERIAL

Potassium ferrocyanide ($K_4Fe(CN)_6 \cdot 3H_2O$)	Sigma
Precision Plus Protein Standards	BioRad
ProLong Gold Antifade Reagent	Invitrogen
Propidium iodide solution	Sigma
Protease inhibitor cocktail	Invitrogen
Recovery™ Cell Culture Freezing Medium	Life Technologies
RNAse Zap	Ambion
Roswell Park Memorial Institute medium (RPMI-1640)	Cellgro
Skim milk powder	BD
Sodium bicarbonate ($NaHCO_3$)	Cellgro
Sodium chloride (NaCl)	VWR
Sodium dodecyl sulfate (SDS)	Fisher
Sodium hydroxide (NaOH) 2N solution	Fisher
Sodium pyruvate ($C_3H_3NaO_3$) solution	Cellgro
Tris	Fisher
Triton X-100	Sigma
Trypan blue solution	Cellgro
Tween-20	BioRad
Vectorstain Elite ABC reagent	Vector Laboratories
Vector ImmPact DAB Peroxidase substrate	Vector Laboratories
VEGF-A (recombinant)	Sigma
X-GlcA	RPI
Xanthine	Merck
Xylazine	Lloyd Laboratories
Xylene Substitute	Sigma

MATERIAL

2.2   Buffers and solutions

Agarose histology buffer

0.25% Triton X-100

1 x PBS (pH 7.4)

Agarose histology blocking buffer

0.25% Triton X-100

5% Normal goat serum

1 x PBS (pH 7.4)

Citrate buffer

0.1 M Citric Acid

0.1 M Sodium Citrate

ddH_2O (pH 6)

CMC overlay medium

1.5% Carboxymethylcellulose

2% FBS

1% A/A

1 x DMEM medium

Crystal violet staining solution

1.3 g crystal violet

5% ethanol

30% formaldehyde (37%)

dd H_2O

RBM tissue homogenization buffer

50 mM TrisHCL

2 mM EDTA

1 tablet protease inhibitor complete mini

1x PBS (pH 7.4)

MATERIAL

VEGF ELISA wash buffer	0.05% Tween-20
	1x PBS (pH 7.2)
VEGF ELISA reagent diluent	1% bovine serum albumin
	1x PBS (pH 7.2) filtered 0.2 µm
Propidium Iodide solution	0.2 mg/ml DNAse free RNAse
	0.02 mg/ml propidium iodide
	0.1% (v/v) Triton X-100
	1x PBS (pH 7.4)

2.3   Cell lines and media

CV-1	African green monkey kidney fibroblast (ATCC)
	DMEM with 10% FBS
HUVEC	Human Umbilical Vein Endothelial Cells (Lonza)
	EBM basal medium with EGM SingleQuot Kit Suppl. & Growth Factors
T-98 G	Human glioblastoma multiforme (ATCC)
	EMEM with 10% FBS
U-87 MG	Human glioblastoma, astrocytoma (ATCC)
	DMEM with 10% FBS
U-118 MG	Human glioblastoma, astrocytoma (ATCC)
	DMEM with 10% FBS

MATERIAL

2.4 Kits

Kit	Manufacturer
ApoLive-Glo^{TM} Multiplex Assay	Promega
Cell Proliferation Kit II (XTT)	Roche
DC^{TM} Protein Assay	BioRad
DNAse-*free*™ DNase Treatment & Removal	Ambion
FLAG® Immunoprecipitation Kit	Sigma
Human VEGF DuoSet Elisa	R&D Systems
ImProm-II™ Reverse Transcription System	Promega
Mesa Green qPCR™ Mastermix Plus for SYBR® Assay	Eurogentec
RNEasy Mini Kit	QIAGEN
VECTASTAIN ABC Kit Rabbit IgG	Vector Laboratories

2.5 Synthetic oligonucleotides

Target	Sequence
Human GAPDH fwd	5'-ACAAGAGGAAGAGAGAGACC-3'
Human GAPDH rev	5'-GCACAGGGTACTTTATTGAT-3'
Human TK1 fwd	5'-CTGCTTAAAGCTTCCCTCTC-3'
Human TK1 rev	5'-AGAAACTCAGCAGTGAAAGC-3'

2.6 Antibodies

Primary antibody	Origin	Manufacturer
anti-A27L (CAKKIDVQTGRRPYE)	rabbit	Genscript
anti-mouse CD31	rat	BDPharmingen
anti-DDDDK	rabbit	Abcam
anti-γH2AX	mouse	Abcam

Secondary antibody	Origin	Manufacturer
anti-mouseAlexa-Fluor647	goat	Invitrogen
anti-rabbit-DyLight^{TM} 594	donkey	Jackson Immunoresearch
anti-rabbit-HRP	goat	BioRad
anti-rat-Alexa Fluor 594	donkey	Jackson Immunoresearch
anti-rabbit IgG	goat	Vector Laboratories

2.7 Recombinant vaccinia virus strains

All recombinant viruses used within this work have been constructed at Genelux Corporation, San Diego. GLV-1h68 is a genetically engineered VACV derived from the Lister strain (LIVP). It has been shown to locate, enter, replicate in and ultimately lyse cancer cells while sparing normal cells. GLV-1h68 was constructed by insertion of three expression cassettes, Renilla luciferase-Aequorea green fluorescent protein (RUC-GFP) fusion, β-galactosidase (LacZ), and β-glucuronidase (GusA) into the F14.5L, J2R (thymidine kinase) and A56R (hemagglutinin) loci of the LIVP genome of the LIVP strain [65]. The gene for the Ruc-GFP fusion protein is under control of a synthetic early/late promoter whereas the marker gene beta-galactosidase is under control of the p7.5 promoter. The transferrin receptor gene (*RTFR*) cDNA was inserted in the reverse orientation to vaccinia synthetic early/late promoter to serve as a negative control for a TFR-expressing recombinant virus. The third genetic insertion, β-glucuronidase was inserted under control of the p11 promoter.
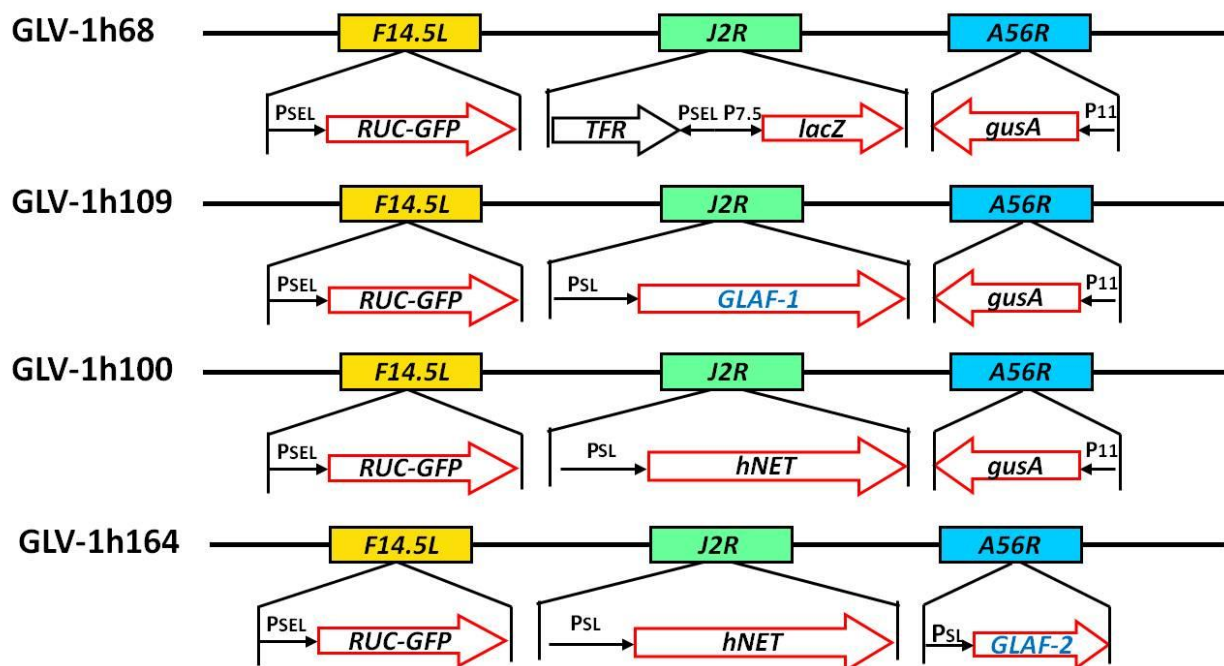
MATERIAL

Fig. 12 Schematic representation of engineered VACV used in this study
GLV-1h68 presents the 'parental' virus that is currently undergoing clinical testing (GL-ONC1 is clinical grade GLV-1h68). It has three gene insertions, namely RUC-GFP fusion, LacZ and GusA into the F14.5L, J2R and A56R loci, respectively, into the genome of the LIVP strain. GLV-1h109 is identical to GLV-1h68 with the difference that the gene for GLAF-1 is inserted into the J2R locus. GLV-1h100 is derived from GLV-1h68 as well and has the gene for hNET in the J2R locus. GLV-1h164 has in addition to hNET in the J2R locus the GLAF-2 gene in the A56R locus.

GLV-1h109 was engineered from GLV-1h68 with the insertion of GLAF-1, which encodes for a scAB targeting human and murine VEGF with a FLAG tag under control of the synthetic late promoter, into the J2R locus replacing the genes for lacZ and the inverted TFR gene. GLV-1h100 was also constructed form the GLV-1h68 backbone and has the hNET gene cloned into the J2R locus instead of GLAF-1 under control of the same promoter. GLV-1h100 represents the intermediate between GLV-1h68 and GLV-1h164 since GLV-1h164 was constructed using the GLV-1h100 backbone with the additional insertion of GLAF-2 under control of the synthetic late promoter. GLAF-2 also encodes for a single-chain antibody targeting human and murine VEGF, identical to GLAF-1, but without the FLAG tag.

Another VACV used in this work is LIVP 1.1.1 which represents a less virulent wild-type isolate of the LIVP strain. LIVP 1.1.1 has a naturally occurring disruption in the TK gene locus.

2.8   Laboratory animals

Animal studies were carried out with male athymic nude FoxN1 mice purchased from Harlan. The mice exhibit a non-functional rudimentary thymus weakening the immune system due to a lack of T-cells. While the innate part of the immune response remains functional, mice are lacking an adaptive part of the immune system. This condition enables the growth of species different xenografts such as human tumors. In addition to this immune impairment, the mice exhibit an autosomal recessive mutation in chromosome 11 inducing the hairless phenotype which facilitates observation of treatment effects on tumor xenografts grown in these mice.

Mice were cared for in accordance with approved protocols by the Institutional Animal Care and Use Committee of LAB Research International, Inc. and Explora Biolabs (San Diego Science Center).

2.9   Laboratory equipment and other materials

Equipment	Manufacturer
5-0 Coated Vicryl Sutur	Ethicon
Accu Pro X-ray Measurement	Rad Cal
Amicon Ultra-15 Centrifugal Filter Unit 10 kDA cut-off	Millipore
Argus-100 Low Light Imaging System	Hamamatsu
Balance PL1501-S	Mettler-Toledo
Biosafety cabinet	The Baker Company
Carestream Imaging System	Carestream
Cell culture cluster 6-, 24- and 96- well Costar	Corning
Cell culture flasks	Corning
Cell Lab Quanta SC Flow Cytometer	Beckman Coulter
Cell scraper	Corning
Centrifuge Centra CL2	Thermo Scientific
Centrifuge Micro CL 21	Thermo Scientific
Centrifuge Micro 1816	VWR
Centrifuge Sorvall RC 6 Plus	Thermo Scientific

MATERIAL

Centrifuge Sorvall Legend RT	Thermo Scientific
Combitips Plus 1, 2.5, 5 and 25 ml	Eppendorf
Cryotubes 2 ml	Nalgene
CK30 culture microscope	Olympus
Digital caliper	VWR
Digital dry bath incubator	Boekel Scientific
Dish 100 mm	Fisher Scientific
Drill (0.8 mm)	Robos Surgical Instruments
Embedding Mold TISSUE-TEK®	IMEB Inc
Falcon 15 and 50 ml tubes	BD
FireWire DFC/IC monochrome CCD camera	Leica
Hamilton Syringe	Chromtech Inc.
Havels stainless steel surgical scalpel size 15	Braintree Scientific
Heater	VWR
Hotplate stirrer 375	VWR
Hybond-P PVDF membrane	Amersham Biosciences
Incubator	Forma Scientific
Incubator HERA Cell 150	Thermo Electron
Insulin syringe U-100 27G, 29G	BD
IX71 inverted fluorescence microscope	Olympus
MagNA Lyser	Roche
MagNA Lyser green beads	Roche
MicroAmp® Fast Optical 96-well reaction plate	Applied Biosystems
Microfuge tubes easy open cap 1.5 ml	Saarstedt
Microplate reader SpectraMax MS	Molecular Devices
Microscope cover glass	Fisher Scientific
Microslides Premium Superfrost®	VWR

MATERIAL

Microtome Leica RM 2125	IMEB Inc.
Microwave Carousel	Sharp
Mini-Sub® Cell GT	BioRad
Multipipette	Eppendorf
MZ 16 FA stereo fluorescence microscope	Leica
Nikon Eclipse 6600 microscope	Nikon
Parafilm laboratory film	Pechiney Plastic Packaging
pH Meter Accumet AR15	Fisher Scientific
Photometer Biomate3	Thermo Spectronic
Pipet Aid	Drummond
Pipet Tips 10, 200, 300 and 1000 µl	VWR
Pipettes 20, 200 and 1000 µl	Rainin
Pipettes 5, 10 and 25 ml	Corning
Radsource RS2000 Irradiator	Radsource
Repeater® stream pipette	Eppendorf
Rocking platform	VWR
Sonifier 450	Branson
Space Drape, 4"x5" mouse pouch	Braintree Scientific
StepOnePlus Real-Time PCR System	Applied Biosystems
Stereotactic frame	David Kopf Instruments
Stereo fluorescence macroimaging system	Lighttools Research
Sterile disposable scalpel	Sklar Instruments
Surflo Winged Infusion Set	Terumo
Syringe 1, 30, 60 ml	BD
Syringe 20G	BD
Syringe Driven Filter Unit Millex®-VV PVDF 0.2 µm	Millipore
Tissue culture dish 60 mm	BD
Tissue Embedding Center	Reichert-Jung

Tissue Processing/Embedding Cassettes with Lid	Simport
Titer plate shaker	Thermo Scientific
Ultracell Surgical Sponge	Braintree Scientific
Illumatool Tunable Lighting System	Lightools Research
Vibratome VT 1200S	Leica
Vortex VX100	Labnet
Water bath	Boekel Scientific
Water bath Isotemp202	Fisher Scientific
X Cell Sure Lock™	Invitrogen

2.10 Statistical analysis

Statistical analysis of data generated from animal experiments involving more than one treatment, here IR and VACV, was performed with SPSS, version 11 (SPSS, Inc.). One-way analysis of variance (ANOVA) was used to compare the tumor volumes among different treatment groups at each time point. The differences between the groups were analyzed with Bonferroni tests when the ANOVA showed an overall significance at a time point.

To determine significance between only two treatment groups a two-tailed unpaired t-test was used (Excel 2007 for Windows).

For orthotopic mouse studies differences in survival were analyzed using Log-rank method.

3   Methods

3.1   Cell biological methods

3.1.1 Analysis of viral replication

Standard viral plaque assays were used to quantify viral replication in three human glioma cell lines (U-87, U-118 and T-98). Cells were seeded into 6-well plates and after 24 h in culture infected with GLV-1h68 at a multiplicity of infection (MOI) of 0.01. U-87 cells were also infected with LIVP 1.1.1 at the same MOI to analyze differences in cell sensitivity to both oncolytic viruses. Infection was carried out for 1 h at 37 °C in cell medium containing 2% FBS. The amount of input virus needed was calculated by the following formula:

$$Input\ Virus = \frac{Number\ of\ Wells\ x\ MOI\ x\ Cell\ Count/\ Well}{Viral\ Titer}$$

Virus containing medium was replaced by fresh growth medium (both infectious medium and fresh growth medium are supplemented with antibiotic antimycotic solution 100 U/ml penicillin G, 250 ng/ml amphotericin B and 100 units/ml streptomycin). Infected cells were harvested in triplicate at 24, 48 and 72 hours post infection (hpi). To release viral particles from cells all samples underwent three freeze and thaw cycles followed by three rounds of 30 s sonication. To determine viral titers a dilution series of each sample was made and used to infect a CV-1 monolayer. Each sample was plated in triplicate. One hour after infection, 1 ml of CMC overlay media is added to each well to limit viral spread to adjacent cells. Consequently, an area of lysed cells, called a "plaque" is produced by each infectious particle. After 48 hours of incubation all wells are stained with crystal violet which stains remaining viable cells and allows counting of all plaques produced. Viral titer per ml is calculated by the number of plaques divided by the dilution and the volume of used for infection. Viral titers are expressed as plaque forming units (pfu)/ml, pfu/10^6 cells or fold increase in viral particles.

3.1.2 Irradiation of cells in culture or irradiation of VACV

All irradiation was carried out using a Radsource RS 2000 x-ray biological irradiator for small animals and cell irradiation. The radiator is equipped with an adjustable shelf to regulate radiation dose. As can be seen in Fig. 13 the different shelf levels exhibit different dose rates. The closer the shelf is placed to the x-ray source the higher is the radiation dose rate and at the same time the smaller is the field that receives irradiation. All irradiation carried

out in this work is done at shelf level 3. Since the radiation is delivered at a dose rate with constant value for each shelf level the required dose can be adjusted by the time the radiation is delivered.
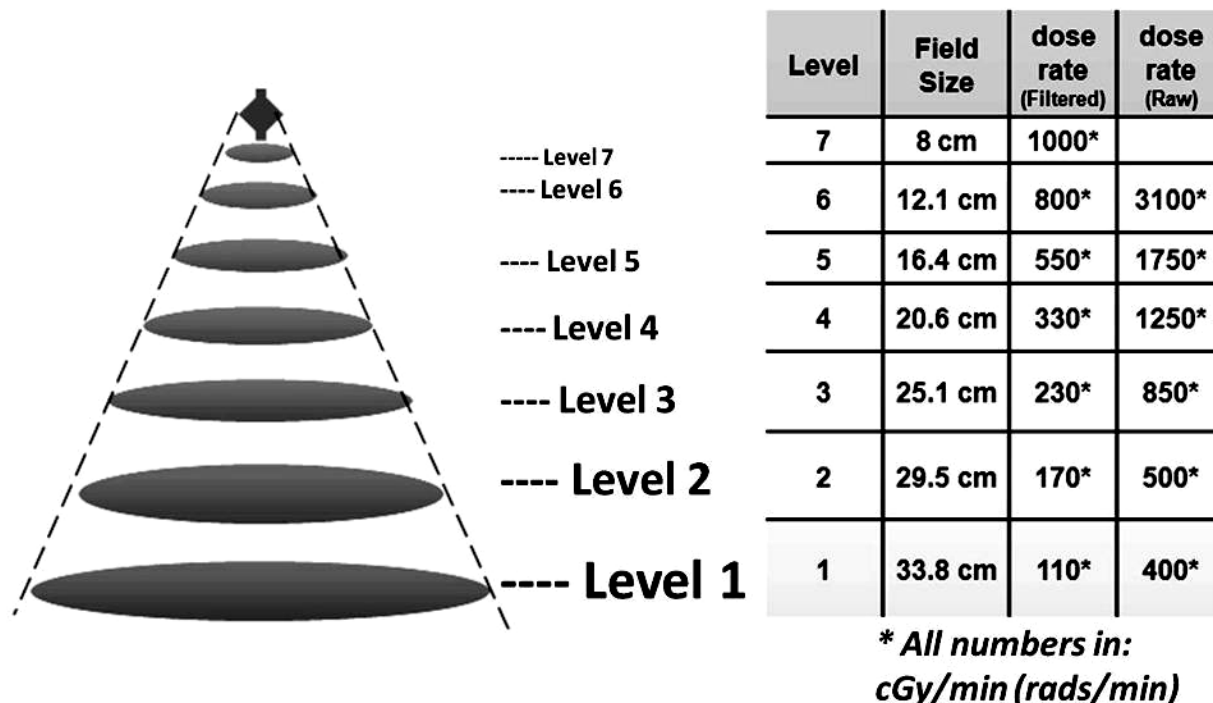
Level	Field Size	dose rate (Filtered)	dose rate (Raw)
7	8 cm	1000*	
6	12.1 cm	800*	3100*
5	16.4 cm	550*	1750*
4	20.6 cm	330*	1250*
3	25.1 cm	230*	850*
2	29.5 cm	170*	500*
1	33.8 cm	110*	400*

* All numbers in: cGy/min (rads/min)

Fig. 13 Regulation of radiation doses by adjustable shelves
The higher up the shelf in the radiator the higher the dose rate per minute and the smaller the field that is exposed.

Cells that undergo radiation treatment are placed into shelf level 3 of the radiator and irradiated with the appropriate dose. Non-irradiated control cells are placed outside of the incubator for the time of the irradiation.

For irradiation of virus a 10^{-1} dilution was made in CV-1 media containing 2% FBS and transferred onto a 24-well plate. Three wells per plate were radiated with increasing doses of IR while control virus was kept on ice for the time of irradiation. Following irradiation, all samples were sonicated for 30 s three times and a dilution series was made to be titered on CV-1 monolayers equivalent to the determination of viral concentration in samples for replication assay as described previously. The viral pfu is determined by following equation:

$$Virus\ pfu/ml = Counted\ Plaques \times Dilution/Volume\ of\ Infection$$

3.1.3 Analysis of cell cycle

Human U-87 glioma cells were grown in 60 mm dishes and after 24 h in cell culture assigned to a treatment group of either control, irradiation alone, virus alone or a combination of both. In irradiated cells, a single fraction of 6 Gy was delivered to the cells. In virus infected groups, cells were infected with GLV-1h68 at an MOI of 1 6 h after irradiation. Twenty four hours after virus infection, cells were trypsinized and centrifuged at 1100 g for 10 min. The pellet was resuspended in ice-cold phosphate buffered saline (PBS) and the cell suspension was added slowly to 70% ethanol (EtOH). Cells were repeatedly washed with ice-cold PBS. Subsequently cells were treated with 0.2 mg/ml DNAse-free RNAse A and stained with 0.02 mg/ml propidium iodide in 0.1% (v/v) Triton X-100 in PBS. Samples were analyzed by flow cytometry within 24 hours.

3.1.4 Immunofluorescence γ-H2AX staining in irradiated and non-irradiated virus-infected cells

Human U-87 glioma cells were grown on glass microscope cover slips. After 24 h in cell culture, cells were mock infected or infected at an MOI of 5 with GLV-1h68 or LIVP 1.1.1, respectively. One set of cells was irradiated with 6 Gy 1 h after virus infection. One, 6 and 24 h after irradiation cells were fixed in duplicate with 4% paraformaldeyde (PFA) in PBS for 15 min. Cells were permeabilized with PBS containing 0.25% Triton X-100 (PBST) and subsequently blocked with 1% Bovine serum albumin (BSA) in PBST. A mouse-monoclonal antibody against γ-H2AX in blocking solution was added to the cells to stain DNA double-strand breaks. Detection of the primary antibody was carried out with an Alexa-Fluor647-labeled goat anti-mouse secondary antibody. Cells were counterstained with 4, 6-diamidino-2-phenylindole (DAPI) and mounted onto microscope slides. All samples were analyzed on a Nikon Eclipse 6600 microscope (magnification 60x). Images were captured using the Diagnostics Instruments model 24.4 camera and image processing software (Metamorph 7.7) with band pass filter sets allowing visualization of the Alexa647 dye for the γ-H2AX identification and DAPI as the nuclear counterstain. After 2D convolution was applied to the pictures to increase contrast, γ-H2AX foci were counted. To calculate foci per cell the number of cells per image was determined using the DAPI staining. For each treatment condition, γ-H2AX foci were scored from 75 to 100 cells.

3.1.5 Analysis of RNA expression in irradiated and non-irradiated glioma cells

Human U87 glioma cells were grown in 6-well plates. After 24 h in culture cells were irradiated at a dose of 6 Gy. At 2, 6, 12 and 24 h post irradiation cellular RNA was isolated using the RNeasy Mini Kit followed by DNase treatment to eliminate interfering DNA using DNA-free Kit. RNA concentration was determined and 0.5 µg of RNA of each sample was converted to cDNA by ImProm-II™ Reverse Transcription System. All cDNA samples were analyzed by semi quantitative PCR using primers for gene transcription of thymidine kinase (TK). Semi-quantitative PCR was performed using the MESA GREEN qPCR MasterMix for SYBR®Assay. Human GAPDH was used for the internal control and all values were normalized in regard to TK-1 expression of non irradiated cells by the delta delta C_T method.

3.1.6 Quantitation of VEGF expression in irradiated and non-irradiated glioma cells

U-87 glioma cells were seeded into 6-well plates at low confluency. Cells remained non-irradiated or were radiated with 10 and 20 Gy, respectively. VEGF levels in supernatants were analyzed 24, 48 and 72 hours after irradiation with a VEGF Elisa. Cell number per well was determined by trypzinization and counting of cells and VEGF concentration was plotted as pg VEGF per 10^6 cells.

3.1.7 Purification of GLAF-1 from VACV infected cells

Two flasks of confluent CV-1 cells were infected at an MOI of 1 with GLV-1h109 expressing GLAF-1 under the synthetic late promoter in 15 ml of CV-1 media containing 2% FBS. Two days after infection the virus and GLAF-1 containing medium was filtered (0.2 µm) to remove all viral particles. To concentrate the media from 15 ml to 1 ml, the suspension was loaded on Amicon Ultra-15 columns with a molecular mass cut off of 10 kilo kDa. The samples were centrifuged using a rotating swing bucket 4000 rounds per minute (rpm) for 15 min. Functional GLAF-1 was purified from the concentrate with a FLAG Immunoprecipitation kit which allows immunoprecipitation and elution of an active FLAG-tagged protein. Purified GLAF-1 was analyzed for the correct molecular weight on a Coomassie stained gel and protein concentration was determined using BioRad DC™ Protein Assay kit using a protein standard created from bovine plasma gamma globuline.

3.1.8 Manipulation of VEGF levels on endothelial cells and tumor cells

Human endothelial cells (HUVECs) and human lung adenocarcinoma cells (A549) were seeded into 96-well dishes. One set of cells was treated with increasing concentrations of recombinant VEGF (0, 1, 5, 10 and 50 ng/ml) and the other set with increasing concentrations of purified GLAF-1 protein (0, 10, 50, 100 and 200 ng/ml). All cells were either pretreated with 10 ng/ml GLAF-1 or 100 ng/ml VEGF in HUVEC medium containing all supplements. Four h after cell treatment, cells were irradiated with a dose of 10 Gy. Six days after irradiation cell viability was assessed using a XTT cell viability assay and survival was plotted in relation to untreated control cells that did not receive any radiation.

3.2   Animal studies

3.2.1 Subcutaneous and orthotopic tumor cell implantation

Animals used within this work were five- to six-week old male Hsd:athymic Nude-*Foxn1^{nu}* mice purchased from Harlan. For subcutaneous tumor xenografts, 5×10^6 U-87 glioma cells in 0.1 ml PBS were injected with a 27G needle into the right or bilateral flanks. Treatment was initiated when tumors reached a size of 200–300 mm^3. To evaluate therapeutic efficacy, tumor growth was recorded twice a week in three dimensions using digital calipers and calculated as follows:

$$Tumor\ Volume = 0.5x\ (Height - 5)x\ Length\ x\ Width$$

Tumor volume is shown as fractional tumor volume (FTV) which is the tumor volume at each given time point divided by tumor volume at initiation of treatment.

To monitor general well being of the mice, body weights of all mice is recorded once a week. To exclude the tumor mass net body weight is defined as:

$$Net\ Bodyweight\ (NBW) = Bodyweight - Tumor\ Volume/1000$$

Similar to tumor volume, net body weight is expressed as fractional net body weight meaning net body weight at one particular time point divided by the initial net bodyweight at treatment initiation.

For intracranial glioma xenografts, athymic nude mice were stereotactically implanted with 1×10^5 U-87 cells (in 2 µl U-87 media). Mice were anesthetized with a mixture of Ketamin (100 mg/kg) and Dexmedetomidine (0.25 mg/kg) and fixed using a small animal stereotactic frame. A small incision was made into the skin of the skull and cells were inoculated into the right frontal lobe (1 mm anterior und 2 mm lateral to bregma at 2.5 mm depth) using a Hamilton syringe and a drill (size 0.8 mm) to form a hole in the skull. The incision was

closed with sutures and tissue adhesive. Mice were recovered with antisedan (Altipamezole) (0.5 mg/kg) and analgesia (Burprenophine) (0.1 mg/kg) was administered for 3 consecutive days. Bodyweight of mice was recorded twice a week and expressed as fractional net body weight in regard to initial body weight.

3.2.2 Systemic administration of oncolytic VACV

Oncolytic VACV was administered by retro-orbital inoculation. Each virus used within this work was sonicated for 1 min and diluted to a final concentration of 2×10^6 pfu in 0.1 ml PBS. Mice were anesthetized using isofluorane and the virus was administered into the retrobular sinus with a 29G syringe. To confirm virus concentration, a small aliquot of injected virus was titrated. A dilution series is made in CV-1 media containing 2% FBS and a standard plaque assay is carried out on CV-1 monolayers as described previously.

3.2.3 Irradiation of animals

All irradiation of animals was carried out using a Radsource RS2000 irradiator, Fig. 14A. For irradiation, mice were anesthetized by intraperitoneal (i.p) injection of a mixture of Ketamine (3 mg/mouse) and Xylazine (0.2 mg/mouse). The entire body was shielded with lead except for the tumor bearing hind limb blocking 95% of the given dose under the lead shield as determined by RadCal device, see Fig. 14B. For mice with bilateral flank tumors, only the tumor on the right flank was exposed to IR. A single dose of 6 Gy was delivered locally to the tumor bearing hindlimb either one day prior (day -1) or one day after (day +1) viral injection. In studies with fractionated radiation regimens two fractions of 3.5 Gy were administered at day -1 and day +1 or four 4 Gy fractions at days -1, +1, +6 and +8 in respect to viral administration on day 0. In experiments analyzing the toxicity of VACV in combination with IR, non- tumor bearing mice were restrained on their backs, the lower body was shielded with lead and their whole upper body was irradiated with multiple doses of 2 Gy at day -2, -1, +1 and +2 in respect to viral administration.
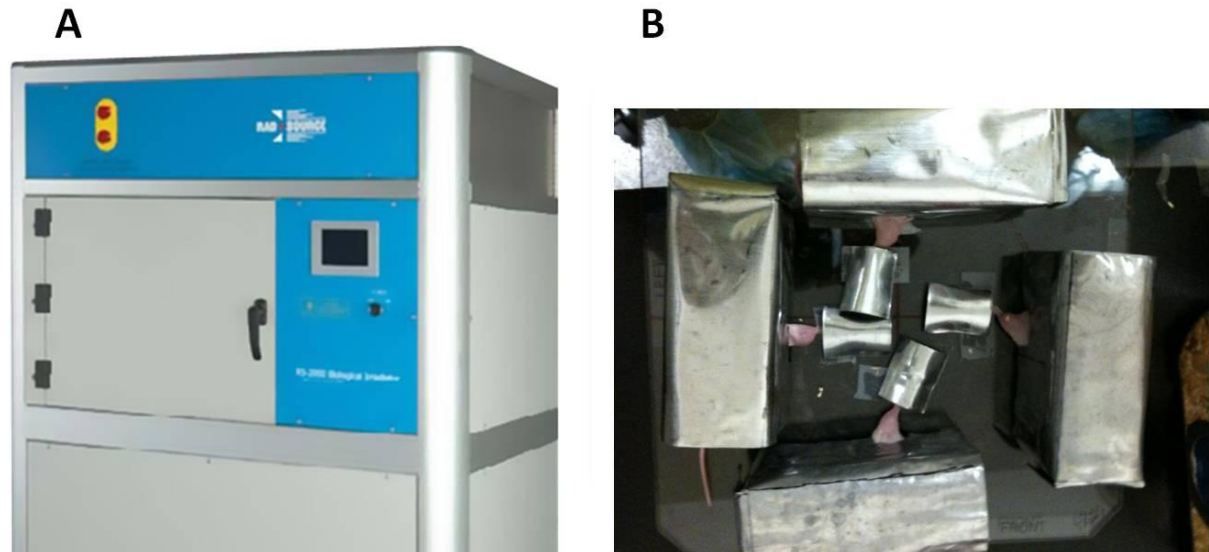
A **B**

Fig. 14 Irradiation of mice
    A) All irradiation of cells and animals is carried out using a Radsource RS200 irradiator. **B)** In irradiated mice only the tumor bearing hind limp mps exposed to IR with the remainder of the mouse shielded by lead.

3.2.4 Marker gene expression in tumors

All VACV used in this work, except LIVP 1.1.1, express the RUC-GFP protein. Virus encoded GFP expression within tumors was monitored under UV light using a Stereo-Fluorescence macroimaging system. GFP expression was scored once a week by observation using a four point system: 0) no GFP signal, 1) one GFP spot, 2) two or three local GFP spots, 3) >3 GFP spots and 4) diffuse GFP signal. Pictures of individual mice for bright field and GFP were taken at day 7 dpi. For GLV-1h68-encoded luciferase expression, 5 µl coelenterazine (0.5 µg/µl) in 95 µl PBS was administered by tail vain injection. Mice were warmed on heating pads to facilitate injection into the tail vain. Immediately after coelenterazine injection, mice were anesthetized using a mixture of Ketamine (3 mg/mouse) and Xylazine (0.2 mg/mouse) and photon emission was recorded for 1 min using the Argus100 Low Light Imaging System.

3.2.5 Tumor homogenates for viral titers in tumor xenografts, protein detection and immune-related profiling

To generate tumor homogenates, tumors were excised and combined with two volumes of RBM tissue homogenization buffer supplemented with one Complete Protease Inhibitor

Cocktail Tablets per 50 ml buffer. Tumors were homogenized using MagNA Lyser at a speed of 6500 for 30 s (three times). After three freeze and thaw cycles, the supernatants were collected by centrifugation at 6500 rpm for 5 min.

Tumor homogenates were used to quantify viral distribution in tumors of treatment groups at different days post viral injection. Viral titers were determined in duplicate by standard plaque assay on CV-1 monolayer. Tumor viral load is expressed as pfu per gram (g) tumor.

To analyze VEGF expression in tumor homogenates at day 3, day 7 and day 14, the total protein concentration in each sample was determined by BioRad DC™ Protein Assay kit using a standard created from bovine plasma gamma globuline. Quantitative analysis of VEGF levels in tumor samples was carried out with a VEGF ELISA according to manufacturer's instructions. VEGF levels were expressed as percent of total protein.

In addition, tumor homogenates, generated as described above, for different treatments (n=2 per group) on day 7 were analyzed for immune-related protein antigen profiling by Multi-Analyte Profiles (Rules Based Medicine) using antibody-linked beads. Results were normalized based on total protein concentration and cut off was set at minimum 1.5 fold increase in treated samples compared to control.

3.2.6 Immunohistochemical staining for VACV

Vaccinia virus staining in tumors of individual groups was performed 7 and 10 days post viral injection. Tumors were excised and fixed with 10% neutral buffered formalin over night. The following day tumors were dehydrated in increasing concentrations of dehydration alcohol and subsequently embedded in paraffin. The detailed protocols follows, each step is carried out for 1h:

Dehydration:

1. 0.9% NaCl
2. 30% EtOH in 0.9% NaCl
3. 50% EtOH in 0.9% NaCl
4. 70% EtOH in ddH$_2$O
5. 90% EtOH in ddH$_2$O
6. 100% EtOH
7. 100% EtOH

Embedding in paraffin:

1. 100% ethanol, at room temperature
2. EtOH/xylene 1:1, at room temperature
3. Xylene, at room temperature
4. Xylene/wax, at 58°C
5. Paraffin, three times at 58°C

METHODS

Following infiltration, tissue is embedded in small paraffin blocks and embedded tumors were sectioned at 5 µm thickness and mounted onto object slides. Sections were stained for the presence of VACV-encoded late protein A27L. Prior to staining individual sections were rehydrated and antigen retrieval was performed with citrate buffer at pH 6. The tissue was blocked with normal goat serum and treated with hydrogen peroxidase (H_2O_2) to block endogenous peroxidase activity. Samples were incubated with an anti-A27L antibody custom-made against a VACV synthetic peptide. Detection of the primary antibody was done using a goat anti-rabbit IgG as a secondary antibody. The secondary antibody was detected with Vectorstain Elite ABC reagent and Vector ImmPact DAB Peroxidase substrate. All sections were counterstained with hematoxylin and examined with low magnification (2x) on a Nikon Eclipse 6600 microscope. Images were taken using the Diagnostics Instruments model 24.4 camera and Metamorph v. 7.7 software.

3.2.7 Analysis of vessel numbers in agarose embedded tumor sections

U-87 glioma xenografts were grown subcutaneously as described previously. Mice were either mock-infected or injected with GLV-1h68 or GLV-1h164, respectively. Irradiated mice received four fractions of 4 Gy at days -1, +1, +6 and +8 with respect to viral delivery on day 0. Mice were sacrificed on day 14 after viral injection, and tumors were excised and snap frozen in liquid N_2. Tumors were then fixed in 4% PFA in PBS over night and embedded in 5% low-melt agarose in PBS. One hundred µm sections of embedded tumors were cut using a VT1200S vibratome. Sections were subsequently permeabilized in PBS containing 0.25 % Triton-X 100 and 5 % normal goat serum and stained with a rat α-mouse CD31 antibody. The antibody was detected using an Alexa-Fluor594 labeled donkey α-rat secondary antibody. Strength of GFP expression was used as an indicator for viral distribution within the tumor. Images of fluorescent-labeled tumor sections were examined using a Leica MZ 16 FA Stereo-Fluorescence microscope equipped with a FireWire DFC/IC monochrome CCD camera. Digital images were processed with GIMP2 (freeware) and merged to yield pseudo-colored images. To quantitate vessel numbers, 4 pictures at higher magnification were taken and a grid was overlaid on each image using ImageJ (freeware). All vessels crossing the grid lines were counted in four pictures of four slides of each tumor.

3.2.8 Assessment of tumor vessel permeability in non-irradiated and irradiated glioma xenografts

Tumor vessel permeability was analyzed using an Evans Blue Dye assay. U-87 glioma xenografts were grown s.c. as described above. Irradiated tumor xenografts received a dose of 6 Gy focally to the tumor. Twenty-four hours after irradiation, similar to virus administration in other studies, mice were injected with 0.1 ml of 1.5% Evans Blue dye in PBS via retro-orbital inoculation. The dye was allowed to circulate for 45 min before the mouse was sacrificed. The chest was opened and all mice were intra-cardial perfused with 20 ml PBS to flush all remaining dye from the vessels. Following perfusion, tumors and spleens were harvested and placed in 1 ml of N-, N-Dimethylformamide per 0.1 g tissue. Dye extraction was performed at 55 °C for 72 h and absorbance was quantified at 620 nm. Tumor measurements were normalized to dye extracted from the spleen of the same mouse.

4   Results

4.1   Combining oncolytic VACV with ionizing radiation

In initial experiments we analyzed how IR might influence oncolytic VACV in terms of replication, specificity as well as toxicity.   Furthermore we delivered increasing doses of radiation to the virus to evaluate possible IR mediated damage to VACV.

4.1.1 IR does not damage VACV at clinically relevant doses

Since the primary target for IR is DNA and VACV has a double-stranded DNA genome, we first analyzed the possibility of IR damaging the virus and inhibiting VACV replication.   Here, virus was diluted in PBS and radiated on ice with increasing doses of IR.   Standard viral plaque assay on CV-1 cells was carried out to determine viral titers in irradiated and non-irradiated VACV samples, Fig. 15.
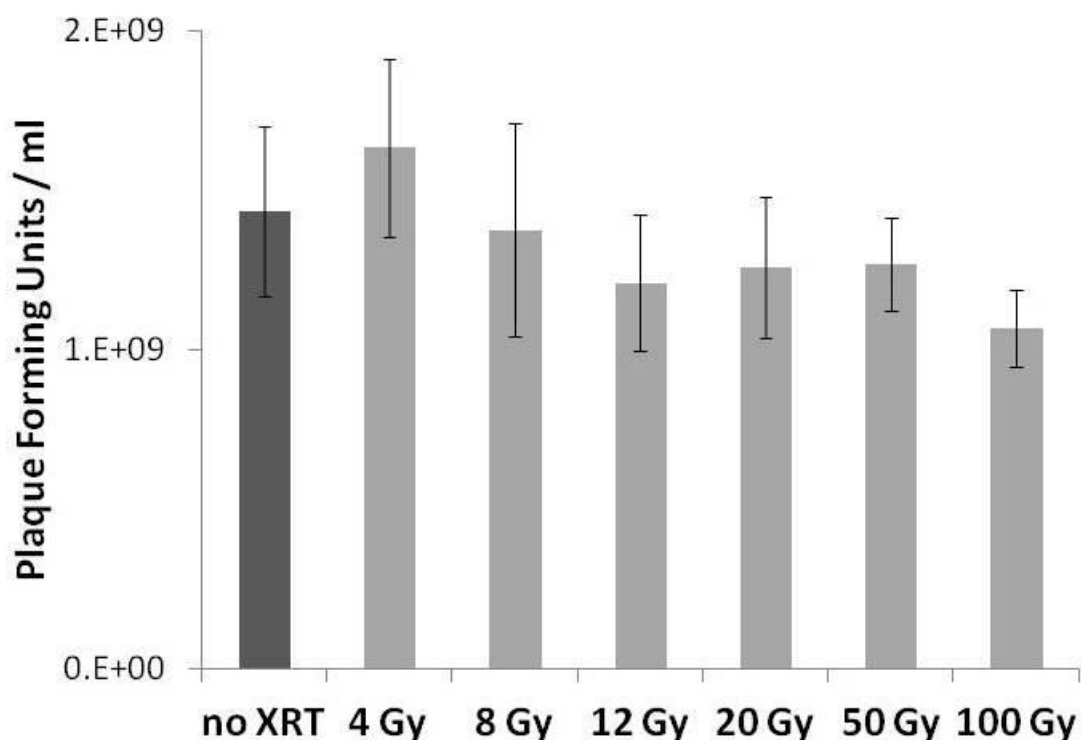

Fig. 15 Viral titers after increasing doses of IR
   GLV-1h68 in PBS was irradiated with increasing doses of radiation. Standard plaque assay was carried out to determine viral titers (pfu/ml) immediately after irradiation.

RESULTS

Table 1 shows how viral titers were affected by increasing doses of irradiation. Viral titers remained constant up to doses of 50 Gy. The samples that received a single dose of 100 Gy showed a minimal reduction of infectious viral particles from 1.4×10^9 to 1.1×10^9 pfu/ml. Since the highest IR dose we used within this work in combination with VACV was 6 Gy, there is absolutely no danger of damaging the virus by IR.

Table 1. *Viral Titers (pfu/ml) after increasing doses of IR*

	No XRT	4 Gy	8 Gy	12 Gy	20 Gy	50 Gy	100 Gy
Viral Titer (pfu/ml)	1.4×10^9	1.6×10^9	1.4×10^9	1.2×10^9	1.3×10^9	1.3×10^9	1.1×10^9
STDEV	2.7×10^8	2.8×10^8	3.3×10^8	2.1×10^8	2.2×10^8	1.5×10^8	1.2×10^8

4.1.2 IR has no influence of VACV replication

In the following study we tested how IR affected viral replication in cell culture. A major concern was that IR might inhibit viral replication in tumor cells, which might compromise oncolytic VACV efficacy in the in vivo setting. The alternative scenario would be that delivering IR to cells increases viral replication. To analyze whether different IR delivery schedules in regard to time of viral infection have an influence on replication behavior, we infected U-87 cells with an oncolytic VACV and delivered small doses of IR to different time points prior to and after viral infection. Cells were infected with GLV-1h68 at an MOI of 0.01 and 5 Gy IR was delivered 12 h prior as well as 2, 8 and 20 h post irradiation. Samples were harvested in triplicate and standard viral plaque assay was carried out to determine viral titers for all treatment groups.
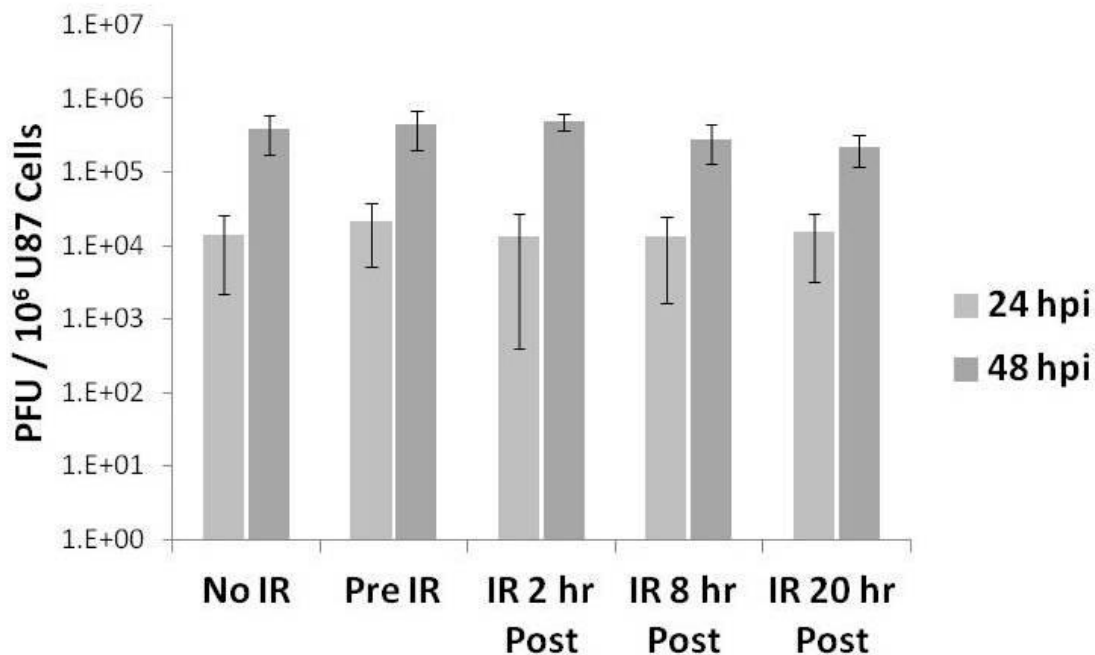
Fig. 16 Influence of different IR schedules on VACV replication.
U-87 cells were grown in 6-well dishes and infected with GLV-1h68 at an MOI of 0.01. Cells were irradiated at different time points either before or after viral infection with a dose of 5 Gy. Viral titers were determined 24 and 48 hpi on CV-1 monolayer and are shown as PFU/ 10^6 cells.

In this experimental model, we did not detect any differences in number of viral particles recovered from irradiated versus non-irradiated infected U-87 cells, regardless of the timing of IR delivery in relation to VACV infection, Fig. 16. Viral titers were comparable for all treatment groups at both analyzed time points. This shows that viral replication is not affected by low doses of IR in cell culture.

4.1.3 IR does not increase VACV toxicity to healthy tissue

The attenuated triple mutant oncolytic VACV GLV-1h68 exhibits a remarkable safety profile as reported in previous studies [66]. Upon intravenous injection, GLV-1h68 specifically targets the tumor while sparing surrounding normal tissue. Such high tumor specificity results in only minimal colonization of normal body organs. To analyze whether combining viral treatment with irradiation changed the safety profile of GLV-1h68, we conducted a study analyzing viral distribution in healthy organs. One group of mice was treated with focal irradiation at a dose of 2 Gy on five consecutive days given to the upper part of the body. Mice were anesthetized and restrained lying on their backs. The lower part of the body, below the chest, was shielded with lead to block 95% of the given dose. GLV-1h68, at a dose of $2x10^6$ pfu, was administered at day 3 intravenously through retro-orbital injection. The other group of mice received only GLV-1h68 without irradiation of tissue. Control mice did not receive any treatment. Seven and 14 days post systemic virally injected mice were

sacrificed and brain, liver, lungs, spleen and also tissue of the irradiated neck area were excised, homogenized and analyzed for viral colonization. No enhanced viral distribution was observed in tissues after irradiation. In fact, only one mouse that received GLV-1h68-treatment alone exhibited viral particles in the brain at day 7, and at a very low dose of 5.7 x 10^1 pfu per total brain. In all other mice no viral colonization of organs was detectable regardless if mice were treated with multiple doses of irradiation or not. In summary, we showed that systemic injection of GLV-1h68 in non tumor xenograft-bearing mice does not induce viral colonization of healthy organs. In addition, we showed that multiple doses of irradiation given to non-transformed tissue do not alter viral tropism. Therefore, combining GLV-1h68-treatment with irradiation has no detrimental effect on the safety of the virus.

4.2 Therapeutic potential of combining systemic GLV-1h68 and focal IR in a murine model of human glioma

4.2.1 Replication of GLV-1h68 in three different glioma lines

Initial experiments were carried out in cell culture to determine a suitable cell line for further animal studies. Ideally, we were looking for a glioma line that is not that efficiently infected by oncolytic VACV alone. If monotherapy with virus only is efficacious it would be difficult to demonstrate any further treatment improvement by adding a second anti-tumor therapy. Three different human glioma lines, T-98, U-87 and U-118, were seeded into 6-well plates and infected with GLV-1h68 at an MOI of 0.01. Cells were harvested at 24, 48 and 72 hpi and viral particle load was measured using standard plaque assay on CV-1 cells. Fig. 17 shows the replication efficiency of GLV-1h68 in these three tested glioma lines.
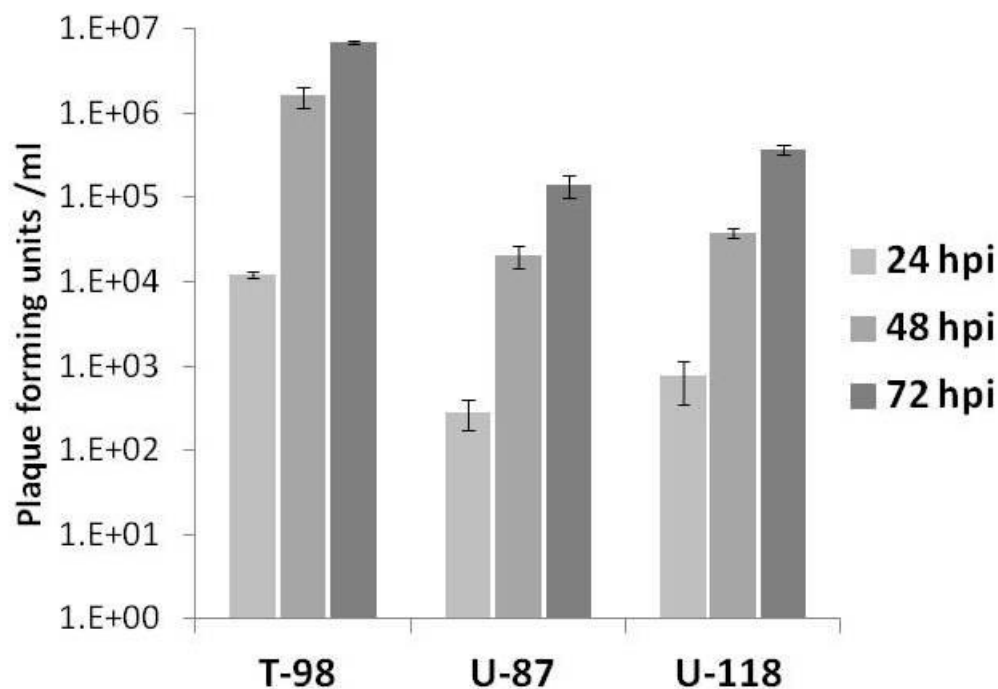
Fig. 17 Replication efficiency of GLV-1h68 in three different glioma cell lines
Three human glioma cell lines (T-98, U-87 and U-118) were seeded in 6-well dishes and infected with GLV-1h68 at an MOI of 0.01. Samples were harvested in triplicate at 24, 48 and 72 hpi and viral titers were determined by standard plaque assay on CV-1 monolayer.

GLV-1h68 replicated exponentially in all three glioma lines tested. However, T-98 glioma cells had higher viral titers than U-87 and U-118 glioma cells following GLV-1h68 infection. By 72 hpi, GLV-1h68 replicated 19-fold higher in T-98 cells compared to U-118 cells and 49-fold higher in T-98 cells compared to U-87 cells. Since in U-87 glioma cells GLV-1h68 did not replicate as efficiently, we used this human glioma line for studying the interaction of IR and oncolytic vaccinia virus in murine glioma xenograft models.

4.2.2 Inhibition of glioma xenograft growth by the combination of systemic GLV-1h68 and focal IR in a subcutaneous glioma model

Since our initial cell culture experiments showed the U-87 glioma line was the least susceptible for GLV-1h68 infection, we used this human glioma line in animal models. The rationale was to study a glioma cell line that is radio-resistant as well as not completely curable with GLV-1h68 alone to exploit a possible benefit by combining both modalities. First, we assessed the efficacy of combination of GLV-1h68 and a single dose of IR in a subcutaneous U-87 xenograft model. U-87 glioma xenografts were established in the right hind limb of athymic nude mice. When tumors reached a size of approximately 200-300

mm³ treatment was initiated. A dose of 2x10⁶ pfu GLV-1h68 in 0.1 ml PBS was delivered
systemically be retro-orbital injection on day 0. In irradiated groups, 6 Gy of focal IR was
given to the tumor bearing hindlimb. In these experiments, we used a dose of IR that was
therapeutically suboptimal and would result in tumor growth delay without tumor regression.
Radiation was delivered focally to the tumor while the rest of the mouse was shielded with
lead to block out 95% of the given dose as determined by RadCal device. To analyze
whether there was a sequencing effect of combining IR and oncolytic VACV, we delivered 6
Gy either one day prior (day -1) to viral administration or one day post (day +1). Tumor
volumes were measured twice a week and plotted as mean fractional tumor Fig. 18. FTV at
each time point is defined by tumor volume at that day divided by tumor volume at treatment
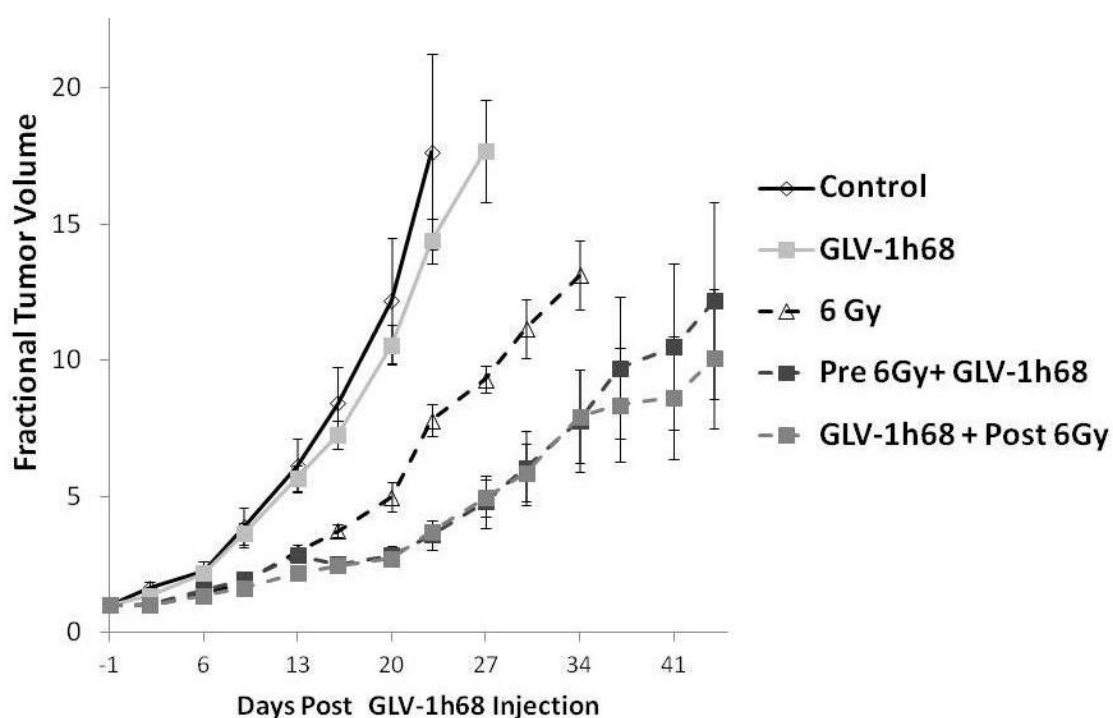start.

**Fig. 18 Inhibition of glioma xenograft growth in animal treated with combination of
systemic GLV-1h68 and focal 6 Gy**
Subcutaneous U-87 xenografts were grown in flanks of athymic nude mice. Mice were treated with
systemic GLV-1h68 and focal 6 Gy IR either 1 day before or after virus injection. Glioma xenografts
were measured twice a week and plotted as mean FTV.

As can be observed in Fig. 18, the untreated control glioma xenografts grew exponentially
and by day 23 all mice had to be sacrificed, secondary to tumor burden. Treatment of mice
with systemic injection of GLV-1h68 alone had minimal effect on tumor growth delay and all
animals were sacrificed by day 27, secondary to tumor burden. Mice that received a single 6
Gy fraction showed an initial tumor growth delay induced by radiation, but then xenografts
grew exponentially. We found that combining 6 Gy with GLV-1h68, regardless of the timing

RESULTS

of IR and VACV, resulted in tumor xenograft growth delay compared to either GLV-1h68 or IR alone. Tumors of mice treated with GLV-1h68 and 6 Gy were significantly smaller ($p<0.05$) compared to all other treatment groups by day 27. Sequencing of IR, either one day before or one day after systemic viral injection, produced a similar effect on U-87 xenograft growth delay. The response of individual glioma xenografts for each experimental group is shown in Fig. 19.
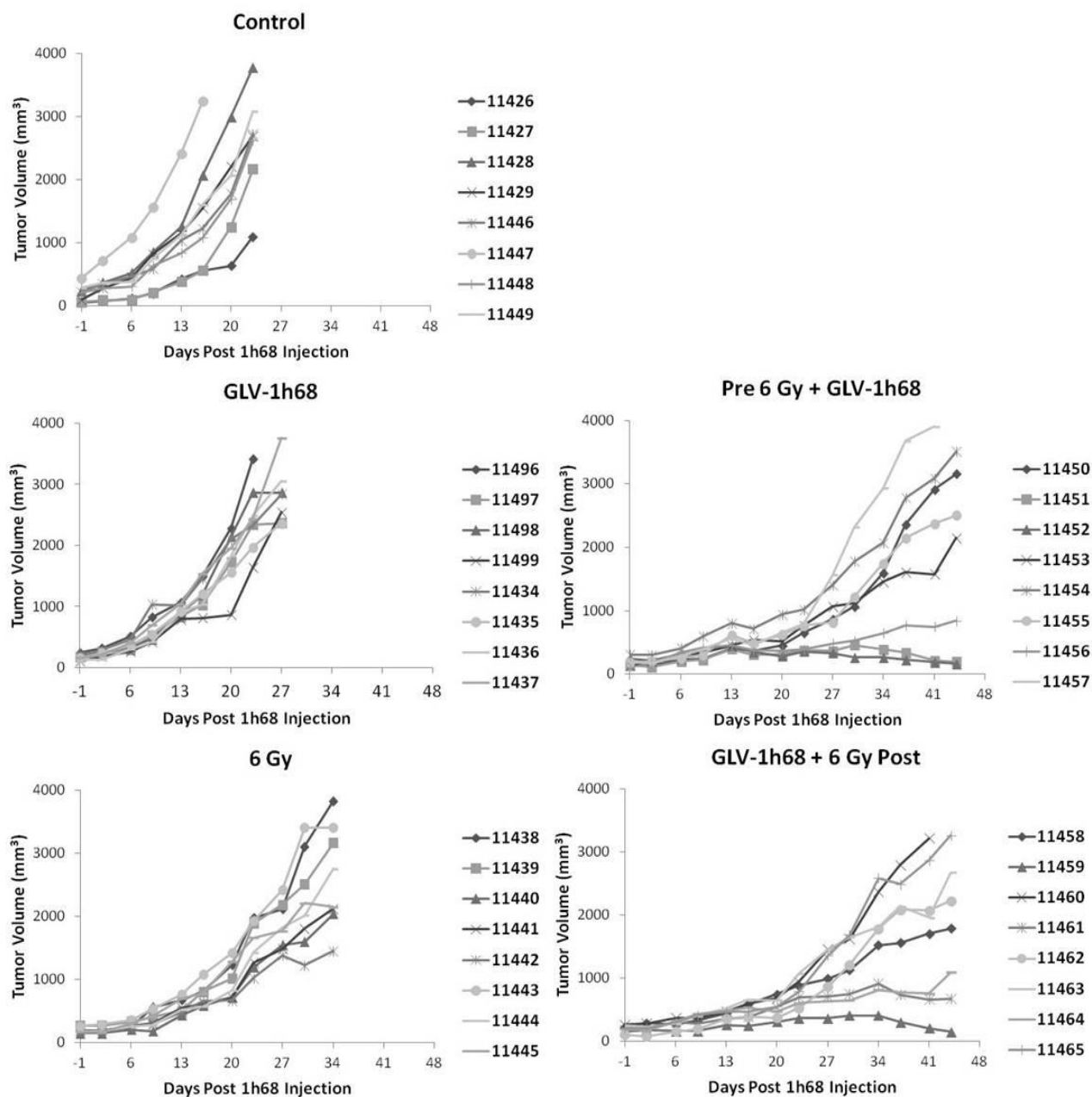

Fig. 19 Glioma xenograft growth delay of individual mice in all treatment groups
Subcutaneous U-87 xenografts were grown in flanks of athymic nude mice. GLV-1h68 was injected systemically on day 0. IR was given as a single 6 Gy fraction either one day before or after GLV-1h68 injection. Glioma xenografts were measured twice a week. The individual volume responses of U-87 glioma xenografts in all experimental groups are shown, 8 mice per experimental group.

RESULTS

To further quantitate the effects of combination of GLV-1h68 and IR on glioma growth delay, we calculated the mean time to reach 10 times the initial starting volume, FTV=10V(0), for each of the groups, Table 2. U-87 xenografts of control mice grew to FTV=10V(0) by 17.8 days. Treatment of mice with systemic injection of GLV-1h68 alone caused minimal tumor growth delay increasing FTV=10V(0) by 2 days. A focal dose of 6 Gy caused a 10 day increase in FTV=10V(0) over control tumors. In both groups that were treated with the combination of systemic GLV-1h68 and focal IR, given either 1 day before or after GLV-1h68 injection, an increase of more than 20 days of FTV=10V(0) was observed.

Table 2. *Time to reach ten times the starting tumor volume and tumor growth delay with GLV-1h68, 6 Gy or the combination*

	Time to reach FTV=10 (Days)	Tumor Growth Delay Over Control Tumors (Days)
Control	17.8	-
GLV-1h68	19.7	1.9
6 Gy	28.4	10.6
Pre 6 Gy + GLV-1h68	39.2	21.4
GLV-1h68 + Post 6 Gy	41	23.2

To monitor the general well-being of animals, mice were weighed once a week. We calculated net bodyweight to exclude to tumor mass. Bodyweight is plotted as fractional net bodyweight which is defined by bodyweight at a certain time point divided by bodyweight at initiation of treatment. A drop in bodyweight is often indicative of a decrease in health due to viral toxicity, other infections, increasing tumor burden or development of metastases. As can be observed in Fig. 20, all mice show constant bodyweight during the duration of the study. This is not surprising for mice treated with GLV-1h68 alone since it was previously shown to be safe [66]. More importantly, mice treated with the combination of IR and VACV also exhibited stable bodyweights, indicating that safety of the virus is not compromised when it is combined with radiation.
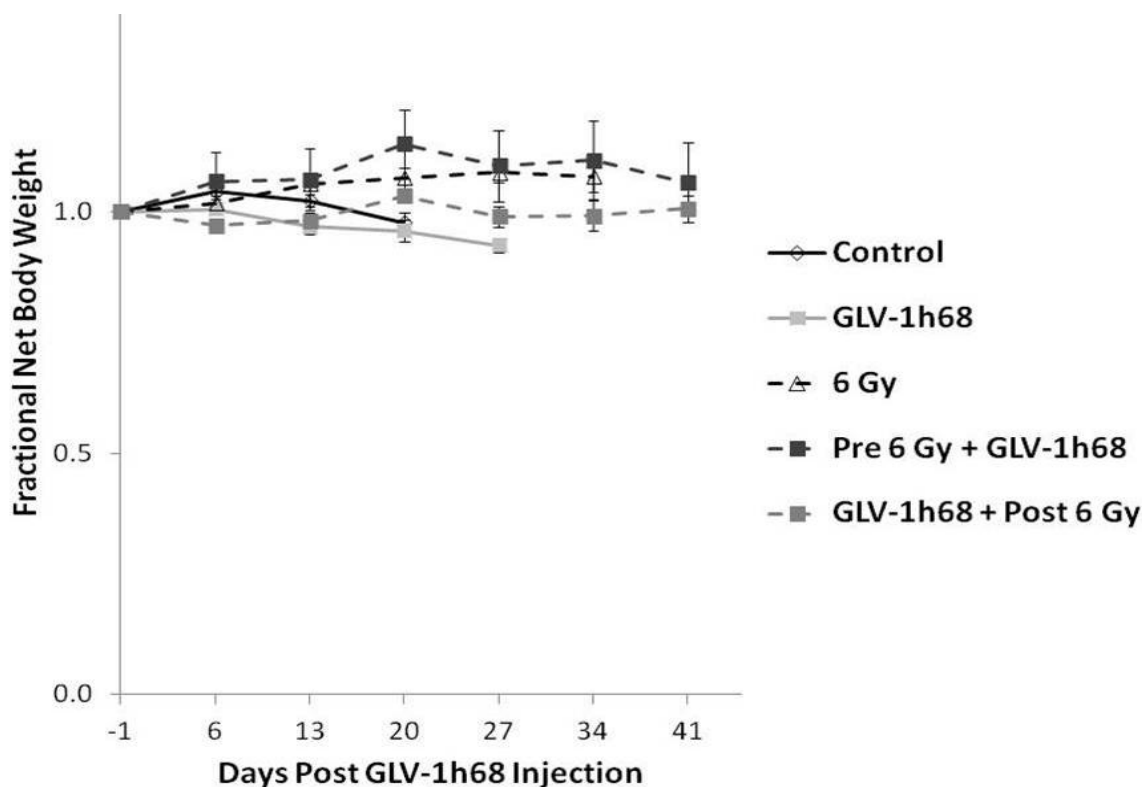
Fig. 20 Fractional net bodyweight of mice with U-87 glioma xenografts treated with GLV-1h68 and IR.
Subcutaneous U-87 xenografts were grown in flanks of athymic nude mice. Mice were treated with systemic GLV-1h68 and focal 6 Gy IR either 1 day before or after virus injection. Mice were weighed to monitor general well-being once a week. Net bodyweight was calculated by subtracting the tumor mass and plotted as fractional net bodyweight.

In this initial study we could demonstrate, tumor growth of subcutaneously implanted glioma xenografts is significantly delayed when systemic oncolytic VACV is given in combination with focal IR.

4.2.3 Survival increased by combining systemic GLV-1h68 and focal irradiation in mice with orthotopically implanted glioma xenografts

Next, we confirmed the efficacy of combining GLV-1h68 and IR in an intracranial U-87 xenograft model. In this study, U-87 glioma cells were orthotopically implanted into the right frontal lobe of nude mice. A single dose of 2×10^6 pfu GLV-1h68 in 0.1 ml PBS was administered by retro-orbital inoculation at day 5 after glioma xenograft implantation. In groups that received irradiation two fractions of 6 Gy each were given to the entire cranium one day prior as well as one day after viral injection. Fig. 21 shows Kaplan Meier survival

curves of all treatment groups. Mice were removed immediately from the study when they showed a sudden drop in bodyweight, any physical impairment and/or signs of weakness.
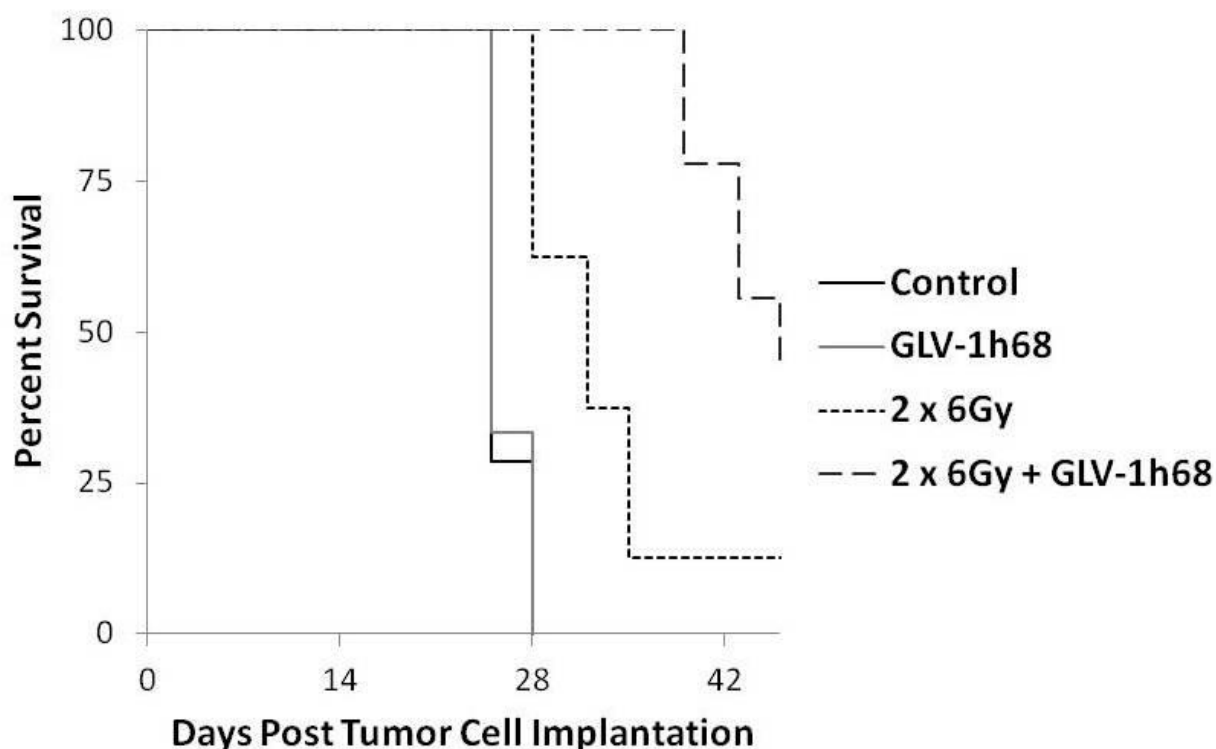

Fig. 21 Kaplan Meier survival curves of mice with intracranial U-87 xenograft
U-87 glioma cells were orthotopically implanted into the brains of nude mice. GLV-1h68 was injected systemically and IR was given to the entire cranium in two 6 Gy fractions one day before and after GLV-1h68 injection. Mice were followed for survival.

The median survival in days post implantation of all treatment groups as well as the survival increase in days over control mice is shown in Table 3. The median survival for control mice was 25 days post implantation. All control mice had to be taken out of the experiment within one week confirming that the stereotactic implantation was technically successful and moreover that the glioma xenografts had homogeneous growth characteristics in their natural location. Treatment of mice with GLV-1h68 did not increase survival. Two fractions of 6 Gy increased survival of mice by one week. All mice treated with the combination of two 6 Gy fractions and GLV-1h68 survived significantly longer (p<0.01) than all other groups and exhibited a survival increase of 21 days over control mice.

RESULTS

Table 3. *Median survival for mice treated with GLV-1h68, 2 fractions of 6 Gy or the combination of both and survival increase over control mice*

	Median Survival (Days post Implantation)	Survival Increase over control mice (Days)
Control	25	-
GLV-1h68	25	-
2 x 6 Gy	32	7
2 x 6 Gy + GLV-1h68	46	21

Since we were not able to measure tumor growth due to its location intracranially, we weighed mice twice a week to monitor their wellbeing and to observe decrease in bodyweight as an indicator for increasing tumor burden in the brain. Fig. 22 shows the bodyweights for all treatment groups. Generally, it could be observed that bodyweight inversely correlated with tumor burden. Weakening of mice by increasing tumor burden was accompanied by a sudden drop in bodyweight. We found that mice treated with the combination of two fractions of 6 Gy and GLV-68 exhibited, after an initial drop in bodyweight due to radiation treatment, a more constant bodyweight than all other treatment groups. Moreover, mice in the combined treatment group appeared healthier and their bodyweights dropped significantly later than all other groups.
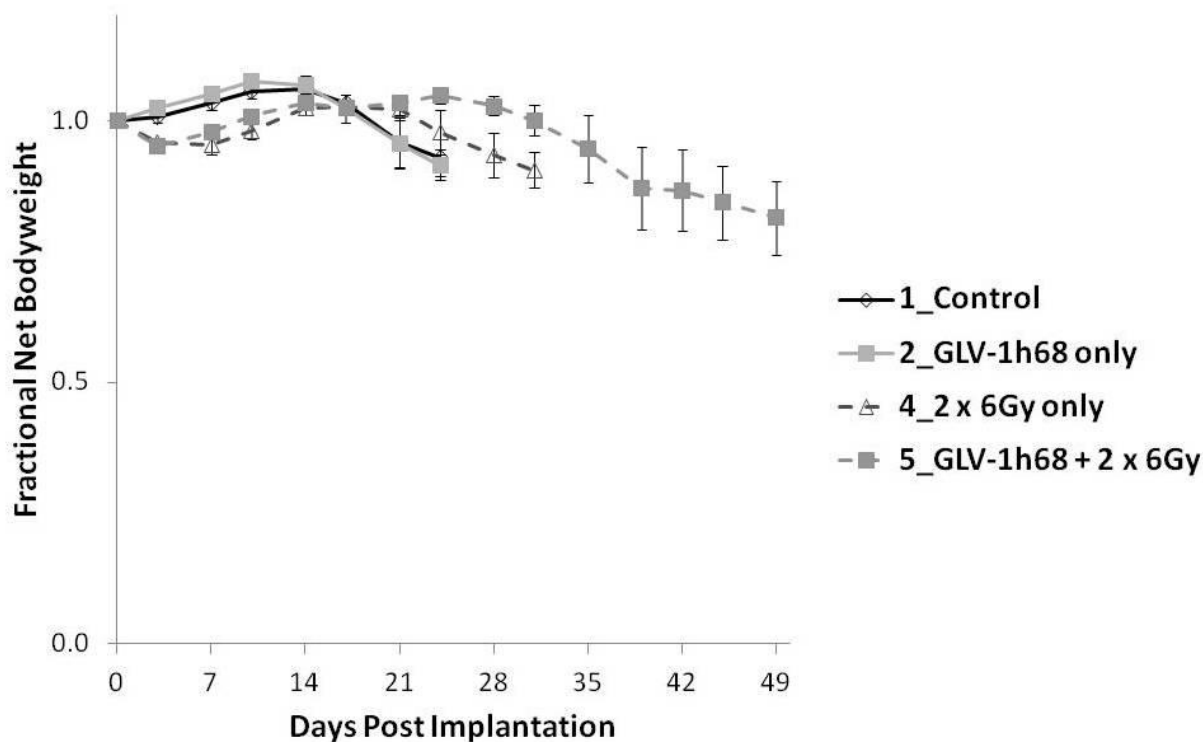
Fig. 22 Net bodyweight of mice with intracranial U-87 xenograft
U-87 glioma cells were orthotopically implanted into the brains of nude mice. GLV-1h68 was injected systemically and IR was given to the entire cranium in two 6 Gy fractions one day before and after GLV-1h68 injection. Bodyweight was recorded twice a week and plotted as fractional bodyweight with respect to animal weight at treatment start.

The effects of combining GLV-1h68 and IR in the intra-cranial glioma model were similar to the results obtained in the subcutaneous glioma model. Since tumors in the flank are easier to monitor in terms of growth as well as viral colonization, we decided to use the subcutaneous glioma model to further characterize the interaction of GLV-1h68 and IR.

4.2.4 Increased GLV-1h68 marker gene expression in irradiated glioma xenografts

To begin to investigate whether and how focal IR and systemic viral delivery interact, we monitored *in situ* real time GLV-1h68 reporter gene expression within tumor xenografts from groups treated with systemic injection of GLV-1h68 with or without focal tumor irradiation. As stated earlier, GLV-1h68 encodes a *Renilla* luciferase-GFP fusion protein enabling the visualization of viral colonization in tumors. Viral GFP expression within the tumors of all treatment groups was monitored under blue light using a Stereo Fluorescence macroimaging system at day 7 and 14 after systemic viral delivery. GFP expression was scored using a four point system: 0) no GFP signal, 1) one spot, 2) two or three local spots, 3) >3 spots and

RESULTS

4) diffuse signal. Tumor xenografts from control mice as well as mice treated with 6 Gy only did not have any detectable GFP expression. One week post systemic injection of GLV-1h68 alone focal spots of GFP were detected in U-87 xenografts, Fig. 26A and Fig. 23 for individual mice. In contrast, when we analyzed mice treated with 6 Gy prior to systemic GLV-1h68 injection we found an increase in GFP in U-87 xenografts which was characterized by a more diffuse signal within the tumor, Fig. 26A and Fig. 24. Interestingly, when a focal dose of 6 Gy was given 1 day after systemic GLV-1h68 injection instead of one day before, GFP expression within the tumor was again focal at day 7 and looked similar to the non-irradiated GLV-1h68 injected alone group, Fig. 26A, Fig. 25. The mean GFP expression of the groups treated with GLV-168 alone or in combination with IR is shown in Fig. 26B.
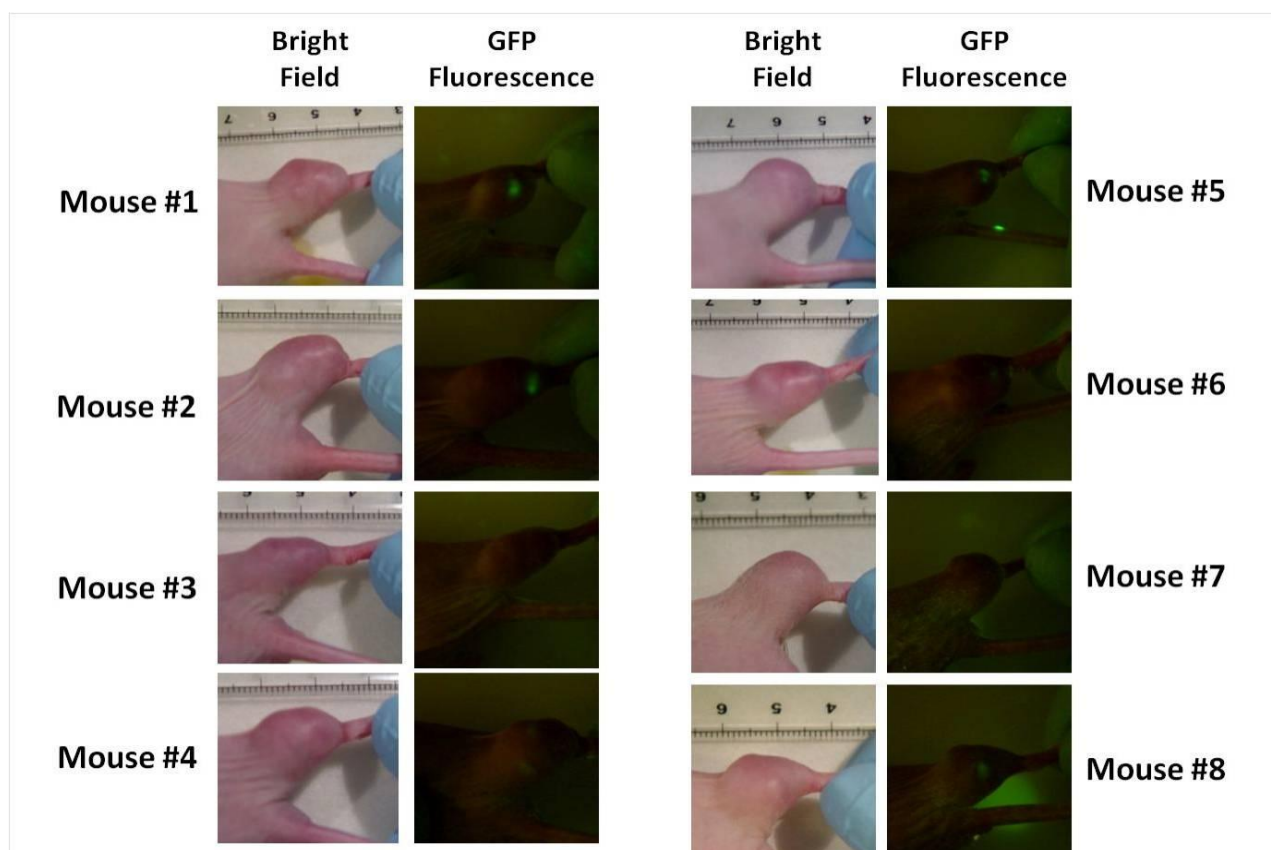

Fig. 23   Viral GFP expression in U-87 glioma xenografts injected with GLV-1h68
U-87 glioma xenografts were injected with GLV-1h68 on day 0. Intra-tumoral GFP expression was monitored. Bright field and corresponding GFP expression images were taken at day 7 post systemic viral injection.
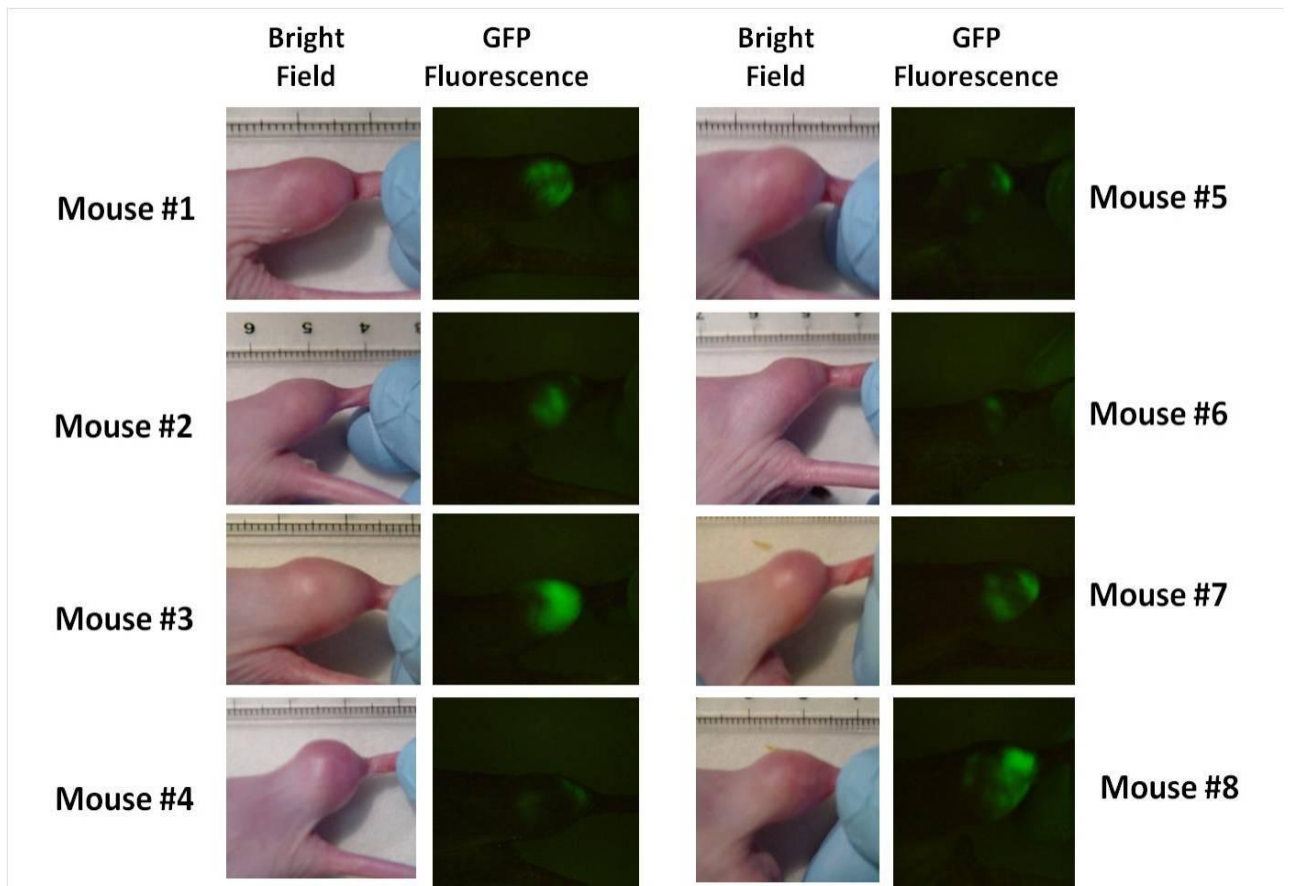
Fig. 24   Viral GFP expression in U-87 glioma xenografts treated with 6 Gy followed by systemic GLV-1h68 injection.

U-87 glioma xenografts were focally irradiated with 6 Gy one day before being systemically injected with GLV-1h68.   Intra-tumoral GFP expression was monitored.   Bright field and corresponding GFP expression images were taken at day 7 post systemic viral injection.

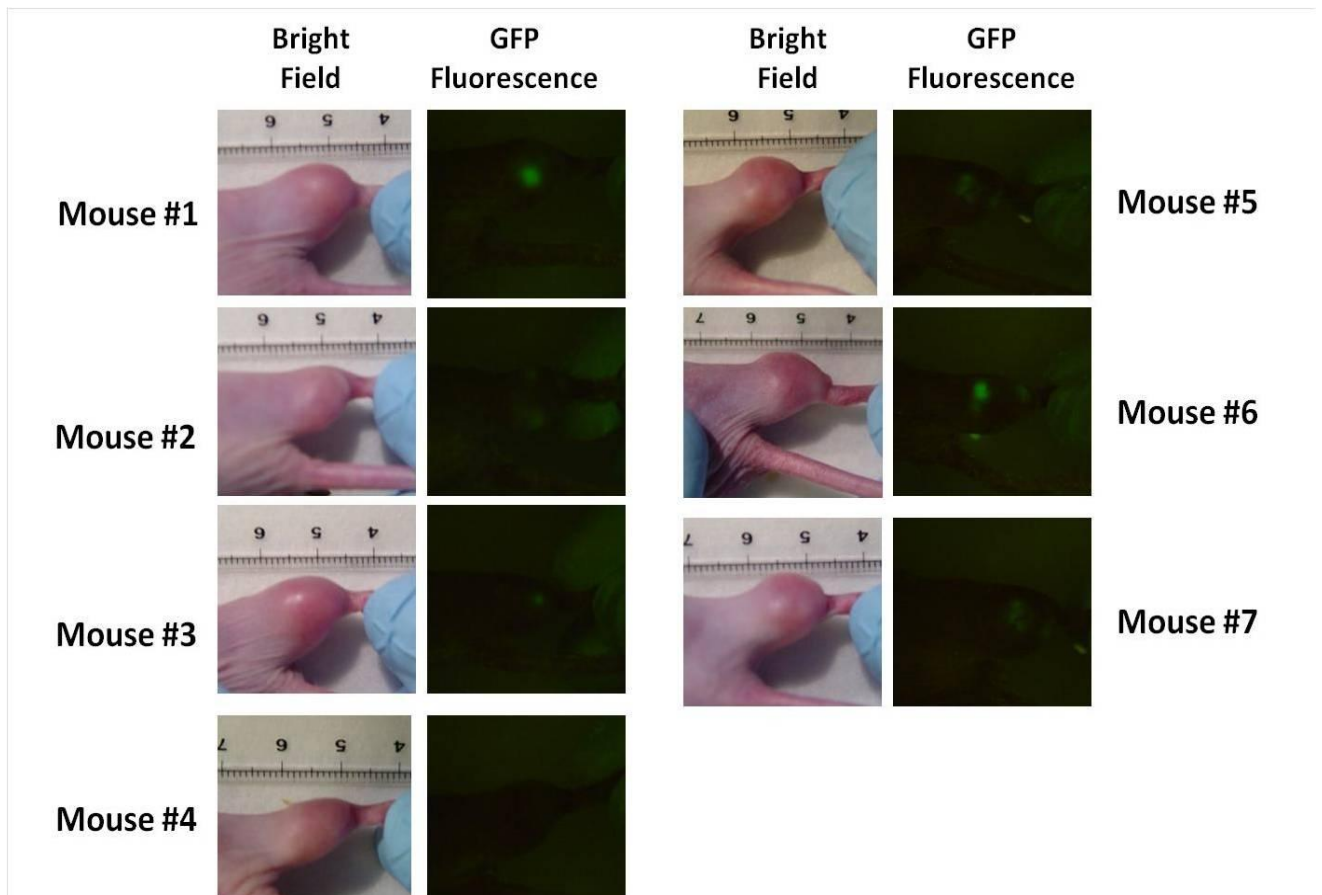**Fig. 25 Viral GFP expression in U-87 glioma xenografts treated with systemic GLV-1h68 Followed by 6 Gy.**

U-87 glioma xenografts were injected systemically with GLV-1h68 on day 0 followed by 6 Gy focally to the tumor one day after viral injection. Intra-tumoral GFP expression was monitored. Bright field and corresponding GFP expression images were taken at day 7 post systemic viral injection.
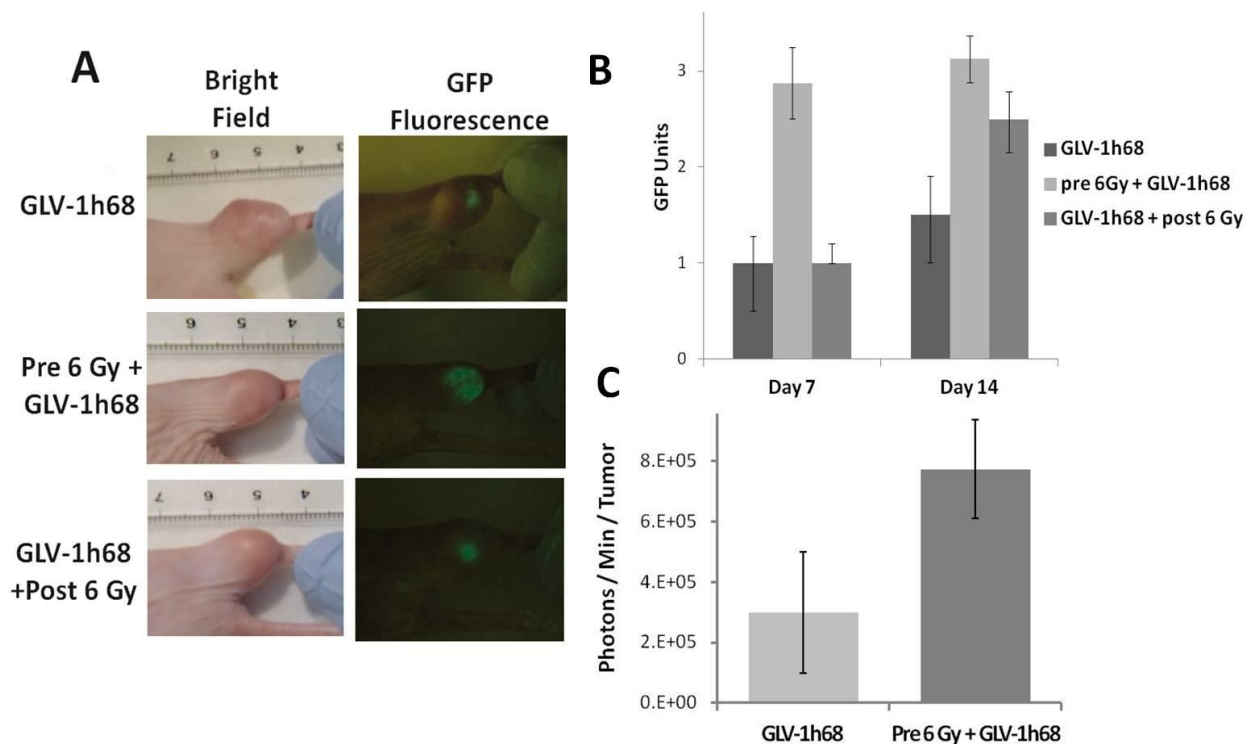
Fig. 26 Expression of viral encoded *Renilla* Luciferase-GFP fusion protein in U-87 glioma xenografts treated with GLV-1h68 and IR
U-87 glioma xenografts were injected systemically with GLV-1h68. IR was given as single fraction of 6 Gy one day before or after viral injection. **A)** Bright field and fluorescence image of representative mice 7 days post GLV-1h68 injection. **B)** Tumoral GFP expression was scored on a 4 point system on days 7 and 14 post systemic viral injection. **C)** Tumoral GLV-1h68 luciferase expression 10 dpi.

While pre-irradiation of tumors led initially to a more diffuse viral GFP signal, we found that by day 14 viral GFP expression was nearly equivalent if IR was given either one day before or one day after viral injection. Importantly, irradiated glioma xenografts had higher viral GFP expression than non-irradiated glioma xenografts that were treated with GLV-1h68 alone, Fig. 26B. To verify higher viral GFP expression in irradiated tumor xenografts, we quantitated viral luciferase activity. GFP and *Renilla* luciferase are expressed as a fusion protein by the virus. Ten days post systemic viral injection mice were injected via tail vain with the substrate for *Renilla* luciferase coelenterazine (2.5 µg) and immediately anesthetized afterwards with a mixture of ketamine and xylazine. Photon emission from GLV-1h68 luciferase activity in 8 non-irradiated and 8 pre-irradiated U-87 glioma xenografts was recorded for 1 min using the Argus100 Low Light Imaging System.
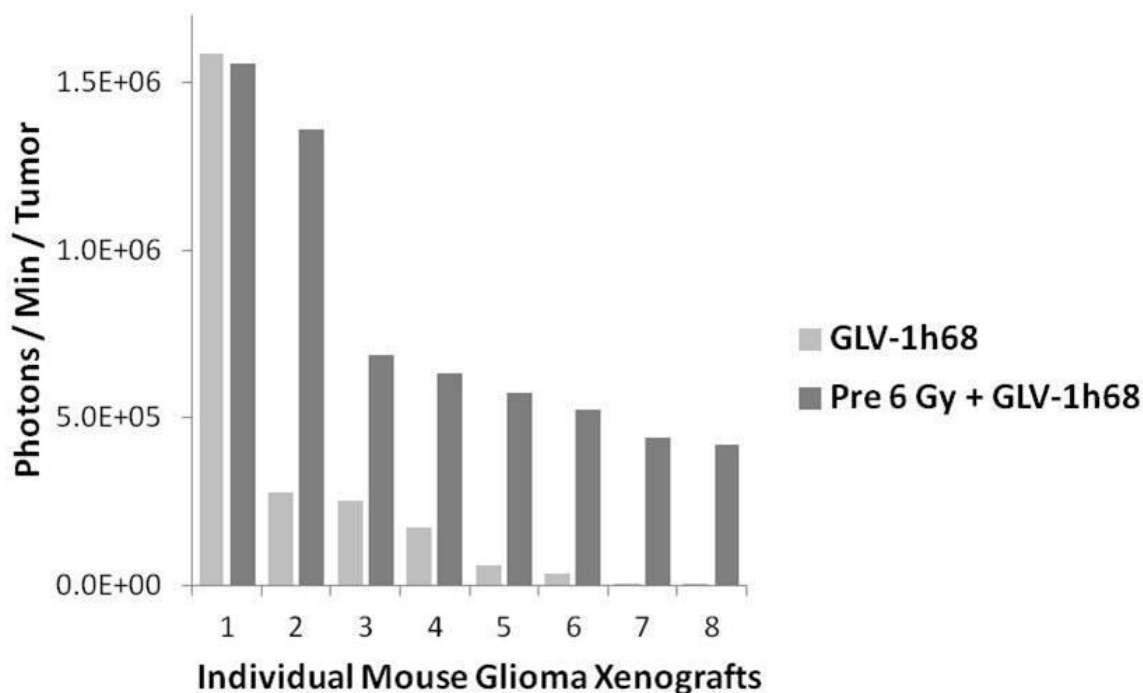
Fig. 27 GLV-1h68 encoded luciferase expression of individual mice in pre-irradiated and non-irradiated glioma xenografts
U-87 glioma xenografts were grown in nude mice and injected systemically with GLV-1h68. IR was given as single fraction of 6 Gy one day before. Tumoral GLV-1h68-encoded luciferase expression is shown for individual mice treated with GLV-1h68 alone or pre irradiated and GLV-1h68 at 10 dpi.

Fig. 27 shows photon emission of individual mice 10 days post systemic injection in groups either treated with GLV-1h68 alone or in GLV-1h68 in combination with pre 6 Gy. As we observed by viral GFP expression glioma xenografts treated with IR showed a higher activity of virally-encoded luciferase, Fig. 26C. In pre-irradiated U-87 xenografts the mean as well as median photon counts from GLV-1h68-encoded luciferase increased significantly ($p < 0.05$) by 2.6-fold and 5.2-fold, respectively, when compared to non-irradiated U-87 glioma xenografts. These data demonstrated IR interacted with oncolytic GLV-1h68 to increase oncolytic VACV gene expression.

4.3 Interaction of oncolytic VACV is not restricted to GLV-1h68 but also observed with an less attenuated strain LIVP 1.1.1

Our initial experiments demonstrated IR can be incorporated with oncolytic VACV GLV-1h68 into treatment of glioma xenografts to increase viral replication which translated to increase tumor control. We next analyzed whether the interaction observed between IR and VACV is a more general phenomenon or restricted to GLV-1h68, which represents a multi-mutated VACV strain with several gene insertions. It is conceivable that IR provides trans-

complementation for deleted viral genes, hence decreasing attenuation ad increasing replication efficacy for certain mutated oncolytic VACV. To follow up on our initial studies we used LIVP 1.1.1, which represents a plaque purified isolate of the non- attenuated LIVP strain of VACV. Compared to GLV-1h68 LIVP1.1.1 is less attenuated although sequencing LIVP 1.1.1 demonstrated it has a natural occurring deletion in VACV thymidine kinase gene.

4.3.1 LIVP 1.1.1 replicates more efficiently in U-87 glioma cells in cell culture

First, we compared replication efficiency of GLV-1h68 and LIVP 1.1.1 in U-87 glioma cells in cell culture. Cells were seeded into 6-well plates and after 24 h in culture infected at an MOI of 0.01 with either GLV-1h68 of LIVP 1.1.1. Wells were harvested at 24, 48 and 72 hpi and titered for viral amounts with standard plaque assay.
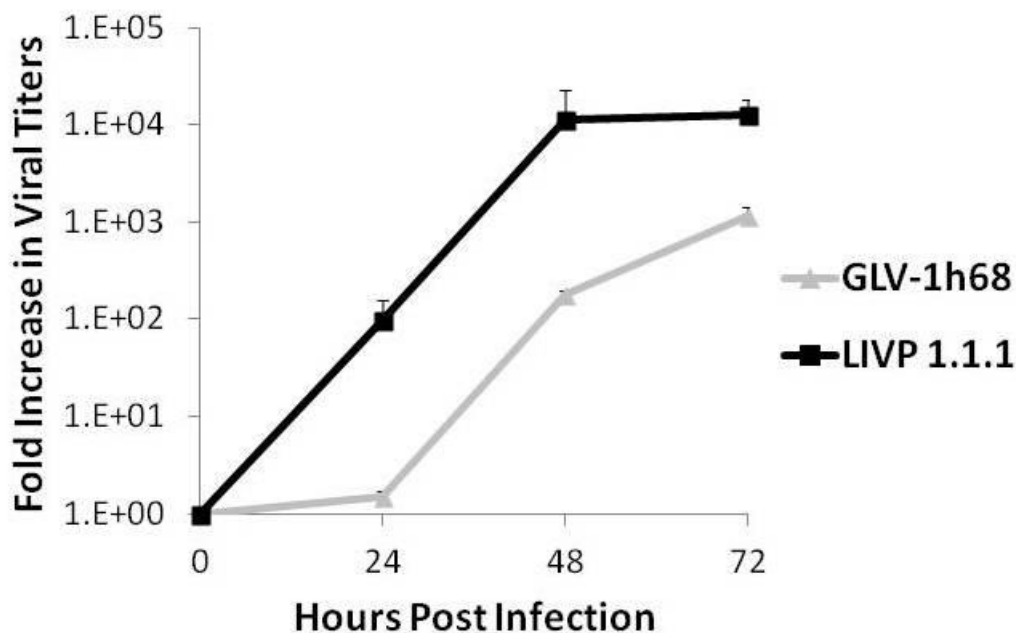
Fig. 28 Increased replication of LIVP 1.1.1 versus GLV-1h68 in U-87 glioma cells
U-87 glioma cells were infected with either GLV-1h68 or LIVP 1.1.1 and harvested 24, 48, and 72 hpi. Viral titers were determined on CV-1 monolayer and normalized to the input virus.

As seen in Fig. 28, LIVP 1.1.1 replicated to higher titers in U-87 cells in culture when compared to more attenuated GLV-1h68. Cells that were infected with LIVP 1.1.1 had a 65-fold higher viral load than GLV-1h68 infected cells by 24 hpi. This promising result indicates that by using a less attenuated VACV strain, efficacy of VACV in U-87 glioma cells could be enhanced due to increased replication when compared to mutated GLV-1h68. Increased

replication in cell culture could translate to an improved tumor control in animal glioma models.

4.3.2 Combining of LIVP 1.1.1 and IR improves glioma tumor control in a subcutaneous model of glioma

Given that we found LIVP 1.1.1 replicated more efficiently in cell culture when compared to GLV-1h68, we next assessed the efficacy of LIVP 1.1.1 and IR in U-87 glioma xenografts to determine whether this combination would further enhance glioma tumor control. As in previous animal studies, U-87 glioma xenografts were grown s.c. in the flanks of nude mice. When tumors reached a size of approximately 200-300 mm^3, treatment was initiated. LIVP 1.1.1 was injected on day 0 systemically by retro-orbital inoculation and a single 6 Gy fraction of IR was delivered focal to the tumor one day prior to viral injection. The mean fractional tumor volumes for all treatment groups are shown in Fig. 29.
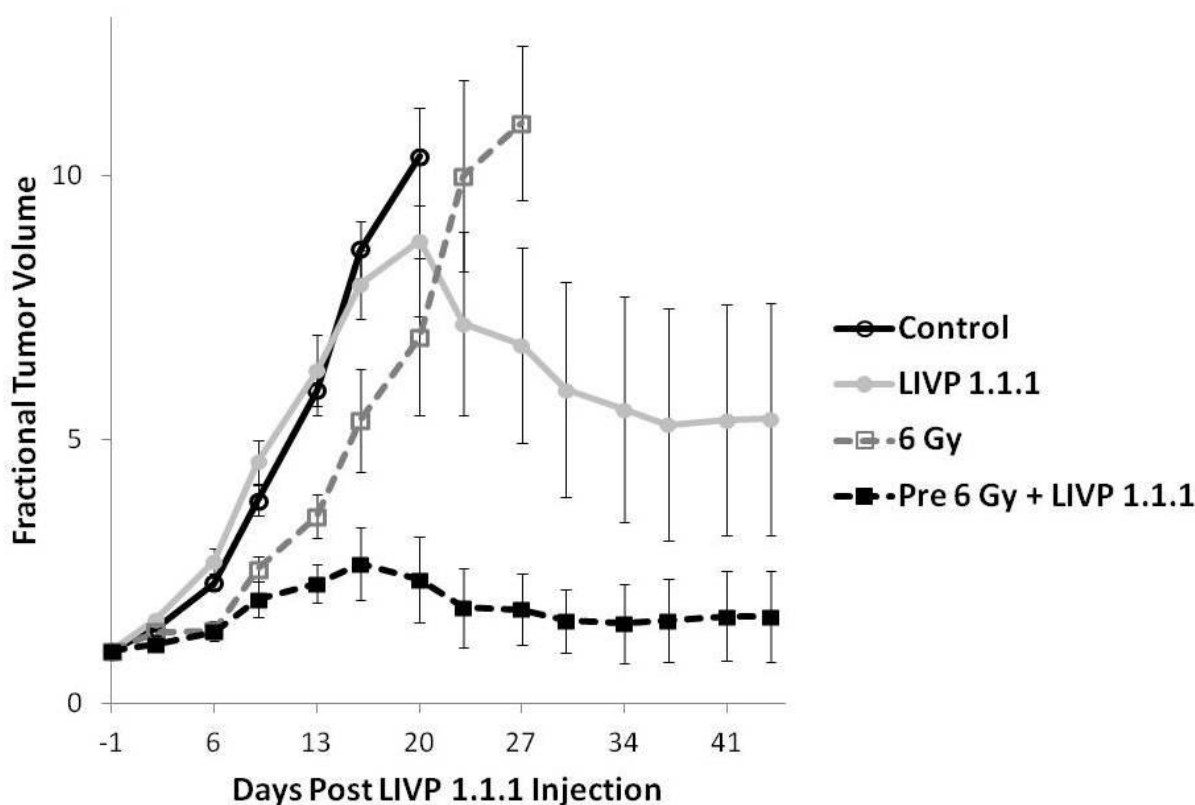

Fig. 29 Increased tumor growth delay by combination of LIVP 1.1.1 with IR
U-87 glioma xenografts were grown in nude mice and systemically injected with LIVP 1.1.1 on day 0. IR was given as a single 6 Gy fraction one day before LIVP 1.1.1. Glioma xenografts were measured twice a week and normalized to the volume at initiation of treatment, FTV.

RESULTS

As expected, untreated control tumor xenografts grew exponentially and all mice had to be sacrificed by day 20, secondary to tumor burden. Ionizing radiation alone, given as a single 6 Gy fraction resulted in an initial growth delay of 7 days as already observed in previous animal studies. Systemic administration of LIVP 1.1.1 alone resulted in a tumor regression pattern previously described for oncolytic VACV. Here, LIVP 1.1.1-treated glioma xenograft growth paralleled untreated control glioma xenografts until day 20, after which the tumor xenografts began to regress. Interestingly, combining LIVP 1.1.1 with IR resulted in a stronger anti-tumor effect as measured by volumetric tumor regression. In the group given 6 Gy, 1 day before LIVP 1.1.1 injection, 5 of 7 tumor xenografts had a FTV≤1 at day 41. In contrast, none of the 7 tumor xenografts treated with LIVP 1.1.1 alone had a FTV≤1. Xenografts of mice treated with 6 Gy prior to systemic LIVP 1.1.1 injection were significantly smaller ($p<0.05$) compared to all other groups.

Again, to monitor general well being of mice we monitored bodyweight once a week. Mice tolerated treatments well as their bodyweights were stable, see Fig. 30.
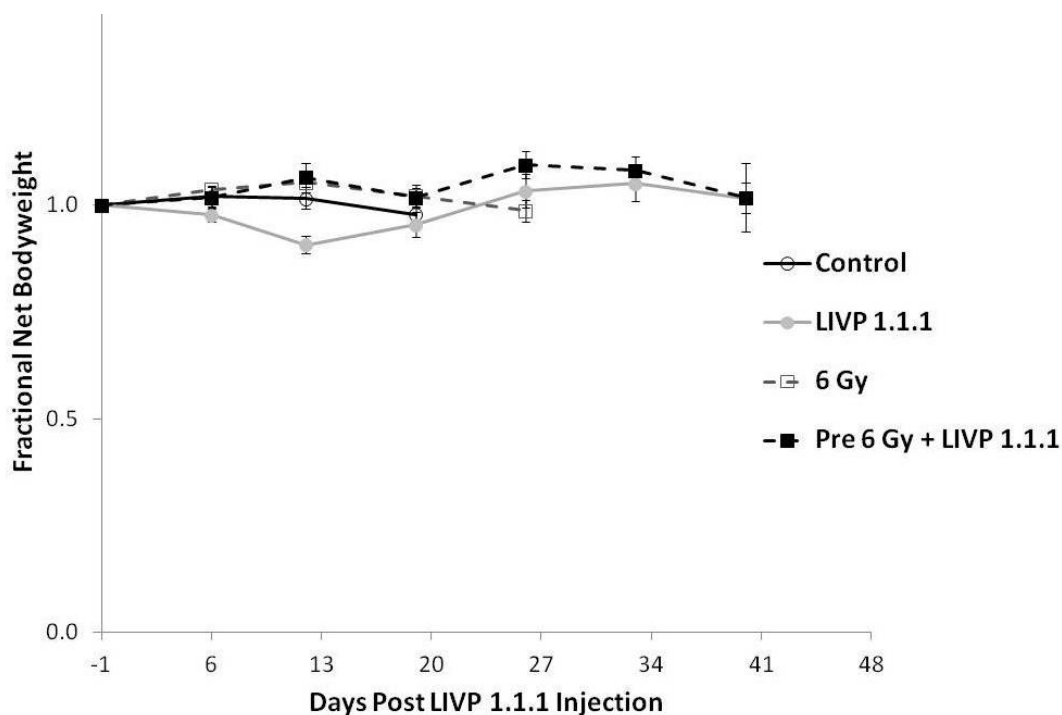
Fig. 30 Fractional Net Body Weight of Mice with U-87 Glioma Xenografts Treated with LIVP 1.1.1 and IR.
Subcutaneous U-87 xenografts were grown in flanks of athymic nude mice. Mice were treated with systemic LIVP 1.1.1 and focal 6 Gy IR one day before or virus injection. Mice were weighed to monitor general well being once a week. Net bodyweight is shown as fractional net bodyweight.

Animals did not show signs of viral toxicity since bodyweights of all treatment groups remained stable through the course of the study.

RESULTS

Since LIVP 1.1.1 is less attenuated than GLV-1h68 and therefore more efficient in destroying the tumor it is conceivable that this lack of attenuation could result in increased toxicity to normal tissue. In particular, we were interested whether toxicity to normal tissue is increased in irradiated mice.

Table 4. *Viral colonization of body organs 3 dpi; Viral titers are shown as pfu/ total organ*

	Liver	Lungs	Spleen	Brain
Control	0	0	0	0
GLV-1h68	0	0	$1.6 \times 10^1 \pm 3 \times 10^1$ 2/4	0
LIVP 1.1.1	0	$8.8 \pm 2.6 \times 10^1$ 1/4	0	$2.1 \times 10^1 \pm 6.0 \times 10^1$ 1/4
Pre6Gy+LIVP1.1.1	0	0	$2.4 \times 10^1 \pm 5.0 \times 10^1$ 1/4	0
LIVP1.1.1+Post6Gy	$2.5 \times 10^1 \pm 7.0 \times 10^1$ 1/4	$1.7 \times 10^1 \pm 3.1 \times 10^1$ 2/4	0	0

Table 5. *Viral colonization of body organs 7 dpi; Viral titers are shown as pfu/ total organ*

	Liver	Lungs	Spleen	Brain
Control	0	0	0	0
GLV-1h68	0	0	0	$1.1 \times 10^1 \pm 3.1 \times 10^1$ 1/4
LIVP 1.1.1	0	$1.7 \times 10^1 \pm 3.3 \times 10^1$ 2/4	$4.7 \times 10^1 \pm 6.7 \times 10^1$ 2/4	0
Pre6Gy+LIVP1.1.1	$3.2 \times 10^1 \pm 9.1 \times 10^1$ 1/4	$2.5 \times 10^1 \pm 7.1 \times 10^1$ 1/4	$2.4 \times 10^1 \pm 5.0 \times 10^1$ 1/4	0
LIVP1.1.1+Post6Gy	0	0	0	0

As can be observed in Table 4 and Table 5 minimal colonization of normal organs was observed in mice treated with GLV-1h68 or LIVP 1.1.1. More importantly, there was no increase in toxicity to normal tissue in irradiated groups indicating that IR does not alter viral tumor-specific tropism.

4.3.3 Combining LIVP 1.1.1 with IR increases survival of mice in an orthotopic model of U-87 glioma

To validate the findings from our subcutaneous animal study, we then used a U-87 orthotopic model. Again, U-87 xenografts were established orthotopically in the brains of nude mice by stereotactic implantation into the right frontal lobe. LIVP 1.1.1 was injected systemically on day 5 and IR delivered to the whole cranium in two fractions of 6 Gy, given at day 4 and 6. Fig. 31 shows the Kaplan Meier survival diagram for all treatment groups.
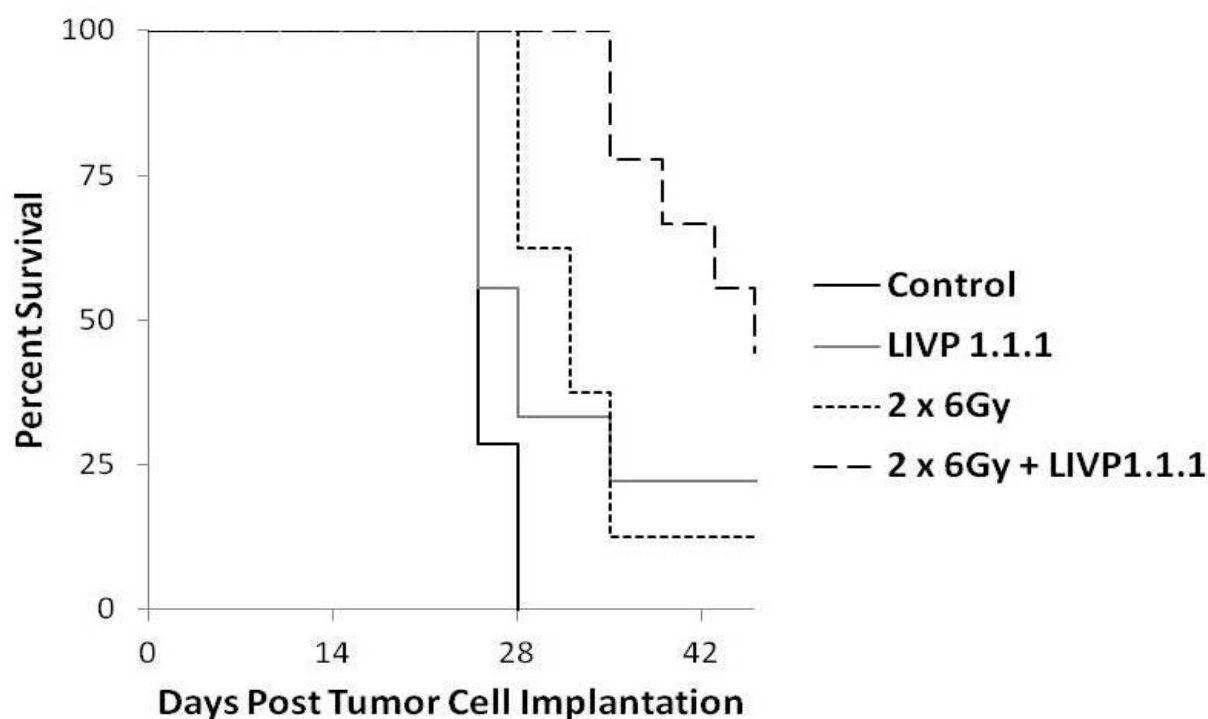
Fig. 31 Kaplan Meier survival curves of mice treated with LIVP 1.1.1 alone, two focal fractions of 6 Gy or the combination of both
U-87 glioma cells were orthotopically implanted into the brains of nude mice. LIVP 1.1.1 was injected systemically and IR was given to the entire cranium in two 6 Gy fractions one day before and after GLV-1h68 injection. Mice were followed for survival.

As can be seen in Table 6, untreated control mice had a median survival of 25 days after U-87 implantation. LIVP 1.1.1 and IR monotherapies resulted in an increase in median survival over control mice of 3 and 7 days, respectively. Again, mice treated with the combination of IR and VACV, here LIVP 1.1.1, showed a dramatic increase in median survival of 21 days over control mice.

Table 6. *Median survival for mice treated with LIVP1.1.1, 2 fractions of 6 Gy or the combination of both and survival increase over control mice*

	Median Survival (Days post Implantation)	Survival Increase over control mice (Days)
Control	25	-
LIVP 1.1.1	28	3
2 x 6 Gy	32	7
2 x 6 Gy + LIVP 1.1.1	46	21

Taken together, the results obtained in the subcutaneous and intracranial murine model of U-87 glioma xenografts indicated that the interaction of IR with oncolytic VACV is not restricted to the triple-deleted GLV-1h68, but is also seen with the less attenuated isolate of LIVP, LIVP 1.1.1. Furthermore, it was demonstrated that when using this less attenuated VACV tumor control can be further improved while toxicity to normal tissue is not affected.

4.3.4 Fractionated IR in combination with oncolytic vaccinia virus achieves similar glioma xenograft regression

Clinically, the radiotherapy is administered in multiple small fractions rather than single large fractions. Radiation therapy for gliomas is delivered in a multi-fractionated regimen. Previously, in our intracranial U-87 model we tested the efficacy of IR given in two fractions of 6 Gy one day before and after viral injection. Hence, we were interested to see whether we can split our single dose into fractions to mimic the clinical practice. To be able to fairly compare different radiation fractionation schedules, in our case one single fraction versus two smaller fractions, similar biologic effective doses (BED) need to be compared. BED is a mathematical approximation by which different fractionation regimens can be compared. It can be calculated by following equation:

$$BED = nD \left(1 + (D / \alpha/\beta)\right)$$

Here, n is the number of fractions, D the fraction size and α/β is a constant which accounts for differences in tissue response and is set as 10 in fast responding tissues such as the tumor. Assuming a α/β ratio of 10 for tumor cell sensitivity, 6 Gy given as a single fraction is equivalent to 3.5 Gy given in two fractions (total dose of 7 Gy). For the two fraction IR schedule, 3.5 Gy was given one day before and one day after LIVP 1.1.1 injection.
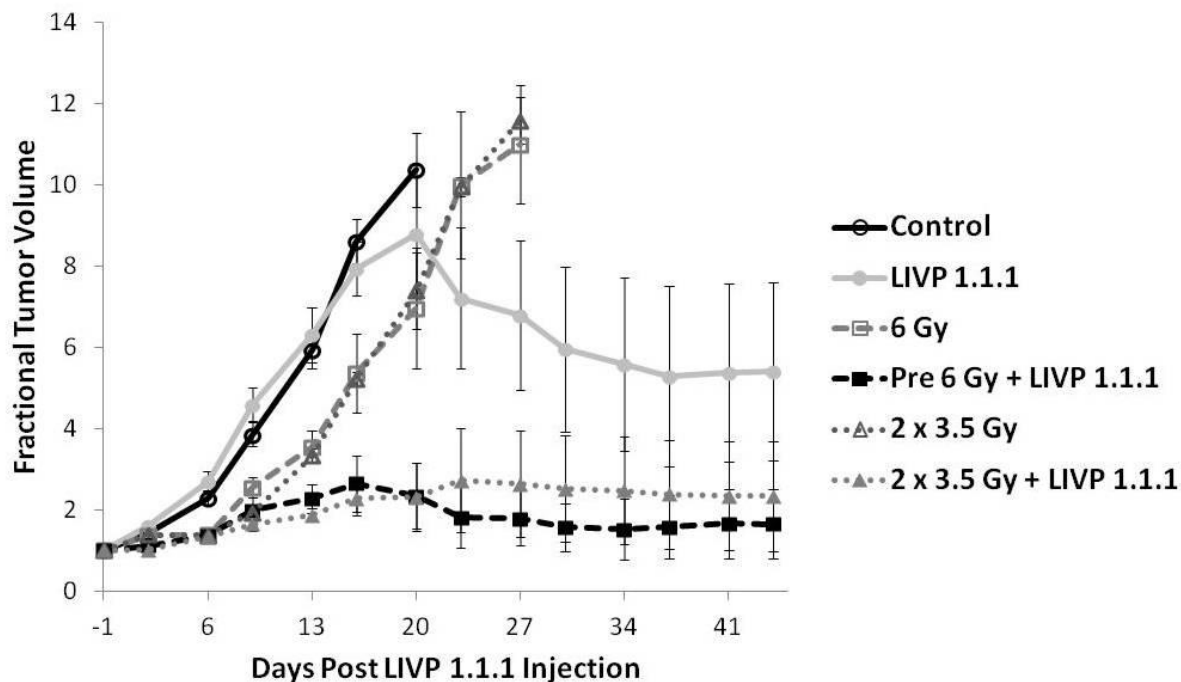
Fig. 32 Splitting one 6 Gy fraction in two 3.5 Gy fractions achieves equivalent tumor growth delay
U-87 glioma xenografts were grown in nude mice and systemically injected with LIVP 1.1.1 on day 0. IR was given either as a single 6 Gy fraction one day before or two 3.5 Gy fractions one day before and after LIVP 1.1.1 injection. Glioma xenografts were measured twice a week and normalized to the volume at initiation of treatment, FTV.

Ionizing radiation alone, given as either one single fraction of 6 Gy or two fractions of 3.5 Gy, one day prior as well as post viral administration, produced equivalent growth delays of approximately 7 days, which is as expected since both IR schedules have an equivalent BED for tumor cell kill, Fig. 32. For the combination groups, splitting of IR in two 3.5 Gy fractions resulted in similar tumor volume regression as seen with 6 Gy and LIVP 1.1.1 and was statistically significant compared to single treatment groups ($p < 0.05$). In this regimen, where the single dose is split into two fractions, 6 of 7 tumors had a FTV≤1 at day 41. These data indicate that IR can be delivered as a large single fraction or as two smaller fractions in combination with LIVP 1.1.1. This is important because in a potential clinical application for combining VACV and IR it is likely that vaccinia virus will be incorporated into a treatment regimen consisting of multiple IR fractions.

4.3.5 IR increases oncolytic vaccinia viral replication and distribution in U-87 glioma xenografts

In our initial U-87 study we saw an increase in marker gene expression of GLV-1h68 in irradiated xenografts. In addition, we have shown that interaction of IR is not restricted to

RESULTS

GLV-1h68 but is also seen for another VACV viral strain LIVP 1.1.1. Next, we determined if IR increased the replication and spread of this oncolytic VACV in glioma xenografts. Since LIVP 1.1.1 does not encode for any reporter genes, we analyzed viral spread within glioma xenografts by IHC in 5 µm thick tumor sections embedded in paraffin by antibody staining to VACV protein A27L at 7 days post LIVP 1.1.1 injection. A27L is a late vaccinia protein which is incorporated into the virus envelope. In this experiment, tumors were excised, fixed in 10% neutral buffered formalin, dehydrated and stained for presence of VACV. As expected, glioma xenografts from control mice showed no staining for VACV protein A27L, Fig. 33A, neither did sections from tumors that received IR only (data not shown). When LIVP 1.1.1 was injected alone 7 days post infection A27L staining showed focal areas positive for VACV, Fig. 33B. Interestingly, in tumors that received irradiation in combination with LIVP 1.1.1 a much more diffuse staining pattern for VACV protein A27L was visible, Fig. 33 C,D.
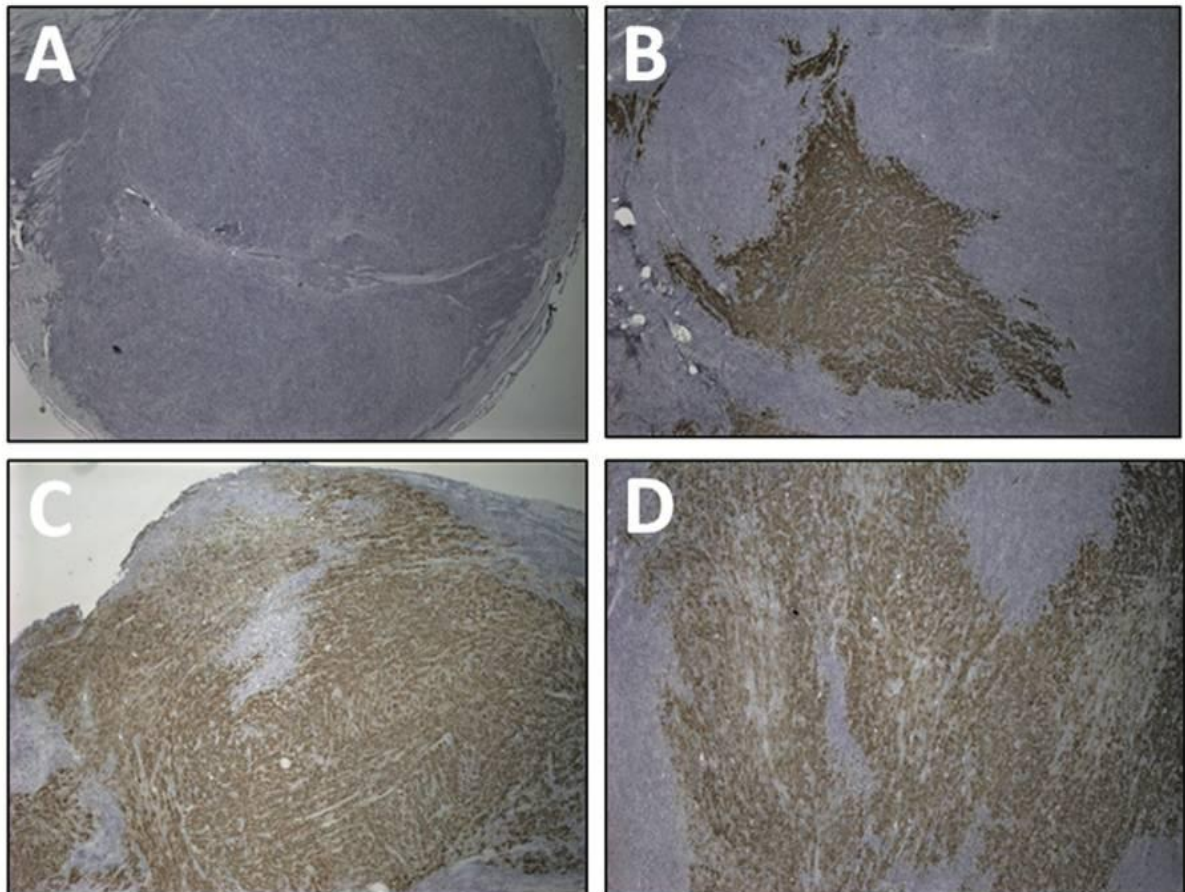
Fig. 33 Distribution of LIVP 1.1.1 in non-irradiated and irradiated U-87 glioma xenografts
IHC to VACV A27L in U-87 glioma xenografts harvested 7 days post LIVP 1.1.1 systemic injection. All pictures were taken at 2x magnification. **A)** Control U-87 xenografts from non-infected mice. **B)** LIVP 1.1.1 treatment alone. **C)** 6 Gy one day before LIVP 1.1.1 injection. **D)** 3.5 Gy one day before and one day after LIVP 1.1.1 injection.

RESULTS

The staining pattern for VACV protein was similar in both combination groups either when 6 Gy was given before LIVP 1.1.1 or if IR was given as 2 fractions of 3.5 Gy, 1 day before and after LIVP 1.1.1 systemic injection. Since the focus of our studies is to analyze interaction of radiation and virus, the IR doses we used in these sets of experiments were therapeutically suboptimal resulting in tumor xenograft growth delay but no extensive tumor damage. Therefore no necrosis was evident on H+E staining in irradiated xenografts compared to control xenografts at day 7. We then quantitated the number of infectious LIVP 1.1.1 viral particles in non-irradiated and irradiated glioma xenografts with the same experimental parameters. IR was given as a 6 Gy fraction one day before LIVP 1.1.1 systemic injection. Animals were sacrificed at day 7 and tumors were harvested. Tumors were homogenized and analyzed for viral amounts with standard plaque assay.

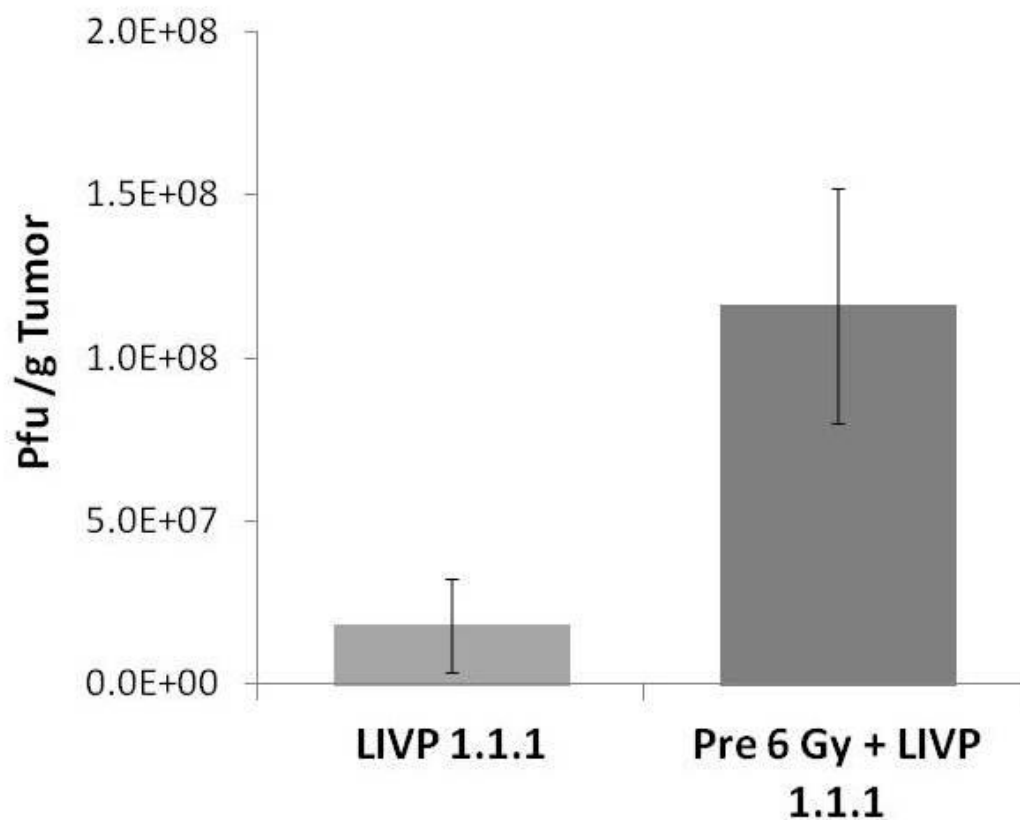**Fig. 34 Infectious LIVP 1.1.1 particles recovered from irradiated and non-irradiated U-87 glioma xenografts**
U87 xenografts were grown in the flanks of nude mice. IR was given as a single 6 Gy fraction one day before systemic LIVP 1.1.1 injection. Glioma xenografts were harvested 7 days post LIVP 1.1.1 injection and infectious viral particles were quantitated by standard plaque assay on CV-1 monolayer.

At day 7, glioma xenografts injected with LIVP 1.1.1 had a mean of 1.8 x 10^7 pfu/gram tumor and irradiated glioma xenografts had a mean of 12 x 10^7 pfu/gram tumor. Irradiation resulted in a statistically significant 6 fold increase in infectious viral particle production (p=0.03), Fig. 34 confirming increased viral replication in irradiated glioma xenografts as already observed for GLV-1h68.

4.3.6 IR in combination with oncolytic vaccinia virus induces a strong proinflammatory tissue response in U-87 glioma xenografts.

Since oncolytic VACV replication was enhanced within U-87 tumor xenografts, we then analyzed how the combination of IR and oncolytic VACV influenced the inflammatory cytokine profile within tumors. U-87 glioma xenografts from control mice and mice treated with LIVP 1.1.1, 6 Gy, or the combination of 6 Gy followed by LIVP 1.1.1, were harvested 7 days post infection. Two tumors of each treatment group were homogenized and analyzed for the expression of murine cytokines and proteins regulating inflammation, Table 7. The cut-off for analysis was set at least 1.5-fold up- or downregulation compared to control in both samples.

RESULTS

Table 7. *Mouse Immune Related Profiling of U-87 Glioma Xenografts*

A) Protein Expression Upregulated

Antigen Name	LIVP 111 / Control Ratio	6 Gy / Control Ratio	LIVP 111 + 6 Gy / Control Ratio
Monocyte Chemotactic Protein 1 (MCP-1)	2.3	1.9	16.4
Interleukin-18 (IL-18)	2.4	2.0	14.9
Monocyte Chemotactic Protein 3 (MCP-3)	2.3	1.9	13.9
Interferon gamma Induced Protein 10 (IP-10)	5.2	1.4	11.4
Interleukin-6 (IL-6)	1.2	3.3	9.8
Macrophage Inflammatory Protein-1 beta (MIP-1 beta)	3.0	1.0	7.8
Eotaxin	1.3	1.2	5.5
Granulocyte-Macrophage Colony-Stimulating Factor (GM-CSF)	5.3	1.4	4.9
T-Cell-Specific Protein RANTES (RANTES)	5.9	1.3	4.6
Macrophage Colony-Stimulating Factor-1 (M-CSF-1)	1.2	1.1	3.0
Lymphotactin	4.4	2.2	2.9
Interleukin-7 (IL-7)	1.0	1.1	2.9
Interleukin-11 (IL-11)	1.1	1.7	2.7
Macrophage Inflammatory Protein-1 gamma (MIP-1 gamma)	1.2	1.1	2.5
Macrophage Inflammatory Protein-1 alpha (MIP-1 alpha)	1.1	1.0	2.4
Vascular Cell Adhesion Molecule-1 (VCAM-1)	1.7	1.2	2.2
Fibroblast Growth Factor basic (FGF-basic)	1.5	2.4	2.2
Interleukin-2 (IL-2)	1.2	1.1	2.1
Tumor Necrosis Factor alpha (TNF-alpha)	1.1	1.1	2.0
Granulocyte Chemotactic Protein-2 Mouse (GCP-2 Mouse)	1.1	1.7	1.9
Interleukin-10 (IL-10)	1.0	1.1	1.9
Stem Cell Factor (SCF)	1.2	1.5	1.9
Endothelin-1 (ET-1)	1.2	1.4	1.8
Interferon gamma (IFN-gamma)	1.6	1.1	1.8
Leukemia Inhibitory Factor (LIF)	1.7	1.3	1.8
Growth-Regulated Alpha Protein (KC/GRO)	1.4	2.0	1.7
Oncostatin-M (OSM)	1.4	1.3	1.7
Macrophage Inflammatory Protein-3 beta (MIP-3 beta)	1.0	1.4	1.6

B) Protein Expression Downregulated

Antigen Name	LIVP 111 / Control Ratio	6 Gy / Control Ratio	LIVP 111 + 6 Gy / Control Ratio
Interleukin-1 beta (IL-1 beta)	1.4	1.2	9.8
Matrix Metalloproteinase-9 (MMP-9)	1.3	3.0	2.9
Tissue Factor (TF)	1.0	3.1	2.5

Fold Upregulation	Fold Downregulation
>1	>1
2-5	2-5
5-10	5-10
>10	

83

RESULTS

Radiation alone had minimal effects on the expression of murine inflammatory cytokines. As expected, LIVP 1.1.1 replication in the tumor resulted in increase in inflammatory cytokines, in particular RANTES, GM-CSF, IP-10, lymphotactin, and MIP-1 beta. Interestingly, the combination of 6 Gy followed by LIVP 1.1.1 injection resulted in a robust proinflammatory reaction within the tumor. Four cytokines were expressed greater than 10 fold (MCP-1, IL-18, MCP-3, and IP-10). In addition, the majority of the remaining cytokines profiled were higher in the combined treatment group compared to LIVP 1.1.1 or 6 Gy alone. IL-1 beta was interesting in that it was the only cytokine strongly down-regulated by the combination of 6 Gy and LIVP 1.1.1.

4.4 In a bilateral glioma tumor model, systemically delivered oncolytic vaccinia virus preferentially replicates in focally irradiated glioma xenografts.

Our experiments so far have indicated that oncolytic VACV increased marker gene expression, viral replication as well as viral spread within the irradiated tumor when compared to non-irradiated tumors derived from mice that received VACV alone. To further pursue whether focal IR could serve to target systemically delivered virus to replicate preferentially within irradiated tumors, U-87 xenografts were grown bilaterally in both flanks of athymic nude mice. Fig. 35 illustrates the experimental setup for this study.
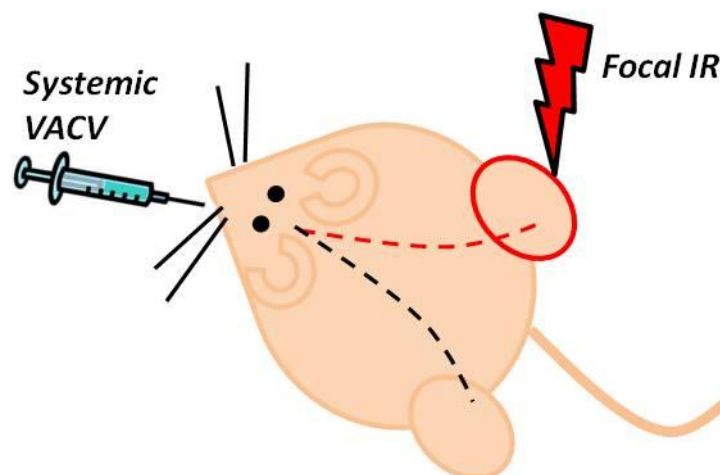
Fig. 35 Individual mouse with bilateral tumors treated with systemic VACV and focal IR to one side
In this model, U-87 glioma xenografts were established in both flanks of individual mice. IR is delivered to only one flank tumor whereas the non-irradiated tumor of the same mouse serves as control.

In each mouse two glioma xenografts were established, one on each hindlimb. GLV-1h68 was injected systemically by retro-orbital inoculation and a single dose of 6 Gy was given

focally to the exposed right flank tumor. The rest of the mouse including the left flank tumor was shielded with lead to block out >95% of the dose as determined by dosimetry. Here, each mouse serves as its own control with identical environmental conditions as well as viral injection; with the only difference that one tumor receives IR while the contralateral tumor is shielded. As a control, to prove IR was focally delivered to one tumor, glioma xenograft volumes were measured until the tumors were harvested at day 9 for histology and viral titers.

Fig. 36 Bilateral flank tumor volumetric response to focal IR or systemic GLV-1h68
U-87 glioma xenografts were grown in the bilateral flanks of mice. **A)** Buffer was injected systemically on day 0. IR was given focally as single 6 Gy fraction to the right flank tumor one day before buffer injection. The remainder of the mouse and the left flank tumor were shielded with lead. Serial measurements of fractional tumor volumes of the left and right flank glioma xenografts were plotted as FTV. **B)** Systemic GLV-1h68 injected on day 0 and no IR was delivered to either flank.

RESULTS

In the group treated with systemic buffer injection and focal IR to the right flank, the shielded left flank tumor grew exponentially whereas the exposed irradiated right flank tumor showed tumor growth delay, Fig. 36A. The difference between the shielded left tumor xenograft volumes and exposed right tumor xenograft volumes was statistically significant by day 9 ($p<0.05$). In the group treated with systemic GLV-1h68 alone, Fig. 36B, both the right and left tumors grew similarly and tumor volumes were not different. In the group treated with systemic GLV-1h68 and focal right flank irradiation, the exposed right flank tumors were significantly smaller than the unblocked left flank tumors ($p<0.05$), Fig. 37.
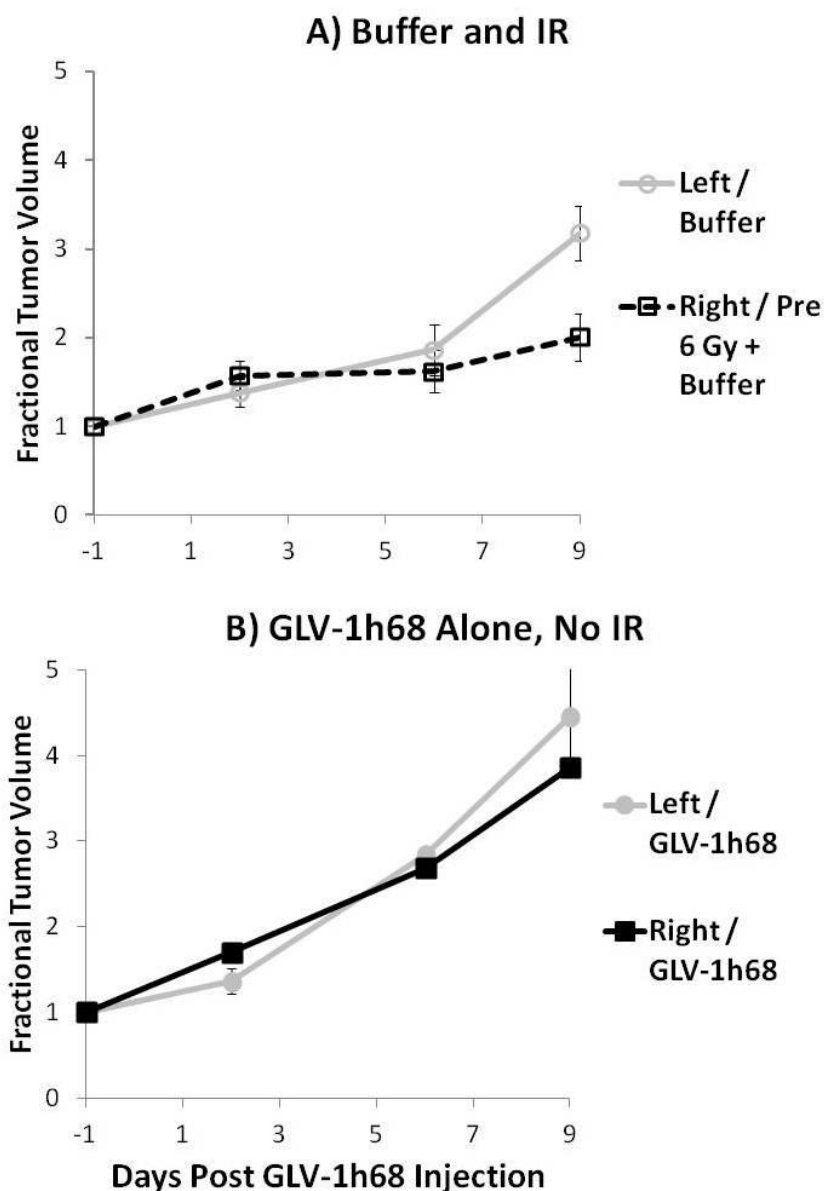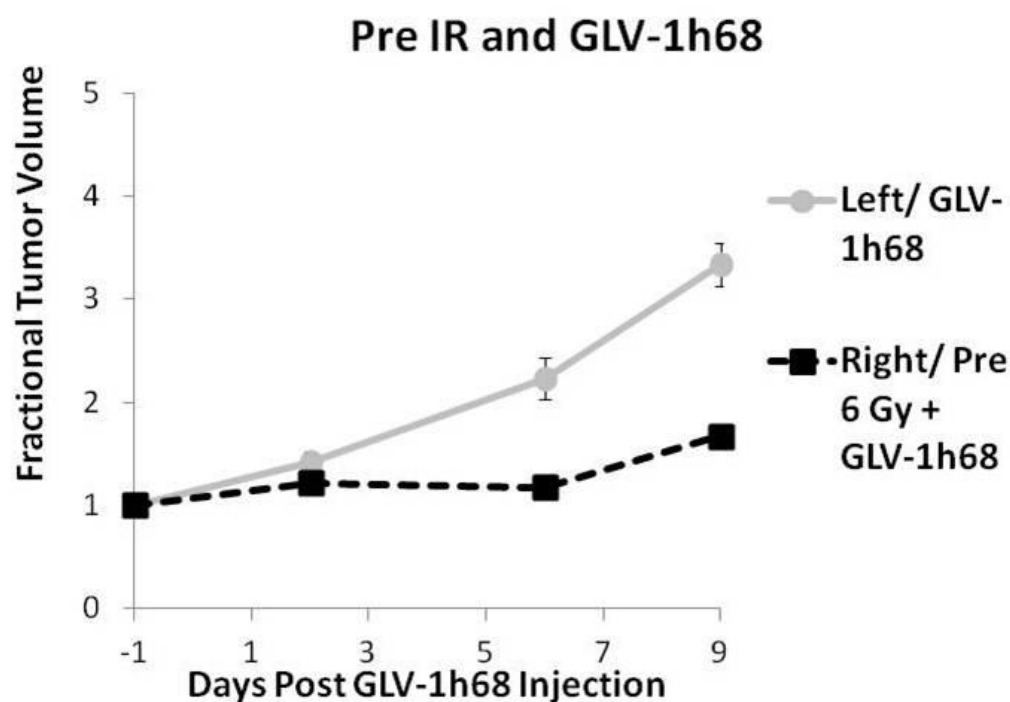

Fig. 37 Bilateral flank tumor volumetric response to focal IR and systemic GLV-1h68
    U-87 glioma xenografts were grown in the bilateral flanks of mice and GLV-1h68 was injected systemically. IR was given focally as single 6 Gy fraction one day before viral injection to the right flank tumor. The remainder of the mouse and the left flank tumor were shielded with lead. Serial measurements of fractional tumor volumes of the left and right flank glioma xenografts are shown.

In these mice with bilateral flank glioma xenografts, we determined how well systemically delivered GLV-1h68 replicated in the shielded left flank tumor compared to the right flank tumor exposed to 6 Gy. First we analyzed virus encoded marker gene expression. Of the six mice treated with systemic GLV-1h68 and focal IR to the right flank, all six mice had higher GFP expression in the irradiated exposed right flank tumor compared to the shielded left flank tumor, Fig. 38A, B.
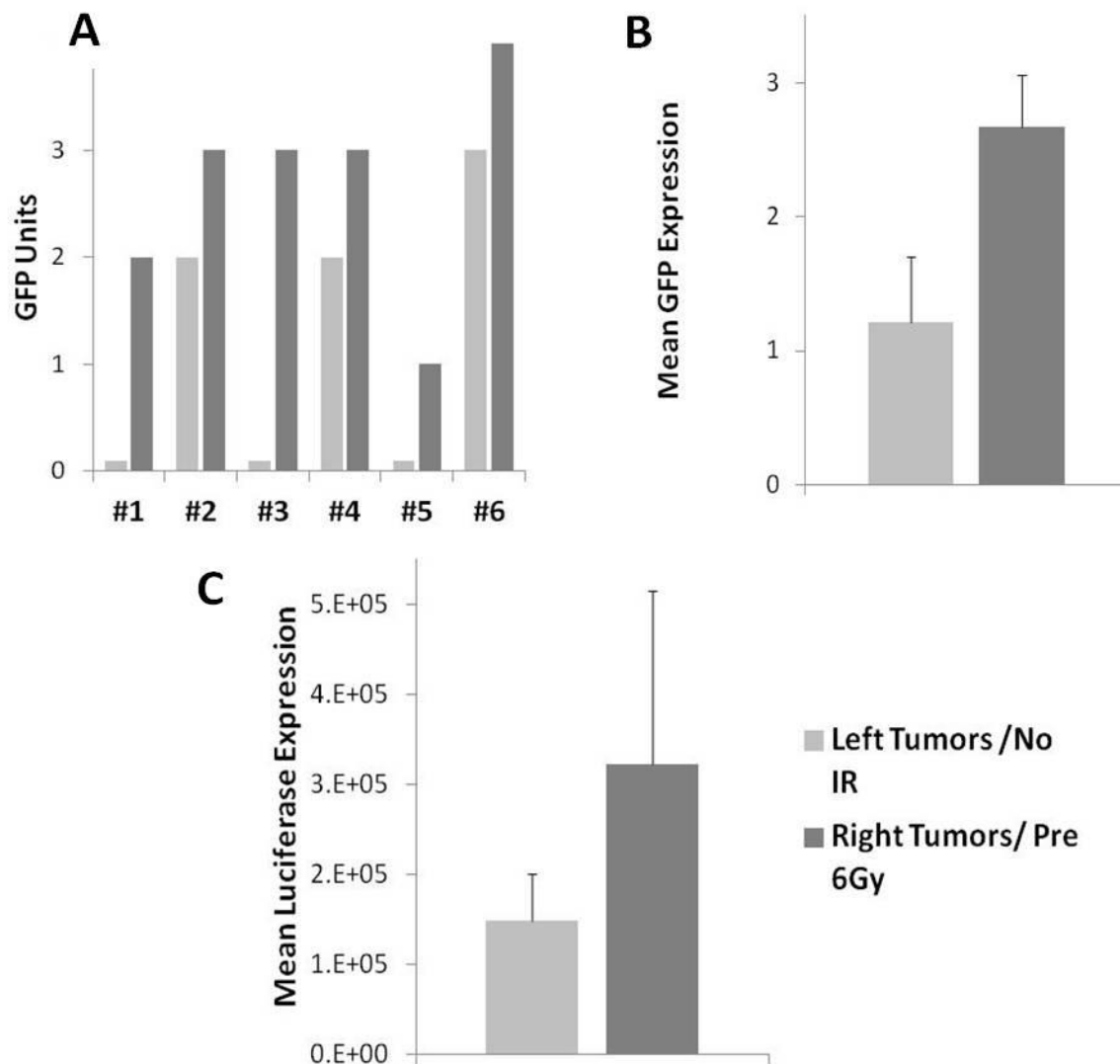
Fig. 38 GLV-1h68 reporter gene expression, A) GFP individual, B) mean and C) luciferase in animals with bilateral glioma xenografts.
U-87 glioma xenografts were grown in the bilateral flanks of mice and GLV-1h68 was injected systemically. IR was given focally as single 6 Gy fraction one day before viral injection to the right flank tumor. Seven days after systemic injection mice were analyzed for GFP and luciferase expression in both tumors.

In accordance with results obtained for GFP, GLV-1h68-encoded luciferase expression was also 2-fold higher in the irradiated flank tumor compared to the contralateral shielded flank tumor, see Fig. 38C. GFP and luciferase expression from two representative mice are shown in Fig. 39. We picked mice with similar size tumors on both sides to prove that GFP or luciferase signal are not masked due to bigger tumor mass. Here, the upper panel shows brightfield and GFP pictures. GLV-1h68 encoded GFP expression was higher in the irradiated right flank tumor (upper flank) compared to the shielded left flank tumor (lower flank). The lower panel shows luciferase activity (photons/minute) as well as an overlay of

luciferase activity with mouse contour. The GFP luciferase expression was higher in the irradiated tumor (upper flank) when compared to its non-irradiated counterpart (lower flank).
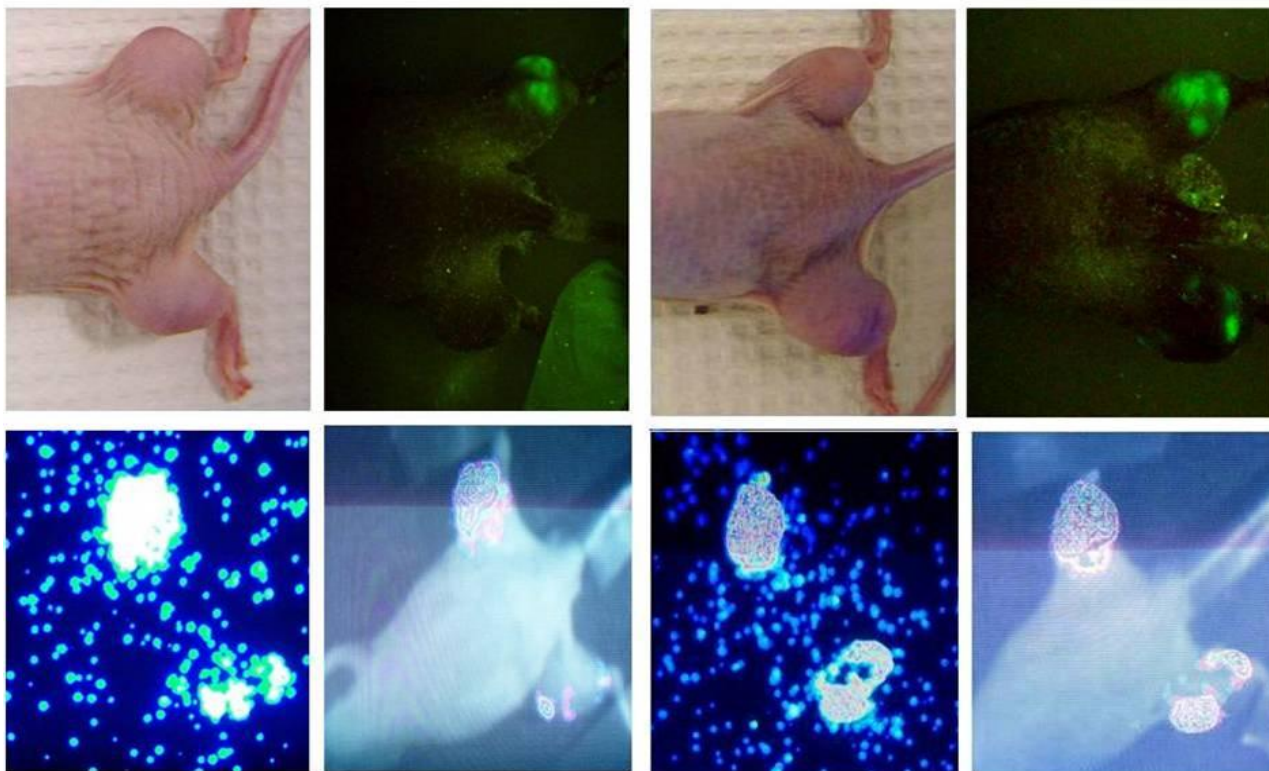
Fig. 39 GLV-1h68 reporter gene expression in two representative mice with bilateral glioma xenografts
U-87 glioma xenografts were grown in the bilateral flanks of mice and GLV-1h68 was injected systemically. IR was given focally as single 6 Gy fraction one day before viral injection to the right flank tumor. The remainder of the mouse including the left flank tumor was shielded with lead. 6 Gy was given focally to the right flank tumor (upper tumor) with the left flank (lower tumor) shielded. Upper left panel: Brightfield, Upper right panel: GFP expression, Lower left panel: Luciferase activity (photons/minute), Lower right panel: Overlay of luciferase activity photon count with mouse contour.

Finally, bilateral xenografts were harvested on day 9 and fixed in neutral buffered 10% formalin followed by dehydration. Tumors were embedded in paraffin and 5 µm sections were cut and stained for VACV protein A27L. Consistent with viral GFP and luciferase expression, IHC staining revealed a greater distribution of VACV protein in the irradiated right flank tumor compared to the shielded left flank tumor, Fig. 40.
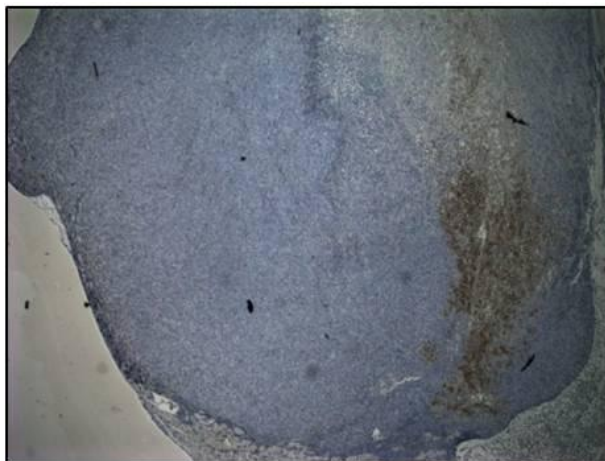
Left Flank Tumor Shielded from IR

Right Flank Tumor Exposed to IR

Fig. 40 IHC to VACV A27L in non-irradiated (left) and irradiated (right) xenografts
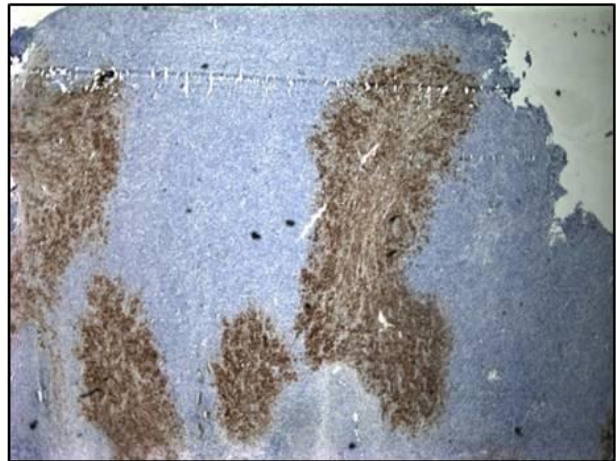U-87 glioma xenografts were grown in the bilateral flanks of mice and GLV-1h68 was injected systemically. IR was given focally as single 6 Gy fraction one day before viral injection to the right flank tumor. IHC to VACV 9 days after GLV-1h68 systemic injection in shielded left flank tumor (left panel) and irradiated right tumor (right panel). Pictures were taken at 2x magnification.

In our bilateral animal tumor model, where oncolytic vaccinia virus was delivered systemically to infect both tumors equally and focal IR was delivered to the right tumor one day prior to virus administration, we could show that the irradiated glioma xenograft had higher levels of viral gene expression and viral replication.

4.5 Focal IR does not alter tumor vessel permeability of U-87 glioma xenografts.

Our studies so far clearly demonstrated an increase in viral colonization as measured by increase in viral marker gene expression, viral titers and viral distribution in tumors that received a dose of 6 Gy one day prior to VACV administration. To determine whether the focal dose of 6 Gy increases permeability of the tumor vasculature at the time of systemic virus delivery we performed an Evans Blue dye assay. U-87 glioma xenografts were grown in the flanks of nude mice as described previously. When tumor reached a size of approximately 250 mm^3 tumors were irradiated with a focal dose of 6 Gy to the tumor as in previous experiments. One day after irradiation 1.5% Evans Blue dye in PBS was injected systemically, similar to the time of oncolytic VACV injection. Non-irradiated and irradiated tumors along with spleens were analyzed for vessel permeability. The dye was allowed to circulate for 45 min. Mice were sacrificed and perfused with 20 ml PBS to flush excessive dye out of the vessels. Tumors and spleens were harvested and placed in 1 ml of N, N-

RESULTS

Dimethylformamide per 0.1 g tissue. Dye extraction was performed at 55 °C for 72 h and absorbance was quantified at 620 nm. Values were normalized to dye extracted from the spleen of the same mouse. We found that there was no significant difference (p=0.134) in dye extravasation in non-irradiated versus irradiated tumors. The mean normalized Evans Blue extravasation of control and irradiated tumors is shown in Fig. 41.
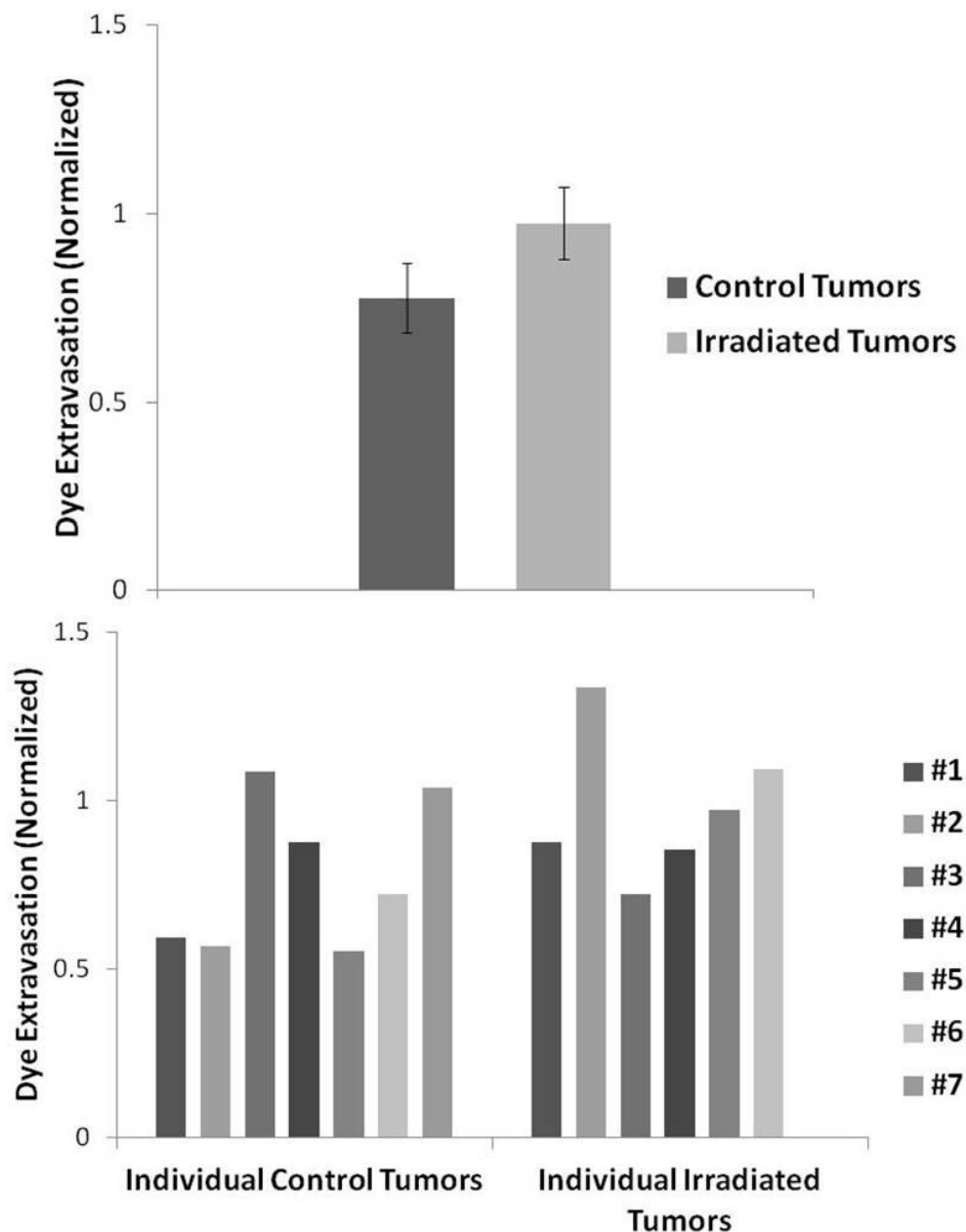
Fig. 41 Tumor vessel leakiness in irradiated and non-irradiated U-87 glioma xenografts
U-87 glioma xenografts were grown s.c. and focally irradiated with 6 Gy. One day post irradiation 1.5% Evans Blue dye was injected systemically and allowed to circulate for 45 min. Mice were perfused with PBS and control (n=7) and irradiated (n=6) tumors were harvested. Evans Blue dye was extracted from tumors tissue with N, N- Dimethylformamide and quantitated spectrometically at 620 nm. All values were normalized to spleen.

These data suggest, that increased viral replication in irradiated tumors is not due to a higher viral dose that reaches the irradiated tumor initially because of increased permeability of vessels.

4.6 Cell culture analysis of interaction of VACV and IR

4.6.1 Influence of combination of VACV and IR on cell cycle

To further elucidate the interaction IR and VACV, we analyzed whether IR and VACV have an influence on cell cycle progression. IR is known to induce an arrest in cell cycle due to DNA damage and VACV was reported to modulate the cell cycle as well [91]. To analyze IR or VACV induced effects on cell cycle U-87 cells were treated with virus or radiation alone or the combination of both. For combination treatment a dose of 6 Gy was given 6 h after viral infection. Propidium iodide staining to label DNA was performed and samples were analyzed for DNA content by flow cytometry. Fig. 42A shows the representative cell cycle response to IR. Here, when compared to non-irradiated cells the percentage of cells in G_2/M phase increases due to activation of checkpoint kinases with a resultant cell cycle block in G_2 as a result of DNA damage by IR.
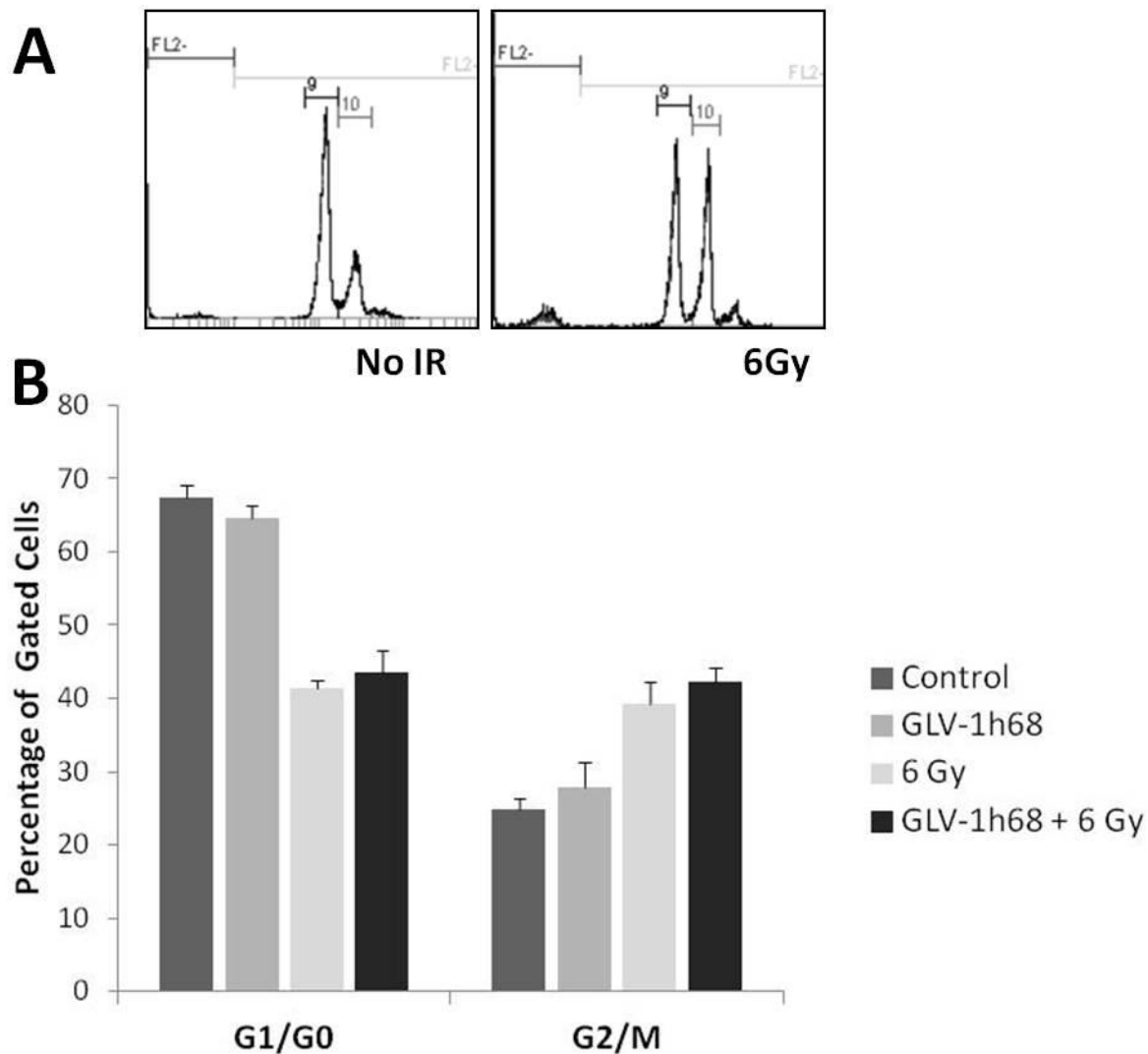
Fig. 42 Influence of IR and GLV-1h68 on distribution of cells in different phases of the cell cycle
Human U-87 glioma cells were grown in dishes and treated with IR or VACV only or the combination of both. Samples were stained for DNA content with propidium iodide and analyzed by flow cytometry. **A)** Increase in cells in G_2/M phase (second peak) upon irradiation **B)** Percentage of gated cells in different cell cycle phases.

In non-irradiated cells the majority of cells were in the G_1/G_0 phase of the cell cycle, 67.5%, whereas approximately 25% of cells were in G_2/M phase of the cycle. Cells that were infected with GLV-1h68 did not show any alterations in distribution of cells in phases of the cell cycle compared to non-irradiated cells. Upon irradiation the number of cells in G_1/G_0 phase of the cell cycle decreased to 42% and cells accumulated in G_2 phase of the cell cycle as a response to IR induced DNA damage, 40%, Table 8.

Table 8. *Distribution of virus infected and irradiated cells in cell cycle*

	Percent of cells in G_1/G_0 phase	Percent of cells in G_2/M phase
Control	67.5	24.8
GLV-1h68	64.6	27.9
6 Gy	41.4	39.3
6 Gy + GLV-1h68	43.5	42.1

Upon virus infection, there were no differences in irradiated and non-irradiated cell cycle populations. Cells treated with the combination of GLV-1h68 and 6 Gy exhibit a similar distribution within the cell cycle than irradiated cells, indicating that in our experimental conditions, VACV has no influence on distribution of cells in the stages of the cell cycle.

4.6.2 Influence VACV on induction of double strand breaks by IR

The critical and most lethal lesion IR induces in cells is DNA double-strand breaks. In this experiment we determined whether infection of cells with GLV-1h68 or LIVP 1.1.1 had an influence on the number of DNA double-strand breaks induced by IR or on the kinetics of their resolution. Human U-87 glioma cells were grown on cover slips and after 24 h in culture infected at an MOI of 5 with GLV-1h68 or LIVP 1.1.1, respectively. Control cells remained uninfected. One hour after virus infection one set of cells was irradiated with 6 Gy. At 1, 6 and 24 hours after irradiation cells were fixed, permeabilized, blocked and incubated with a mouse-monoclonal antibody against γ-H2AX to label DNA double strand breaks. γ-H2AX is serine 139 phosphorylated histone protein H2A, and is one of the first proteins phosphorylated upon DNA damage and recruited to the site of DNA damage. The primary antibody was detected by an Alexa-Fluor647 labeled goat anti-mouse secondary antibody and cells were counterstained with DAPI. For each treatment condition, the number of γ-H2AX foci was scored in 75 to 100 cells, Fig. 43.
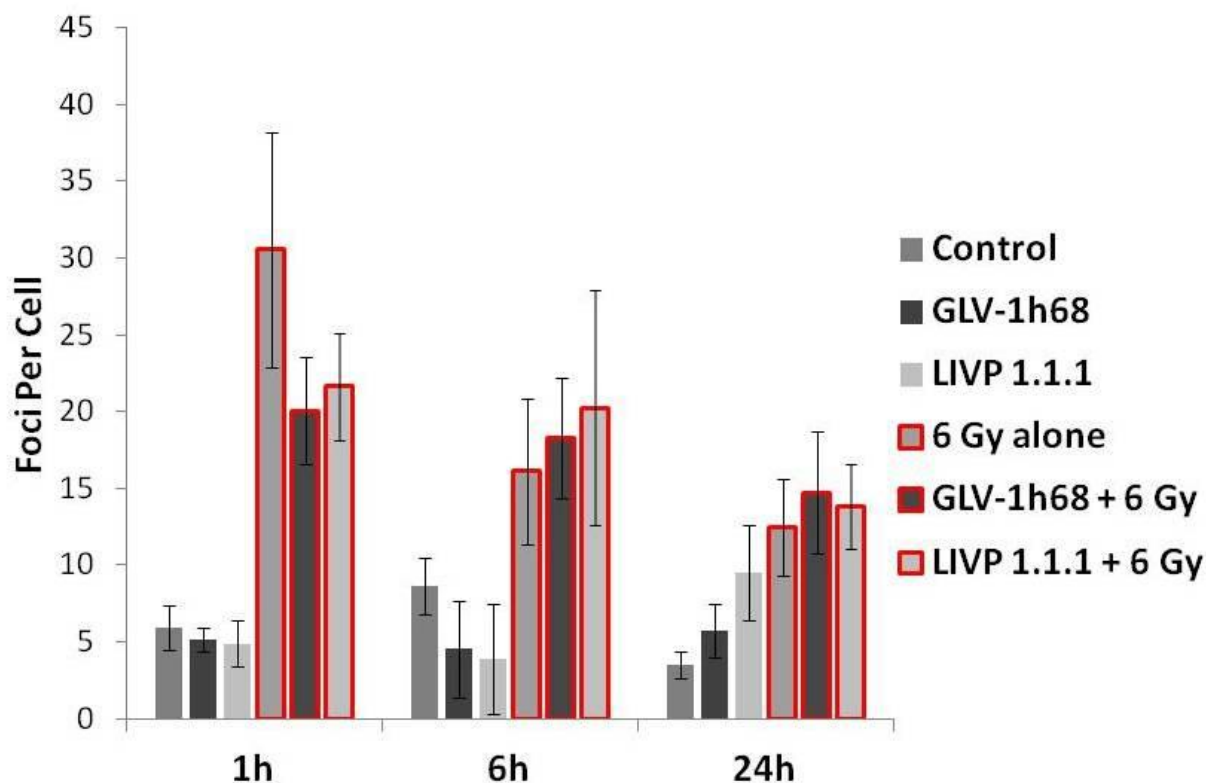
Fig. 43 γ-H2AX Foci per cell upon infection with GLV-1h68 or LIVP 1.1.1 in irradiated and non-irradiated glioma cells
Human U-87 glioma cells were grown on cover slips and infected with GLV-1h68 or LIVP 1.1.1 with an MOI of 5, respectively. Control cells remained uninfected. One hour after virus infection cells were irradiated with 6 Gy. Double-strand breaks were labeled by staining IHC staining of γ-H2AX. Foci were scored in 75 to 100 cells

Immunohistochemistry staining of γ-H2AX foci as an indicator of DNA-double strand breaks after irradiation, showed an expected pattern. Shortly after IR, a clear increase in γ-H2AX foci was observed. While levels of γ-H2AX were found to remain elevated 6 h post IR they decreased towards baseline by 24 h after IR when DNA damage is either resolved or cells begin to die. We were not able to detect any significant differences in number of γ-H2AX foci in cells that were in addition to being irradiated also infected with VACV. Values of γ-H2AX foci were comparable amongst control, GLV-1h68 or LIVP 1.1.1 infected samples and also amongst irradiated and irradiated plus VACV infected samples.

4.6.3 Influence of IR on the expression of thymidine kinase 1 (TK-1) in U-87 cells in cell culture

We have established in animal models that both VACV tested so far, GLV-1h68 and LIVP 1.1.1, interacted with IR and showed a preferential replication in irradiated tumors. A possible mechanism is that IR upregulates specific genes in the host cell that provide trans-

completion of genes deleted from the viral genome to achieve attenuation and safety. In this scenario, oncolytic VACV replication would be increased since the virus is temporarily reverted towards a more wild-type state, which has an inherent ability to replicate more efficiently. The only gene disrupted in both GLV-1h68 as well as LIVP 1.1.1 is vaccinia encoded thymidine kinase. In order to carry out replication in a host cell oncolytic VACV utilizes cellular TK-1. This is in part a reason for the tumor cells restricted replication of VACV, since TK-1 is often upregulated in cancer cells. We were interested to see if IR can further increase expression of cellular TK-1 and hence, potentially increase replication of the virus.

Human U-87 glioma cells were grown in culture and irradiated at a dose of 6 Gy. At 2, 6, 12 and 24 hours post irradiation total cellular RNA was isolated and 1 µg of RNA from each sample was converted to cDNA. Samples were analyzed mRNA expression changes by semi quantitative PCR using primers to cytosolic thymidine kinase-1 (TK-1). Human GAPDH a housekeeping gene necessary for glycolysis was used as an internal control gene. TK-1 expression was normalized to expression in non- irradiated control cells and human GAPDH was used for the internal control.

.

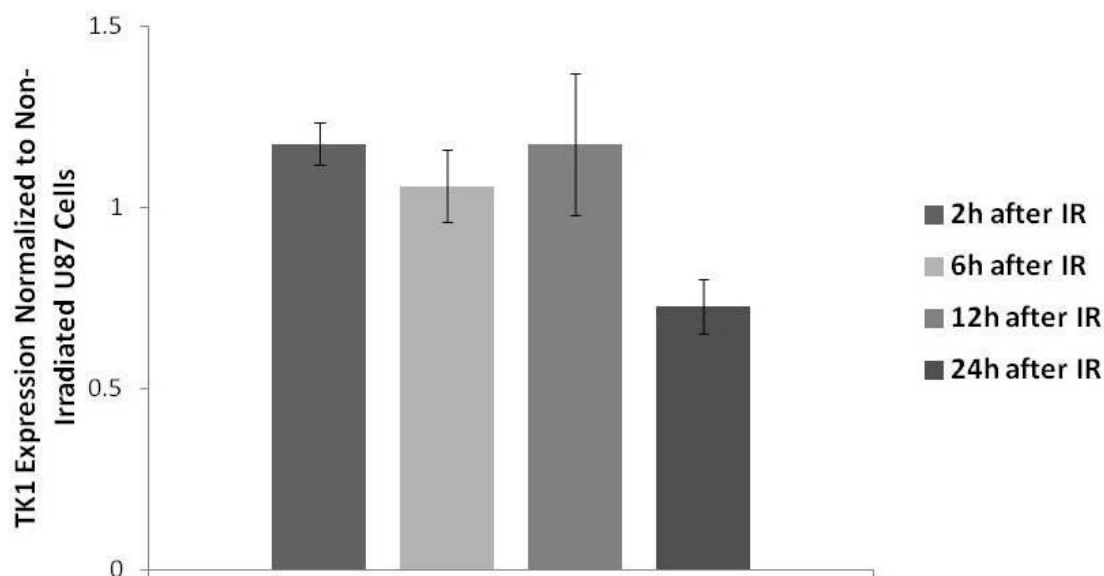**Fig. 44 Cellular levels of cytosolic thymidine kinase after IR**
Human U87 glioma cells were grown in 6-well plates and irradiated at a dose of 6 Gy. At different times after IR total cellular RNA was isolated and converted into cDNA. Samples were analyzed by semi-quantitative PCR using primers for gene expression of TK 1. GAPDH served at as internal control. TK-1 RNA transcription was normalized to non-irradiated cells.

Fig. 44 shows the expression of cytosolic thymidine kinase 1 in irradiated U-87 glioma cells at 2, 6, 12 and 24 hours after irradiation normalized to non-irradiated control cells. At 2, 6 and 12 hours post irradiation TK-1 expression remained comparable to non-irradiated cells. However, 24 hours post irradiation we found a slight decrease in TK-1 expression most likely due to an overall decrease in gene transcription in regard of irradiation of cells. We concluded that increased replication of VACV is not secondary to higher levels of TK-1 in irradiated cells.

4.7 Tumor radiosensitization through the use of an anti-angiogenic VACV

In the initial series of experiments we established that oncolytic VACV and IR interact. We were able to show increased replication followed by improved tumor control in irradiated subcutaneous and orthotopic xenografts. In an attempt to further improve tumor control we decided to analyze interaction of IR with a VACV carrying a therapeutic backpack to increasing responsiveness to radiation and simultaneously to block radioprotective effects on cells induced by IR. In the following series of experiments, we used a VACV that expressed a single-chain antibody directed against human and murine VEGF.

4.7.1 In irradiated tumor cells VEGF is unregulated as part of the cellular stress response to ionizing radiation

Irradiation of cells leads to the induction of a multi-facetted stress response. Studies to date have proposed a connection between induction of angiogenesis and IR, meaning that radiation is involved in initiating the angiogenic process [37]. We were interested in whether irradiation of human glioma cells U-87 leads to an induction of VEGF which in tumors might tip of the angiogenic switch towards neovascularization and angiogenesis. U-87 cells were seeded in 6-well plates at a low confluency (30%) and irradiated with a dose of 10 or 20 Gy. At 24, 48 and 72 h post irradiation, the concentration of VEGF in the cell supernatant was quantitated by ELISA. Cells in each well were trypsinized and counted, to normalize VEGF levels as pg VEGF/10^6 cells
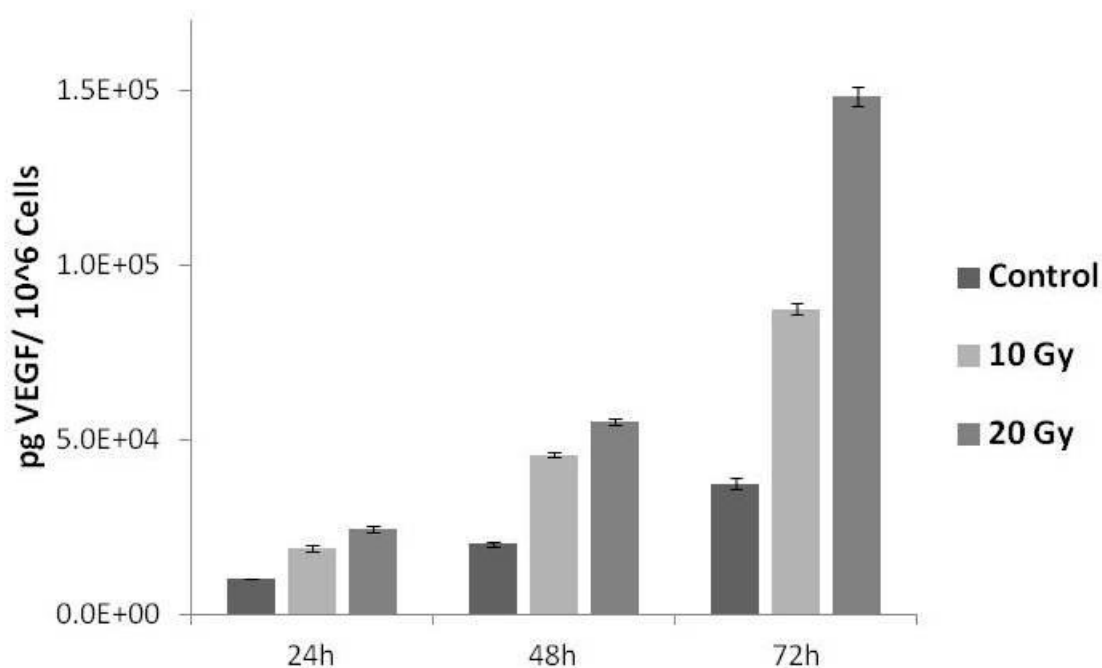
Fig. 45 Time and dose dependent upregulation of VEGF
U-87 cells were seeded in 6-well plates and irradiated with doses of 10 or 20 Gy. At 24, 48 and 72 h post irradiation the VEGF concentration in the cell supernatant was quantitated by ELISA and normalized to cell number.

Irradiation of U-87 glioma cells in culture lead to an upregulation of VEGF, Fig. 45. This upregulation occurred in a time and dose dependent fashion. Seventy-two hours after irradiation the concentration of VEGF has increased 8.7 fold for cells irradiated with 10 Gy and 14.8-fold for a dose of 20 Gy when compared to non-irradiated cells at 24 h.

4.8   Targeting VEGF levels by GLAF-1 to increase the radiosensitivity of endothelial cells

In addition to induction of angiogenesis VEGF is also known to promote radioresistance in endothelial cells [36]. In the next experiment, we analyzed whether increasing concentrations of VEGF affect sensitivity of endothelial cells to IR and whether we can block VEGF induced radioprotective effects, Fig. 46. In this experiment HUVECs were exposed to increasing concentrations of recombinant VEGF-A and irradiated with a dose of 10 Gy 4 h post treatment. HUVEC survival was assessed by XTT assay and normalized to non-irradiated control cells. Relatively low concentrations of VEGF-A (50 ng/ml) increased cell survival following IR by 15%.
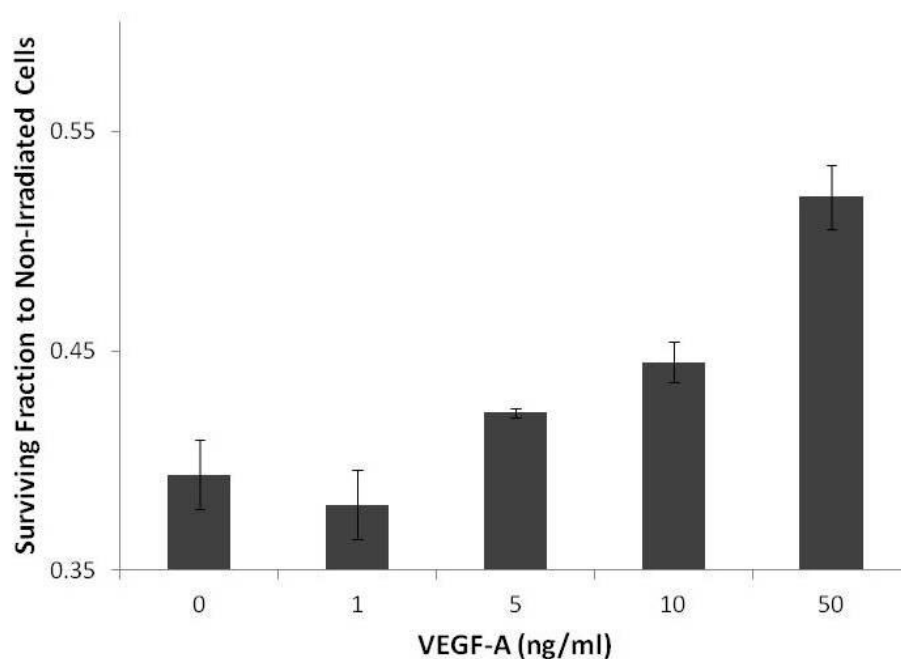
Fig. 46 VEGF-mediated radioresistance of human endothelial cells
Human Umbilical Vein Endothelial Cells were treated with increasing concentrations of recombinant VEGF-A. Cells were irradiated with 10 Gy and cell survival was analyzed 6 days post irradiation and normalized to non-irradiated cells.

We were next interested, whether the effects of VEGF on endothelial cells to decrease VEGF-induced radioresistance could be therapeutically targeted. HUVECs exposed to a constant concentration of VEGF-A were treated with increasing concentrations of GLAF-1. GLAF-1 is a single-chain antibody directed against human and murine VEGF that is expressed by the oncolytic VACV GLV-1h109. CV-1 cells were infected with GLV-1h109 at an MOI of 1 and GLAF-1 was immunoprecipitated from infected cell supernatant using a FLAG immunoprecipitation kit since the GLAF-1 antibody contains a FLAG tag. HUVECs were irradiated at a dose of 10 Gy after treatment with constant concentration VEGF and increasing concentrations of GLAF-1. Simultaneously, the same experiment was performed with glioma cells instead of HUVECs.
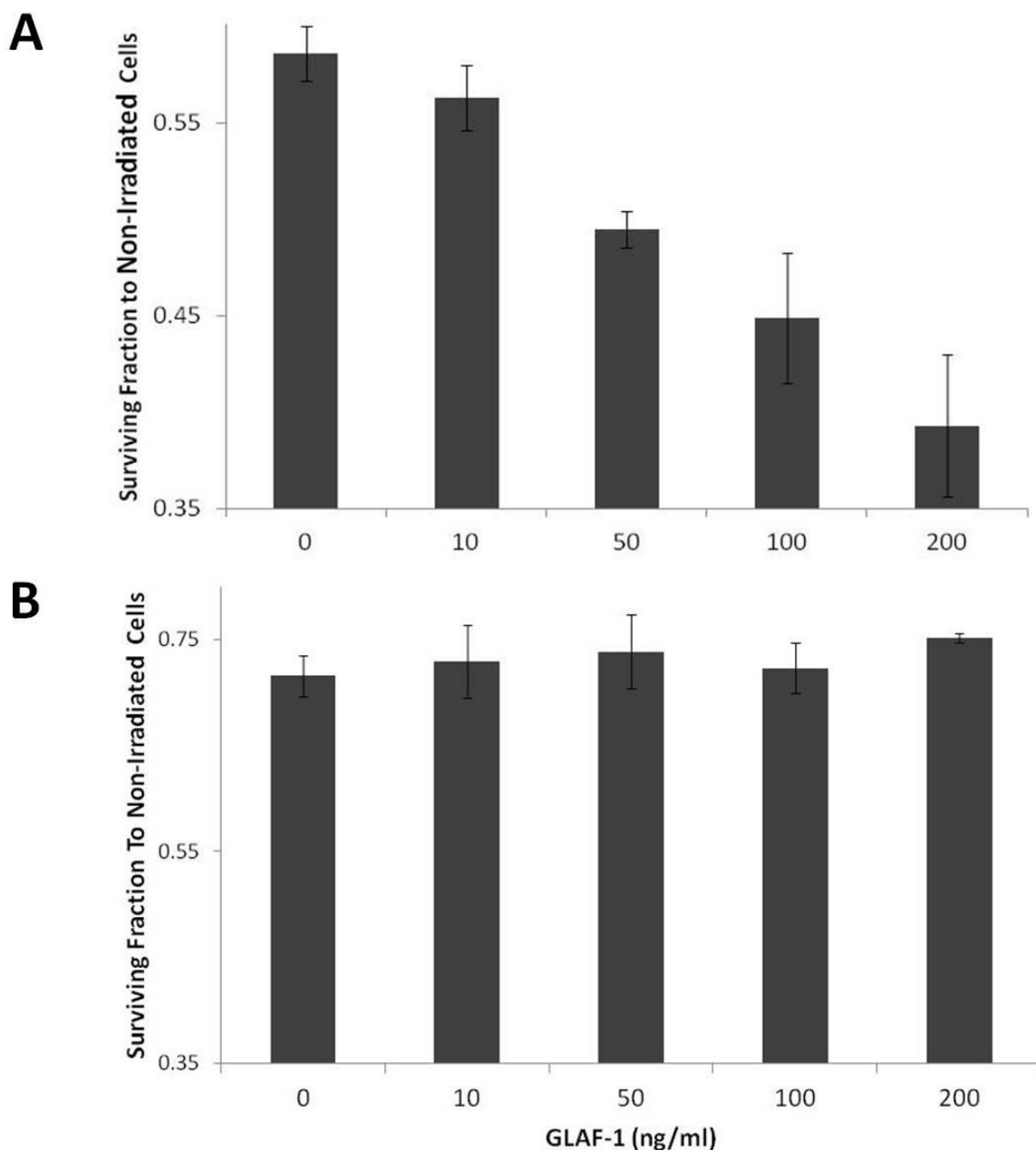
Fig. 47 Manipulation VEGF levels on endothelial (A) and U-87 glioma cells (B)
Cells were treated with increasing concentrations of purified VACV encoded GLAF-1 and constant VEGF-A. Four hours after treatment cells were irradiated with 10 Gy and cell survival was analyzed 6 days post irradiation and normalized to non-irradiated cells.

As shown in Fig. 47 GLAF-1 can block the radioprotective effects mediated by VEGF-A. Increasing concentration of GLAF-1 rendered VEGF exposed HUVECs sensitive to irradiation (Fig. 47A) but GLAFs effects were not observed in U-87 glioma cells (Fig. 47B) making it a phenomenon specific to the tumor vasculature rather than the tumor cells.

By treating tumors with an oncolytic VACV expressing an antibody targeting VEGF, the inherent oncolytic efficacy of the virus can be combined simultaneously with a decrease in VEGF levels within the tumor microenvironment. Such a treatment strategy will allow IR to enhance tumor cell oncolysis by VACV and also radiosensitize the tumor endothelial cells though VACV produced GLAF-1.

4.8.1 Combining IR with and anti-angiogenic VACV improves tumor control in a subcutaneous glioma model

Next, we determined whether we could further improve tumor control when IR is combined with the anti-VEGF expressing oncolytic VACV. The oncolytic virus we used was GLV-1h164 which, like GLV-1h109, expresses a single-chain antibody to target VEGF but without the FLAG tag. In this experiment, we were working with a fractionated radiation scheme, which is more clinically relevant. In addition, to fully exploit anti-angiogenic therapy as a radiosensitizer, increasing the number of fractions of IR potentiates GLAF-1 mediated radiosensitivity of endothelial cells. U-87 glioma xenografts were established in the right hindlimb of athymic nude mice and treatment was initiated when tumors reached a size of approximately 200-300 mm^3. In the irradiated groups, four doses of 4 Gy were given to the tumor bearing hindlimb while the remainder of the mouse was shielded with lead as described previously. The radiation was administered in two fractions per week at day -1, +1, +6 and +8 with respect to virus delivery on day 0. Three different VACV, GLV-1h68, GLV-1h100 and GLV-1h164, were injected systemically at a dose of 2 x 10^6 pfu in 0.1 ml PBS by retro-orbital inoculation. To control for improvement of tumor control by GLAF-1 encoding VACV, we used GLV-1h100. GLV-1h100 represents the backbone virus for GLV-1h164 and the direct intermediate between GLV-1h68 and GLV-1h164, since GLV-1h164 was constructed by insertion of GLAF-2 into the HA locus of GLV-1h100 and GLV-1h100 was constructed by insertion of hNET into the TK locus of GLV-1h68. Tumor volumes were measured twice a week and plotted as mean fractional tumor volume, Fig. 48.
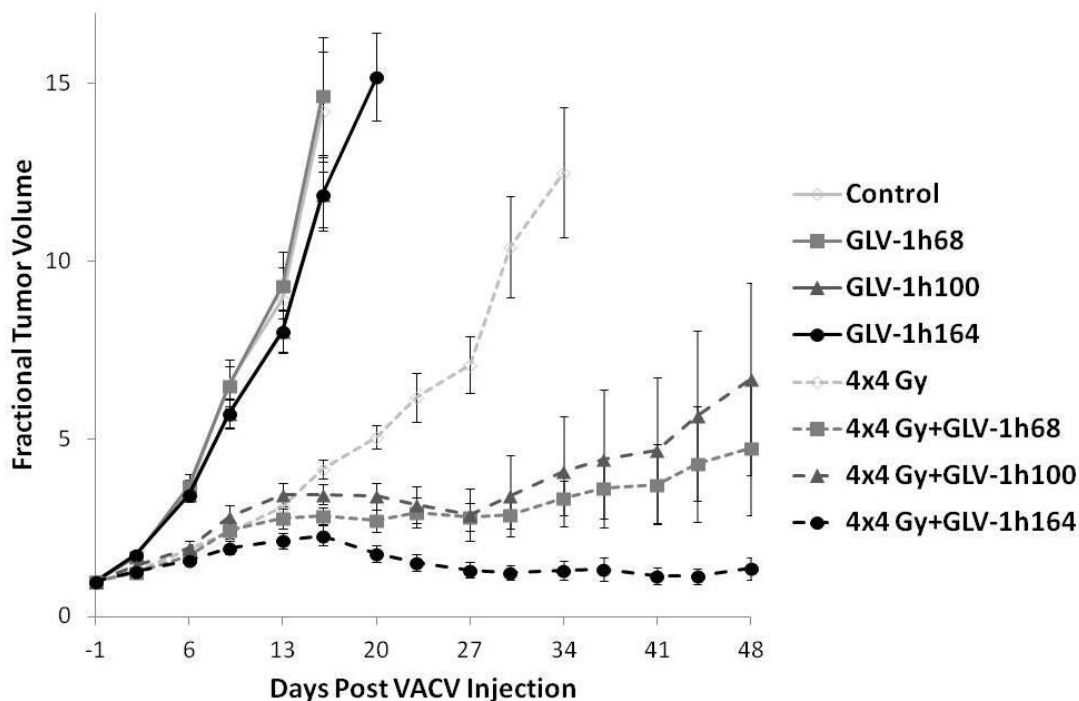
Fig. 48 Inhibition of glioma xenograft growth in animals treated with combination of systemic VACV and focal fractionated radiation.
Subcutaneous U-87 xenografts were grown in flanks of athymic nude mice. GLV-1h68, GLV-1h100 and GLV-1h164 were injected systemically on day 0. IR was given in four fractions of 4 Gy at day -1, +1, +6 and +8 with respect to viral injection. Glioma xenografts were measured twice a week and plotted as fractional tumor volume.

As observed in previous experiments, untreated control xenografts as well as tumors treated with $2x10^6$ VACV alone grew up exponentially and mice had to be sacrificed by day 16 for control, GLV-1h68 and GLV-1h100 injected animals. GLV-1h164 injection alone showed only minimal benefits on tumor control and mice were taken out of the experiment secondary to tumor burden by day 20. Ionizing radiation delivered in four fractions of 4 Gy resulted in an initial tumor growth delay and mice had to be sacrificed by day 38, which was three weeks after control mice. As expected, the tumor growth delay induced by multiple 4 Gy fractions as observed in this study was longer than in previous studies where mice only received a single dose of 6 Gy. Both GLV-1h68 and GLV-1h100 in combination with 4x4 Gy resulted in a strong anti-tumor effect and in both groups 5 out of 8 mice were alive at study endpoint 50 days after viral administration. However, the best volumetric tumor response was observed in animals treated with the combination of fractionated IR and anti-VEGF expressing VACV, GLV-1h164. Tumors in that group were significantly smaller than tumors of all other groups. By day 20 after viral administration 7 out of 8 mice had a fractional tumor volume that was smaller than 2 times the starting volume. In contrast only one mouse out of

RESULTS

8 had a FTV smaller than 2 in groups treated with GLV-1h68 or GLV-1h100 in combination with IR. The response of individual mice for all treatment groups is shown in Fig. 49.
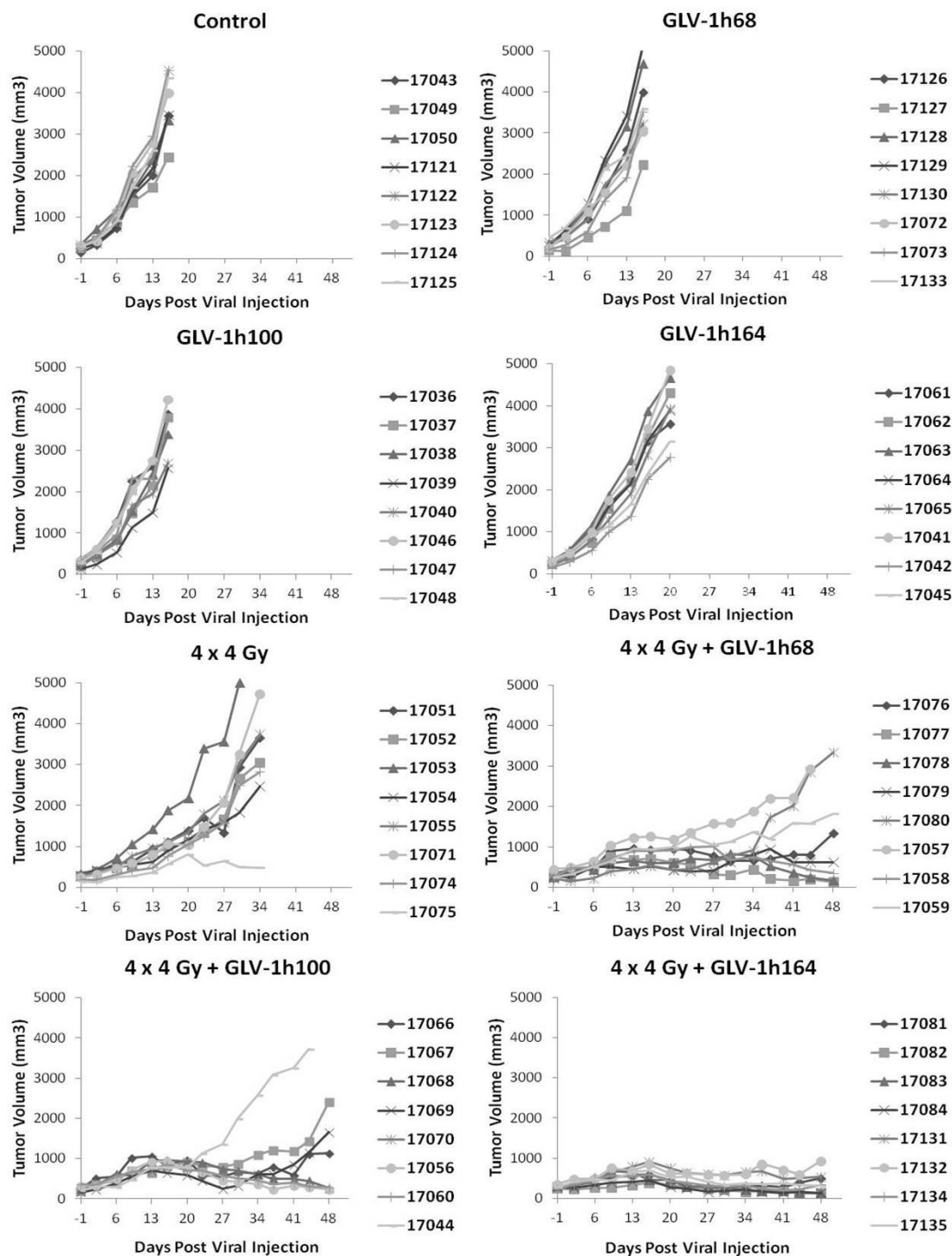
Fig. 49 Individual glioma xenograft response for all treatment groups
Subcutaneous U-87 xenografts were grown in flanks of athymic nude mice. GLV-1h68, GLV-1h100 and GLV-1h164 were injected systemically on day 0. IR was given in four fractions of 4 Gy at day -1, +1, +6 and +8 with respect to viral injection. Glioma xenografts were measured twice a week. The individual volume responses of U-87 glioma xenografts in all experimental groups are shown, 8 mice per experimental group.

RESULTS

Similar to previous experiments shown above, we observed an increase of viral-encoded marker gene GFP in irradiated xenografts when compared to non-irradiated tumors injected with virus alone. This effect was observed for all analyzed VACV, but most obvious for animals injected with GLV-1h68. Fig. 50 shows expression of viral GFP for GLV-168 and GLV-1h164-injected mice and combination of both viruses with fractionated IR.
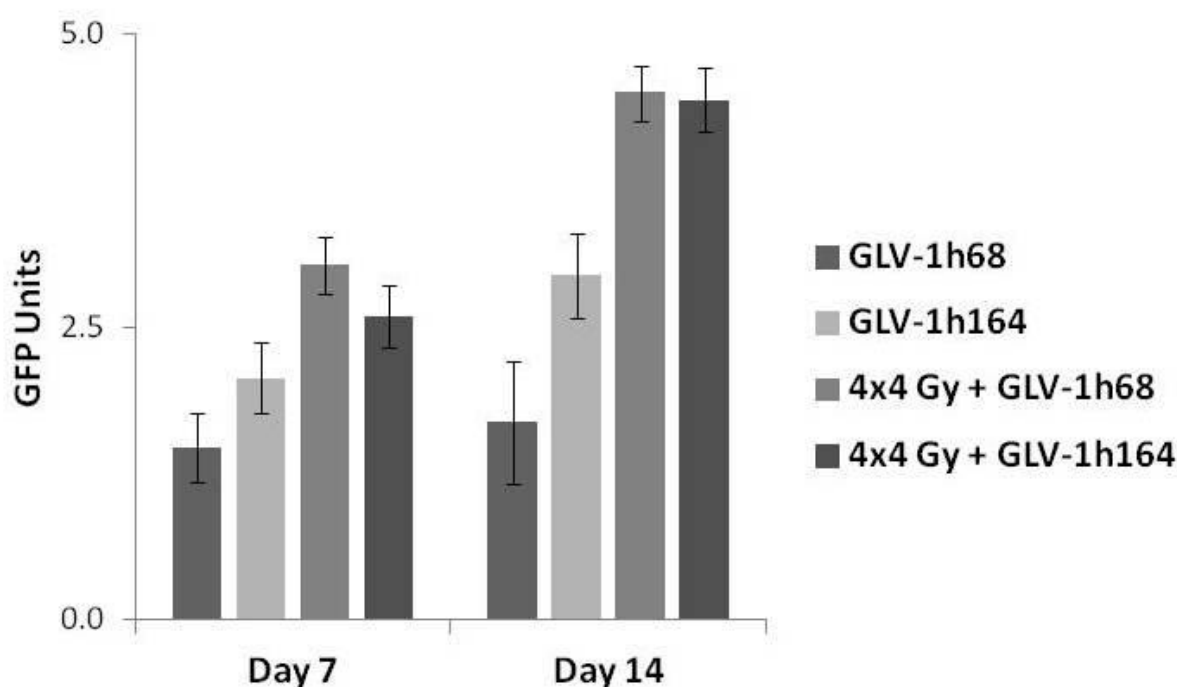
Fig. 50 Expression of viral encoded GFP in U-87 glioma xenografts treated with GLV-1h68 and GLV-1h164 and fractionated IR
U-87 glioma xenografts were injected systemically with GLV-1h68 or GLV-1h164. IR was given as four fractions of 4 Gy. Tumoral GFP expression was scored on a 5 point system on days 7 and 14 post systemic viral injection.

4.8.2 Expression of the single-chain antibody GLAF-2 decreases VEGF levels in tumors

Next, we analyzed how the VACV-mediated expression of an antibody targeting VEGF influenced VEGF levels in tumors. U-87 glioma xenografts were grown in nude mice and retro-orbitally injected with PBS, GLV-1h68 or GLV-1h164, respectively, at day 0. Ionizing radiation was delivered in four fractions at day -1, +1, +6 and +8. Four mice per treatment group were sacrificed and tumors were harvested at day 3, 7 and 14 after viral injection. VEGF concentration of tumor homogenates of all treatment groups was quantitated using a human VEGF DuoSet ELISA and plotted as percent of total protein as measured by protein assay, Fig. 51.
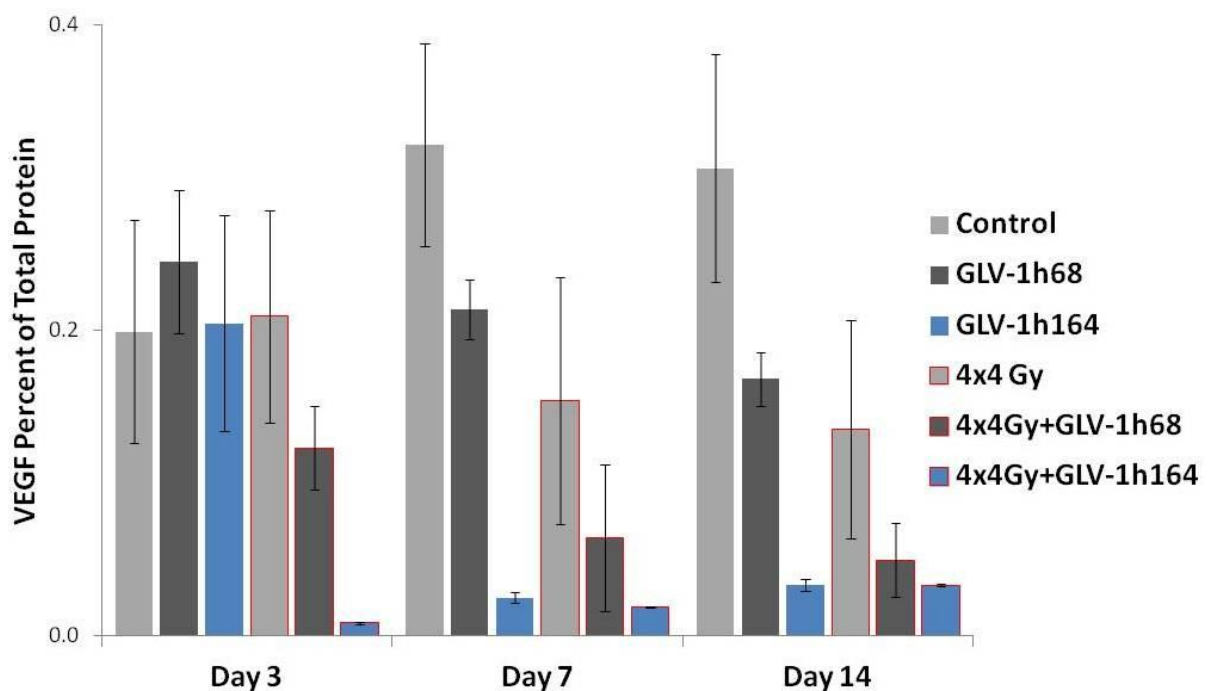
Fig. 51 VEGF concentration in tumor lysates of irradiated and GLV-1h164 injected xenografts
U-87 glioma xenografts were injected systemically with GLV-1h68 or GLV-1h164. IR was given as four fractions of 4 Gy. VEGF concentration in tumor lysates was quantitated at 3, 7 and 14 days after viral injection.

Our studies have demonstrated that VEGF concentration in tumors is decreased by VACV as well as irradiation or the combination of both. Most strikingly, in groups treated with systemic GLV-1h164 and four focal fractions of 4 Gy, VEGF concentration in tumors is dramatically decreased by as early as three days after administration of GLV1h164 to $4\pm3\%$ of control tumors and remained at those very low levels throughout the study. We also observed a decrease of tumoral VEGF concentration in animals treated 4x4 Gy and GLV01h68 to $62\pm22\%$ of control tumors. By day 7 post infection VEGF levels of GLV-1h164 mice are similar regardless if tumors are in addition treated with fractionated IR. In addition we observed a decrease in VEGF in animal treated with the combination of GLV-1h68 and IR.

4.8.3 Tumor vessel number is decreased in glioma xenografts treated with the combination of anti-VEGF VACV and IR

Our studies demonstrated that virus-mediated expression of a single-chain antibody targeting VEGF in combination with fractionated IR reduced concentration of VEGF to 4% of

control tumors as early as 3 days post injection. Low levels of VEGF continued throughout the study. By 7 days VEGF is also strongly decreased in animals treated with GLV-1h164 alone. To assess how a decrease in VEGF would affect the tumor vasculature we performed agarose sectioning of tumors. Here, U-87 glioma xenografts were treated, as described above, with GLV-1h68 and GLV-1h164 and fractionated IR and four tumors per treatment group were harvested 14 days post systemic viral injection. Tumors were snap-frozen in liquid N_2 and subsequently fixed in 4% PFA and embedded in 5% agarose. Tumor sections of 100 µm thickness were prepared and stained for CD31, a cell surface marker of blood vessels. CD31 staining was visualized with a secondary antibody conjugated to anti-rat-AlexaFluor594. Multiple pictures of tumor vessels for all treatment groups were taken covering the whole section to ensure adequate representation of the whole tumor and not only virus-infected areas. A grid was overlaid onto pictures and all vessels intersecting with grid lines were counted. Vessel number in two to four pictures of four sections per tumor from a total of four tumors per group was counted and normalized to vessel number in control tumors.
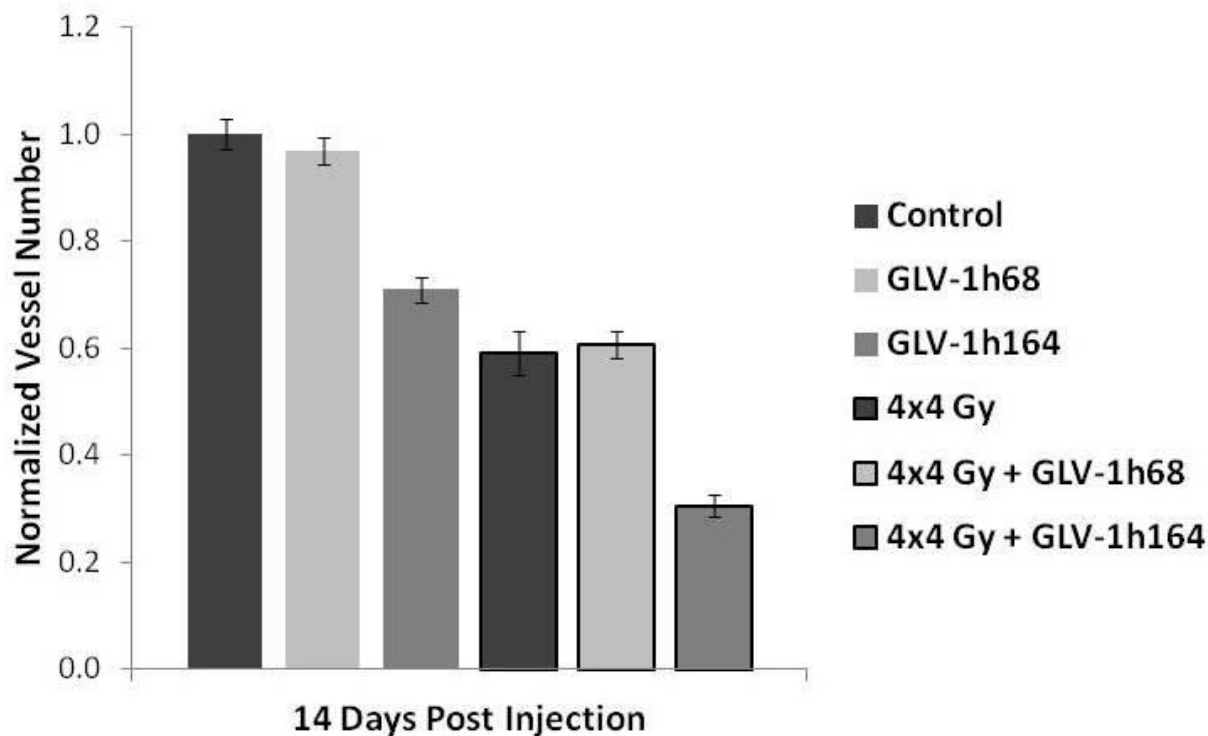
Fig. 52 Decrease in vessel number in tumors treated with focal irradiation and systemic GLV-1h164 injection
Vessel number was scored by CD31 staining in 100 µm thick sections of U-87 glioma xenografts 14 days post systemic injection with either GLV-1h68 or GLV-1h164, and fractionated IR. Two to four pictures of four sections per tumor were counted. Four tumors per experimental group were analyzed.

RESULTS

Fig. 52 shows the vessel numbers of all treatment groups 14 days after systemic viral injection. While GLV-1h68 treatment had no influence on vessel number, a decrease in tumor vessels was observed in tumors of animals treated with GLV-1h164 to 70% of control tumors. Irradiation alone decreased number of vessels in tumor sections to 60% similar to groups treated with GLV-1h68 and IR. The combination of fractionated IR with GLV-1h164 had the greatest effect on tumor vasculature and decreased vessel number to 30% of control tumors. Representative images of tumor vessels in different treatment groups are shown in Fig. 53.
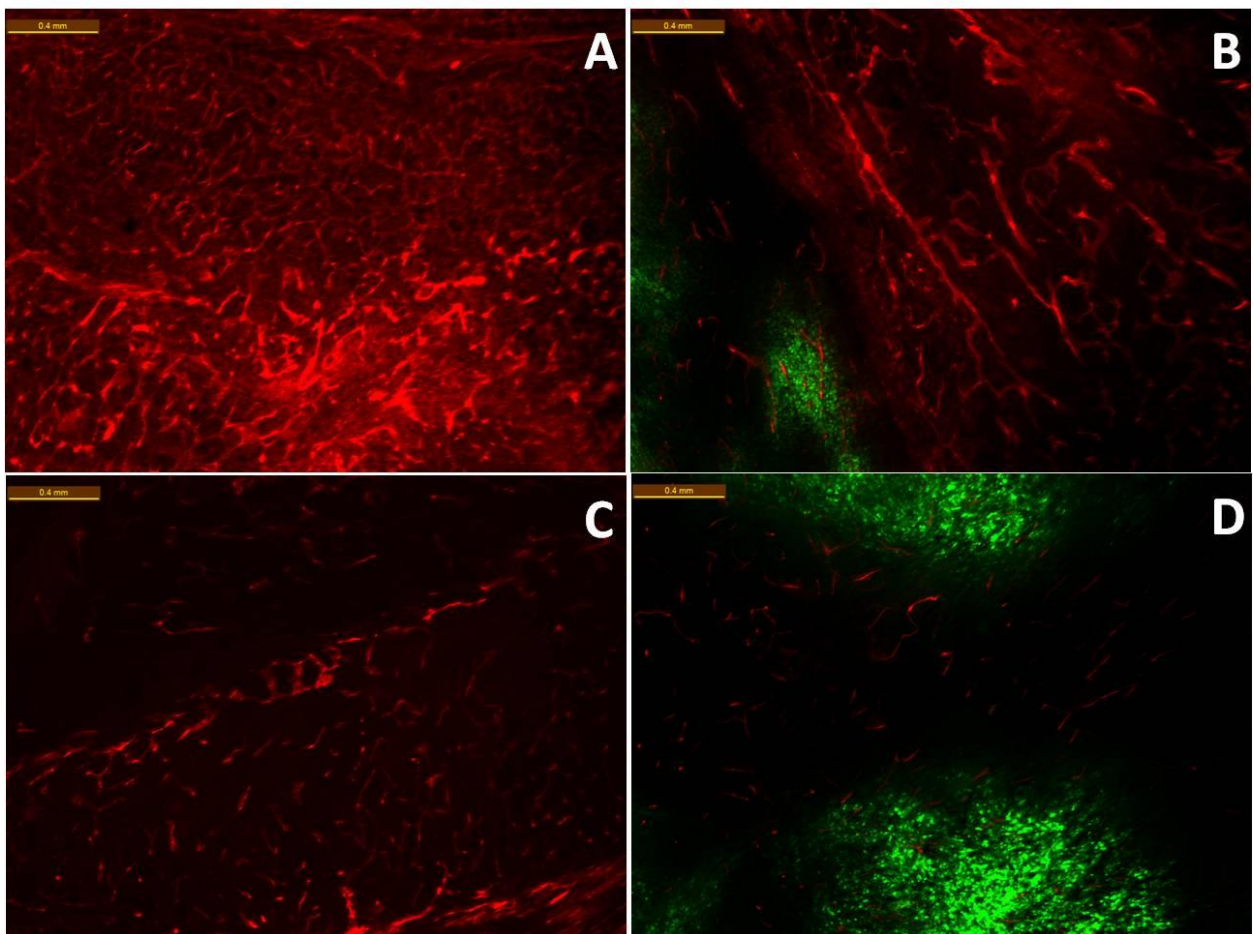
Fig. 53 CD31 tumor vessel staining and GFP marker gene expression in U-87 glioma xenografts
Tumor vasculature was visualized by CD31 staining in sectioned U-87 glioma xenografts of **A)** control tumors, **B)** GLV-1h164 injected tumors, **C)** 4x4Gy treated tumors and **D)** 4x4Gy and GLV-1h64 treated tumors. Tumors were excised at day 14 post injection, fixed, sectioned, and stained for CD31 to label endothelial cells (red). GFP expression was used as marker for viral infection (green). All images are representative examples.

Our studies analyzing interaction of oncolytic VACV GLV-1h164 expressing a single-chain antibody targeting VEGF have shown that tumor control is improved when systemic GLV-1h164 is combined with fractionated focal IR compared to GLV-1h68. We could show that

animals treated with 4 fractions of 4 Gy and GLV-1h164 exhibited the best tumor volumetric response and low levels of VEGF-A within tumors as early as 3 days post injection. Treatment of animals with GLV-1h164 and fractionated IR significantly decreased the number of tumor vessels. This was particularly striking in glioma xenografts from animals treated with the combination of GLV-1h164 and IR. We conclude that GLV-1h164 is a promising candidate oncolytic VACV to be used in combination with IR.

5   Discussion

Glioblastoma multiforme is a WHO grade IV astrocytoma and represents the most aggressive form of malignant brain tumors. The overall prognosis for patients diagnosed with GBM has not significantly improved in the last 20-30 years and remains grim with a median overall survival of 12-14 months. In essence, GBM is considered incurable with ineffective treatment options. GBM is characterized by a highly vascularized phenotype exhibiting areas of hypoxia and necrosis with progressing etiopathology. GBM is also one of the most radioresistant tumors. Moreover, the invasive nature of GBM infiltrating deeply into the cerebral parenchyma precludes complete surgical resection. These factors explain the high rates of local tumor recurrence in people diagnosed with GBM tumors. Standard of care consists of maximal safe surgical resection followed by radiotherapy with concomitant and adjuvant temozolomide. However, median survival is approximately 1 year and the majority of patients suffer from local tumor recurrence imploring the need for new more effective treatment options. Intense research in the field has resulted in the testing of oncolytic viruses as a novel therpay to improve tumor control. Oncolytic viruses represent a class of anti-cancer agents that exploit the inherent capacity of viruses to infect and lyse cells for tumor therapy. In oncolytic viral therapy, replication and cell killing is restricted to tumor cells resulting in tumor cell death while cells leaving surrounding normal cells unharmed. Currently, a variety of oncolytic viruses are being evaluated for their ability to be used in anti-cancer therapy and a few have entered clinical trials. One of the viruses being studied as an oncolytic virus is vaccinia virus. Vaccinia virus belongs to the family of orthopox viruses and gained worldwide fame for its role as a vaccine for smallpox. GLV-1h68 is an oncolytic vaccinia virus engineered by Genelux Corporation with three gene insertions, RUC-GFP fusion, β-galactosidase and β-glucuronidase, and has been successfully used for therapy of various tumor xenografts in preclinical tumor models. GLV-1h68 was shown to specifically target and replicate in tumor tissue inducing tumor shrinkage with minimal toxicity to normal tissue. Recently, a phase I trial was completed at the Royal Marsden Hospital in London, England which demonstrated that administration of GL-ONC1, clinical grade GLV-1h68, is well tolerated with minimal toxicity with preliminary evidence of anticancer activity. In patients treated with GL-ONC1, no does limiting toxicities were observed [92].

Since radiation therapy is a mainstay in glioma therapy, it is of great clinical relevance to evaluate how systemically administered oncolytic vaccinia virus could be combined with targeted ionizing radiation for therapeutic gain. Within this work, we have shown how focal,

tumor targeted IR can be incorporated with a variety of systemically delivered oncolytic VACV constructs to increase viral replication and enhance tumor xenograft regression.

5.1 Ionizing radiation does not damage viral DNA or alter viral tumor tropism

The main cellular target of IR is DNA. Since VACV consists of a linear double-stranded DNA genome of roughly 190 kbp length, we initially analyzed whether IR would damage viral DNA. If IR directly damaged the VACV genome, a decrease in viral activity would be expected rendering the objective of this work to increase viral efficacy by combining it with IR useless. To analyze whether IR affects viral replication, GLV-1h68 was irradiated with increasing doses of IR. Titers of irradiated and non-irradiated viral samples were determined on CV-1 monolayer. It was shown that only a very high non-clinically relevant dose of 100 Gy decreased viral titers to about approximately 80% of the initial titer. The highest dose that was used within this work is 6 Gy in animal model and 10 Gy in cell culture experiments. There is in essence absolutely no risk in damaging viral DNA with those relatively low doses. In addition, doses of IR that are used in conventional fractionated radiation therapy in clinic range between 1.8 and 2 Gy indicating that oncolytic VACV could easily be incorporated into those treatment regimens without any concern of damage to viral DNA. The rationale as to why viral DNA within a tumor cell remains largely undamaged is simply due to the statistical nature or IR mediated cell killing. While one human cell consists of 6×10^9 base pairs in diploid stage, the VACV genome consists of less than 200,000 bp which is only 0.003% of cellular DNA amount. Hence, damage to viral DNA is relatively unlikely.

In previous studies, GLV-1h68 has demonstrated tumor specificity and an improved safety profile due to its attenuation by triple gene inactivation when compared to its parental LIVP strains. Another possible concern in combining IR with oncolytic VACV was that irradiation of target tissue might alter viral tropism for tumor tissue possibly inducing increased toxicity to surrounding normal tissue. To address this issue, two experiments were performed. In the first experiment, we focally irradiated normal tissue over the course of one week with daily doses of 2 Gy mimicking a convention fractionated radiation regimens in mice without tumors and delivered GLV-1h68 systemically in the middle of the radiation treatment. The irradiated healthy tissues (neck tissue, liver, lung, spleen and brain) were analyzed for viral colonization 7 and 14 days after vaccinia virus administration and no viral particles were detected in irradiated normal tissue. In the second experiment, we focally irradiated tumors of tumor bearing nude mice and delivered LIVP 1.1.1 systemically. LIVP 1.1.1 is an

attenuated wild-type isolate of the LIVP strain but is less attenuated when compared with GLV-1h68. Sequencing analysis revealed that both GLV-1h68 and LIVP 1.1.1 both exhibit a disruption of the VACV TK gene locus. In the event that IR alters the tumor specific tropism of oncolytic VACV it would be even more apparent when using a less attenuated viral strain, i.e. LIVP 1.1.1. While we found increased viral replication within harvested irradiated tumors compared to non-irradiated tumors as expected, there was no increase in viral particles recovered from non-irradiated healthy tissues (spleen, liver, lungs and brain) on days 3 and 7 post viral administration.

These studies indicate that IR does not alter the safety profile of VACV and oncolytic VACV tumor tropism is preserved when combined with radiation therapy. These data also demonstrate that the ability of IR to enhance oncolytic VACV replication is specific to tumor cells and not normal tissue.

5.2 Combining focal IR and systemic GLV-1h68-induced tumor growth delay and increase survival in preclinical animal models of glioma

In this series of studies, we demonstrated how focal IR can be incorporated with systemically delivered oncolytic VACV in a treatment paradigm to improve tumor control. In a subcutaneous model of human U-87 glioma in nude mice, we have shown that combining systemically injected GLV-1h68 with a tumor focal dose of 6 Gy resulted in increased tumor growth delay when compared with monotherapy. Our data indicate that delivering IR either one day prior or one day post viral administration had similar effects on tumor growth inhibition. In both cases a tumor growth delay over control tumors to a defined endpoint of 10 times starting volume (FTV=10) of 22 days was observed, while virus alone resulted in 2 days growth delay and IR alone in 7 days growth delay over control tumors. Of note, we observed no decrease in animal well being due to combination treatments since bodyweight remained stable.

To verify whether our results were reproducible in the natural tumor location we implanted U-87 glioma cells orthotopically into the brains of nude mice. Since both the virus and tumor cells were not possible to monitor through the skull, we followed mice for survival following initiation of treatment. While GLV-1h68 treatment alone as well as radiation alone had no or minimal effect on survival, we found a survival increase of 3 weeks over control mice in animals treated with the combination of GLV-1h68 and IR. These results mirrored the result obtained in the subcutaneous model. In both cases combination of systemic oncolytic GLV-1h68 with focal IR resulted in a delayed tumor growth that appears to be greater than just additive from effects of monotherapy.

DISCUSSION

This observation correlates with published data where focal IR in combination with intra-tumoral administered oncolytic viruses induced improved tumor control in subcutaneous animal models or increased survival in orthotopic models for glioma [81-84]. However, here we demonstrate for the first time how this enhancement of viral efficacy by IR is observed when the virus is administered systemically and not directly into the radiated tumor. In this paradigm, we propose a targeting of the virus to the irradiated tumor site.

5.3 Interaction of VACV with IR is not mutant-restricted: Combining IR with the less attenuated oncolytic VACV LIVP 1.1.1 further improves tumor control

In general, the spectrum of cells infected by wild-type viruses is broad, including both transformed and normal cells. The safety concerns in the use of oncolytic viruses has led to the generation of oncolytic viruses genetically engineered with multiple mutations for attenuation and prevention of reversion to wild-type. Genetically engineered oncolytic VACV also results in preferential replication in certain cell types, such as tumor cells, whose genomic composition allows for more robust replication of attenuated viruses when compared to normal cells. We and others have shown that an increase in viral attenuation to increase safety comes at the cost of anti-tumor efficacy. Data reported within this work, are further proof of this concept. LIVP 1.1.1, although exhibiting a naturally occurring TK deletion, represents a less attenuated VACV strain when compared with multi-mutated GLV-1h68 since it is lacking the gene disruptions by insertion of the three expression cassettes. The inefficiency of GLV-1h68 replication in U-87 glioma cells was in part overcome by the use of the less attenuated vaccinia virus LIVP 1.1.1. LIVP 1.1.1 is more virulent which is characterized by a significant increase in replication efficacy in cell culture. In cell lines tested, LIVP 1.1.1 replicated to 100-fold higher titers in U-87 cells than GLV-1h68 during the first 48 hours infection. This increased replication ability translated to a more profound U-87 xenograft growth delay compared to GLV-1h68. These results suggest that the choice of oncolytic virus utilized could in part be dictated by individual tumor intrinsic sensitivity to oncolytic viruses as predicted by cell culture testing of tumor cells from patient biopsies, resulting in a clinical risk adapted stratification strategy. This means that in patients with very aggressive or treatment-resistant tumors a less attenuated VAVC could be used with an increased risk for adverse effects due to the more virulent nature of the virus but simultaneously a possible improved tumor control.

As seen for GLV-1h68, combining LIVP 1.1.1 with IR resulted in an accelerated and enhanced tumor regression in our U-87 glioma murine models. Five out of 7 tumors treated

DISCUSSION

with 6 Gy followed by LIVP 1.1.1 had a FTV of ≤ 1 six weeks after treatment initiation whereas none of the 7 tumor xenografts treated with LIVP 1.1.1 alone had a FTV ≤ 1. Another approach to improve the therapeutic efficacy of attenuated oncolytic viruses is to create a more favorable environment for viral replication. It has been previously shown that a more conducive microenvironment can be created by immunomodulation with cyclophosphamide or rapamycin to enhance the efficacy of systemically delivered oncolytic VACV in experimental glioma models [93]. Altering the tumor composition to support viral replication is similar to what we have achieved with focal irradiation, although probably not in the context of immunomodulation. For both viral strains tested, tumor control was significantly improved when combined with irradiation. This is very attractive from a safety standpoint when by combining the two modalities a lower dose of virus is required to achieve a similar tumor control compared to treatment with virus alone.

Analysis of tumor homogenates for immune-related protein antigen profiling to investigate the inflammatory cytokine pattern within tumors demonstrated that the combination of IR and LIVP 1.1.1 resulted in a robust proinflammatory response. In particular, MCP-1, MCP-3, IL-18 and IP-10 were found within higher levels in the tumor than seen with IR or LIVP 1.1.1 alone. In previous studies conducted in our laboratories, these four cytokines were also observed to be upregulated by GLV-1h68 infection in a pancreatic tumor model, at day 21 and 42 post infection [67]. An intense peri- and intra-tumoral infiltration of mononuclear cells, as seen by immunohistochemistry staining of infected tumors, further confirmed the activation of innate immune mechanisms [65]. It was proposed that tumor regression induced by GLV-1h68 was at least partially mediated through activation of innate immune mechanisms. Our results here show the combination of IR and LIVP 1.1.1 resulted in high expression of these cytokines by as early as 7 days post infection what suggest that the combination of IR and oncolytic VACV can activate a proinflammatory tumor response as well. Additional studies to determine whether cytokine expression mediates an inflammatory tumor response or is secondary to enhanced oncolytic VACV replication mediated by IR could provide further insight into the interaction of innate immunity and tumor regression.

Another important conclusion that could be drawn from these experiments with LIVP 1.1.1 is that the effects or IR on vaccinia virus are not limited to a single mutant virus. GLV-1h68 is attenuated by disruption of three viral genes by insertion of expression cassettes. One plausible scenario of how IR could increase viral replication is that IR induces trans-complementation of mutated viral genes by upregulation of cellular homologues. A similar phenomenon was observed for HSV-1, where the increased replication of one particular HSV-1 strain by IR was explained at least partially by trans-complementation. The used HSV-1 mutant had a deletion of both copies of the $\gamma_1 34.5$ gene which significantly attenuated

to neurovirulence of that particular virus. IR was shown to upregulate cellular GADD34 as part as the stress response to IR in several tumor cell lines [94-96]. Increase of GADD34 which has homology to the viral $\gamma_1 34.5$ gene by IR can thus augment viral protein translation in a $\gamma_1 34.5$ deleted virus [80]. Similarly, HSV-1 viruses deleted of viral ribonucleotide reductase (RR) replicated better in combination with IR because IR increased transcription of cellular RR which complements the viral gene deletion in trans [97]. Since IR potentiated effects of LIVP 1.1.1 as well as GLV-1h68 it is not likely that IR simply induces trans-complementation of disrupted viral genes of GLV-1h68. The only gene both strains have deleted is the thymidine kinase locus. Within this work we have shown by quantitative real time PCR that transcription of cellular TK-1 is not increased upon irradiation of U-87 cells. This was also the case when cells were serum starved to decrease overall transcription before irradiation (data not shown). Thymidine kinase represents one of the many genes that is found dramatically upregulated in cancer cells and should be abundantly present in host cancer cells.

5.4 Preferential replication of systemic oncolytic VACV in irradiated xenografts

Initial animal experiments conducted within this work have demonstrated that U-87 tumor control is improved when systemic VACV is combined with focal IR. In an attempt to further characterize the interaction we analyzed viral encoded marker gene expression as well as viral distribution within tumor xenografts.

In our subcutaneous U-87 xenograft model, viral-encoded GFP and luciferase expression was quantitated seven days after systemic viral injection. We demonstrated that in groups treated with 6 Gy one day prior to viral admistration both GFP and luciferase expression was increased. GFP expression in mice treated with pre 6 Gy and GLV-1h68 also had a more diffuse expression pattern than in groups treated with GLV-1h68 alone or GLV-1h68 and post 6 Gy. Interestingly, by day 14, GFP expression of pre- and post-irradiated groups was similar and more importantly, still higher than in animals treated with virus alone. These data clearly demonstrate that the interaction of IR and VACV results in increased viral gene expression.

We have also shown that IR increased the replication of the less attenuated LIVP 1.1.1. Since this non-engineered viral construct does not encode for any reporter gene, the effect of IR on LIVP 1.1.1 replication was measured by IHC and viral titer determination in irradiated and non-irradiated tumor xenografts. Correlating with the result obtained for GLV-1h68 and IR we found a more diffuse and broader staining pattern for VACV in tumors

DISCUSSION

that received irradiation in combination with LIVP 1.1.1 at 7 days post injection. In addition, when we measured viral load within irradiated and non-irradiated LIVP 1.1.1-infected tumors we found a statistically significant 6-fold increase in infectious viral particle production in irradiated glioma xenografts.

In a bilateral tumor model, we clearly demonstrated that focal IR could serve to target systemically delivered vaccinia virus to preferentially replicate within the irradiated tumor target. In this experimental model system, U-87 glioma xenografts were grown in both the left and right flank of nude mice. GLV-1h68 was injected systemically to be able to equally infect both the left and right sided glioma xenografts. The one variable was that IR was delivered to the right glioma xenograft whereas the left glioma was shielded from IR. Measuring volumetric tumor response of xenografts on both flanks showed tumor growth delay in the exposed irradiated right flank tumors, whereas the lead-blocked left flank glioma xenografts grew exponentially. Interestingly, there was qualitatively a more diffuse GLV-1h68-encoded GFP signal and quantitatively increased GLV-1h68-encoded luciferase activity in the pre irradiated right flank glioma xenografts compared to the shielded left flank U-87 xenografts. This was confirmed by increased VACV staining as well as viral titers in the irradiated flank versus the non-irradiated counterpart. In this model, we showed that by focal irradiation to one tumor viral replication can be increased when compared to non-irradiated glioma xenograft in the same mouse. To our knowledge, this is the first demonstration that focal IR resulted in preferential oncolytic viral replication in an irradiated tumor xenograft compared to non-irradiated tumor xenograft in the same animal [98].

The application of radiation therapy and oncolytic viruses which are injected intra-tumorally has been established by several investigators. However, the utility of combining IR with systemic oncolytic virus administration as in our studies is less clearly defined. Currently, IR is routinely combined with systemically delivered cytotoxic chemotherapies such as cisplatin and temozolomide or more targeted agents such as erlotinib and cetuximab. In addition to target micrometatstasis the systemically delivered chemotherapy can act as radiosensitizer [99-102]. In the treatment paradigm we propose, systemically delivered oncolytic viruses are not sensitizers for radiotherapy as this is the case with systemically delivered chemotherapy. Instead, IR functions as an oncolytic viral sensitizer within targeted irradiated tumors. This means that focal IR to tumors can provide a spatial target for systemically delivered oncolytic virus to promote viral replication. Such "radio-painting" of tumors may result in preferential and enhanced oncolysis within the irradiated tumor target while sparing surrounding normal tissue.

5.5   Scheduling of IR and fractionated radiation regimens

In an attempt to characterize the interaction of oncolytic VACV with IR we analyzed how the delivery sequence of IR to cells and tumors influenced replication of VACV. In an initial experiment in cell culture we irradiated cells at different times before and after virus infection to analyze whether there is a benefit in replication efficacy of VACV when cells are irradiated and in which temporal relationship to viral infection IR should be delivered. Our data showed that viral titers of non-irradiated cells at 24 and 48 hpi were comparable to irradiated cells for all irradiation schedules indicating that at least in cell culture IR does not have a beneficial effect on viral replication. These data also confirm that there is no negative influence of IR on VACV replication.

Next, we analyzed the possible temporal relationship with IR and oncolytic VACV in an animal model of human glioma. To determine if such a temporal relationship existed, a single 6 Gy fraction of IR was delivered either one day before or one day after systemic viral injection. We found both temporal sequences of IR and oncolytic VACV capable of enhancing viral replication which resulted in tumor xenograft regression. Throughout the study, tumors of pre-and post-irradiated virus injected animals showed an almost identical growth pattern. The time to reach a FTV=10, meaning ten times starting volume, for pre-IR or post-IR in combination with VACV were 39.2 and 41 days, respectively, and not statistically different. Interestingly, when we were analyzing virus encoded marker gene expression, we found an earlier peak (day 7) of VACV GFP expression within tumors when IR delivered one day before GLV-1h68 infection. GFP expression of non-irradiated and post-irradiated tumors was similar and lower at this time. By day 14 post infection, VACV GFP tumor expression was similar when IR was given 1 day prior to or after GLV-1h68 infection and in both cases higher than in groups that received virus alone. Therefore, the replication in post-IR groups reached a comparable level which in part may explain why giving IR either before or after oncolytic VACV injection resulted in similar volumetric tumor response. One explanation for these results is that IR delivered after VACV replication works exactly as IR delivered before VACV replication in the context of the VACV replication cycle. The "delayed" increase in virus-encoded GFP expression in tumors with IR after VACV might be due to the fact that post-IR may prime surrounding uninfected cells for infection by progeny virus released by the first wave of tumor infecting VACV. Since the time for completing one VACV life cycle is roughly 24 h, the conditions prevailing within the tumor when radiation is given post viral administration are similar for the first wave of progeny virus than they are for initially injected virus when radiation is given one day before.

DISCUSSION

This observation was in part the reason why for the orthotopic glioma model we chose to deliver two fractions of radiation both prior and post viral injection.

Clinically, conventional radiotherapy to treat gliomas is given in a fractionated scheme. Following maximal safe resection patients commonly undergo fractionated radiotherapy with a total dose of 60 Gy (30-33 fractions of 1.8-2 Gy or equivalent) in combination with chemotherapy. Our experiments have shown that when the biological effective dose of IR was held constant, two fractions of 3.5 Gy produced a similar glioma xenograft growth delay as a single 6 Gy fraction alone. Tumors that were treated with two fractions of 3.5 Gy or one fraction of 6 Gy only resulted in an almost identical tumor growth pattern characterized by an initial stagnation followed by exponential growth. Both fraction schemes, when combined with LIVP 1.1.1, resulted in increased glioma xenografts regression when compared to mono-treatment and a more diffuse LIVP 1.1.1 spread within U-87 xenografts.

Thus, when exploiting a potential clinical application for oncolytic vaccinia virus and IR, it appears that VACV could be incorporated into either larger hypo-fraction or more conventionally fractionated IR. Of course, the choice of radiotherapy fractionation scheme would have to be dictated by clinical relevance and surrounding normal tissue constraints.

5.6   Interaction of IR and VACV

Data presented within this work indicate that focally delivered ionizing radiation enhanced the replication of a systemic delivered oncolytic vaccinia virus. Of note, this interaction is not restricted to a specific viral mutant but also observed with wild-type LIVP 1.1.1 indicating the effect is not due to trans-complementation of viral deleted genes. This is further supported by the result that the expression of thymidine kinase which represents the only gene all viruses analyzed are depleted in is not affected by IR.

One possible explanation for how focal tumor IR can enhance systemically delivered VACV replication in tumor xenografts is that IR transiently increases the vascular permeability in tumors allowing enhanced extravasation of oncolytic VACV into irradiated tumor xenografts. This could explain why IR delivered prior to VACV induces increased viral marker gene expression and viral titers within tumors. To test this hypothesis, an assay was performed measuring the amounts of extravasated Evans Blue dye into irradiated and non-irradiated glioma xenografts 24 hours following IR similar to the time oncolytic VACV was injected in previous studies. In this experimental model, we were not able to detect any significant difference in dye extravasation 24 h following IR. Thus, we concluded focal IR does not appear to result in enhanced oncolytic VACV as a result of IR altering the tumor vasculature. Also it would not explain why post IR achieves similar tumor control. A recent study

DISCUSSION

conducted by Hamalukic and colleges dealt with potential adverse effects of IR by analyzing whether irradiation of normal cells outside of the primary might increase metastasis. The authors demonstrated that systemic injection of tumor cells into immunodeficient mice induced an increase in lung metastasis when mice received whole body irradiation following cell injection. The authors concluded that whole body irradiation altered vessels and increased leakiness thus stimulated tumor cell extravasation [103]. We were not able to observe a similar phenomenon in our experiments. However, in contrast to their publication, in which the authors were delivering IR to normal vasculature, in our model system, we were analyzing IR-induced effects on tumor vasculature which is extremely abnormal and leaky, especially in the case of glioma lines such as our U-87 tumor model. While an alteration of intact vessels by IR is conceivable, we believe, in the context of tumor vasculature, IR has no worsening influence on already abnormal vessel composition.

Since IR predominantly kills cells by inducing double-strand DNA breaks, we measured DNA double-strand breaks by γH2AX foci staining in cells upon irradiation with or without virus infection. Previous studies analyzing interaction of Herpes simplex virus have shown that viral protein IP40 increased radiosensitivity in U-87 glioma cells by degrading the catalytic subunit of DNA-dependent protein kinase thus inhibiting DNA repair [104]. One of the first proteins recruited to the site of DNA damage, as induced by IR, is γH2AX. In our experiments, we found a drastic increase in number of γH2AX foci 1 h after irradiation, as expected. While 6 h after IR the number of foci was still elevated it decreased almost to the normal state 24 after IR when DNA damage is repaired or cells are committed to die. However, we did not detect any differences in number of γH2AX foci in samples which were in addition to irradiation also infected with virus when compared with irradiated cells. Also, VACV alone did not increase the number of γH2AX foci and therefore DNA breaks when compared to control cells. The reason for this is most likely due to VACV exclusively cytoplasmic lifestyle. Unlike to HSV-1 which is known to replicate in the host cell nucleus, VACV never comes near to host DNA and therefore probably hast no influence on DNA breaks and repair mechanisms.

One of the first responses of cells to irradiation is an arrest of cell cycle, primarily in G_2 phase of the cycle, to resolve IR induced DNA damage prior to mitosis. Also, it is known that cells exhibit different radiosensitivity during various stages of the cell cycle, with S phase being most radioresistant. It has also been shown that VACV itself has an influence on cell cycle progression driving cells towards S phase where DNA building blocks as well as TK-1 are abundantly present in the cell which are needed to generate progeny virus [91]. Hence, we analyzed the distribution of cells in different stages of the cell cycle after virus treatment and irradiation or both. As expected, our experiments confirmed an increase of cells in G_2

phase of the cell cycle upon irradiation. However, GLV-1h68 infection of irradiated and non-irradiated cells did not alter distribution of cells throughout cell cycle and samples looked comparable to control or irradiated cells, respectively. Experiments analyzing the interplay of VACV and cell cycle were conducted in primary cells where VACV needed to drive cells to a rate of increased proliferation to carry own its own replication. In tumor cells however, the effects of VACV on cell cycle are not visible or not drastic since tumor cells exhibit a high rate of proliferation and sufficient amounts of TK-1 throughout all stages.

Taken together, we were not able to determine the exact mechanism through which IR increases viral replication in tumors. However, we assume this enhancement of replication is a phenomenon that is only detectable in the in vivo setting. All studies conducted in cell culture did not show any significant differences in either viral replication, cell viability (data not shown) or gene transcription of viral early, intermediate or late genes (data not shown) between virus alone or VACV and IR.

In vivo two different scenarios are possible as to how increased viral titers are found in irradiated xenografts. It is conceivable that higher viral numbers are a result of an initial increased viral infectivity meaning more viral particles initially reach the tumor site or entry into tumor cells is facilitated or accelerated. Our extravasation experiments have shown that increase in viral titers is not due to more viral particles initially reaching the tumor because of changes in tumor vascularity. Experiments that analyze viral attachment or entry into tumor cells of irradiated and non-irradiated could help to determine whether this is of importance. The alternative hypothesis is based on previous studies with IR and oncolytic viruses. We propose that IR creates a more conducive environment for VACV replication. This also explains why IR increases viral replication even after systemic viral infection. IR induces a multi-facetted stress response which is characterized by the upregulation of various signaling pathways. It is conceivable that VACV exploits those micro-environmental changes to increase replication. However, the exact mechanism remains to be elucidated.

5.7   Modulation of the tumor microenvironment to increase tumor radiation responsiveness: VACV with anti-angiogenic payload

In the first part of this work we have shown how focal IR can be incorporated with systemically delivered oncolytic VACV to increase viral replication and enhance tumor xenograft regression. We showed that focal IR can result in preferential replication of systemically delivered oncolytic viruses in a pre irradiated tumor target compared to non-irradiated tumors using a bilateral murine tumor model system.

DISCUSSION

In the next part we focused on the tumor microenvironment, especially in the context of angiogenesis and VEGF. We were interested to see whether we can further improve glioma xenograft regression. We evaluated the interaction of IR and an oncolytic VACV targeting VEGF by virus-driven secretion of a single-chain antibody. VEGF-A is one of the key proteins involved in induction of angiogenesis in tumors to sustain exponential proliferation rates by inducing neoangiogenesis. Inhibition of angiogenesis in tumor therapy has largely focused on anti-angiogenic agents that directly target endothelial cells. A well established way of decreasing angiogenesis is by inhibition of VEGF-A signaling which has been shown to improve tumor control by directly targeting tumor feeding tumor vasculature. The most advanced anti-VEGF agent in clinical use is the anti-VEGF antibody Avastin, a VEGF165 aptamer. A recent study conducted in our laboratories has shown that an anti-VEGF single-chain antibody expressed by oncolytic VACV significantly enhanced anti-tumor therapy when compared with parental GLV-1h68 [105]. GBM is characterized by a highly vascularized tumor with intrinsic elevated levels of VEGF [49, 106]. However, vessels resulting from angiogenesis in GBM, largely driven by VEGF, are structurally as well as functional abnormal, leading to high interstitial pressure and areas of hypoxia and necrosis and contribute the poor prognosis for GBM patients. Emerging preclinical as well as clinical focus is put on targeting angiogenesis in GBM, with promising results and led to the approval of bevacizumab for recurrent GBM [52]. In an initial experiment, we analyzed whether irradiation of glioma cells has further influence on induction of angiogenesis. Since VEGF-A is a critical player of angiogenesis in GBM, we performed experiments evaluating VEGF expression. Our experiments in cell culture demonstrated that IR increased VEGF expression in human U-87 glioma cells. This upregulation was observed in a dose- and time- dependent fashion and correlates with studies conducted by other groups who found similar results [36, 107].

In addition to VEGF involvement of inducing angiogenesis, it is also suggested to play a role in radioresistance of endothelial cells to irradiation by blocking radiation induced cell killing [38]. This effect was also shown for human endothelial cells that were co-cultured with U-87 glioma cells, which resulted in resistance to IR-induced cell death [108]. Authors concluded that resistance was mediated by changes in the transcriptional profile of co-cultured endothelial cells mediated by U-87-driven expression of VEGF. Our experiments are further proof of this concept. When we were growing human umbilical vein endothelial cells in media with increasing amounts of VEGF we found a concentration-dependent increase in radioresistance of cells to IR, given at a dose of 10 Gy. Interestingly, effects of VEGF-A on endothelial cells were reversible by adding purified GLAF-1 to the cells. GLAF-1 is a single-chain antibody targeting human VEGF-A expressed by oncolytic VACV GLV-109. When we

DISCUSSION

added increasing levels of GLAF-1 in media containing VEGF, we were able to block VEGF-induced radioresistance and HUVECS showed a decrease in cell survival which correlated with GLAF-1 concentration.

Next, we wanted to see how the addition of an anti-angiogenic payload to VACV influenced tumor response in the *in vivo* setting when combined with IR. Human U-87 glioma xenografts were grown in the flanks of nude mice and treated with systemic injection of GLV-1h68 or GLV-1h164, expressing GLAF-2 which is identical to GLAF-1 but has no FLAG tag. IR was given in 4 Gy doses at -1, +1, +6 and +8 days in regard to viral administration on day 0. Irradiation was delivered in a fractionated scheme with the intention of maximizing possible payload induced improvement of radioresistance. We have shown that animals treated with GLV-164 and fractionated IR exhibited the best volumetric tumor response with 7 out of 8 mice less than twice the initial tumor volume at day 20 post viral injection. In comparison, only one mouse of 8 animals treated with GLV-1h68 and fractionated IR had a FTV of smaller than 2 at this time. In addition to GLV-1h68, another viral construct was included in this study, GLV-1h100, which represents the parental virus for GLV-1h164. Tumor response of GLV-1h68 and GLV-1h100 looked comparable in irradiated and non-irradiated animals indicating that an improvement in tumor control by GLV-1h164 is due to the payload, it encodes for, GLAF-2. Similar to our previous studies we found an increase of viral-encoded GFP expression in irradiated tumors when compared to animals that received virus alone. This effect could be observed for all viral constructs, again indication that increase in viral replication is not mutant restricted.

In a follow up experiment, we analyzed the influence of IR and viral colonization on tumoral VEGF levels. Tumors were again treated with systemic GLV-1h68 or GLV-1h164, respectively, and in irradiated groups four fractions of 4 Gy were delivered focally to the tumor. Tumor homogenates were prepared at day 3, 7 and 14 post viral administration. Of note, we could show that by day 3 post viral administration in animals treated with GLV-1h164 and IR, VEGF levels decreased dramatically to only 4% of control cells and remained comparably low throughout the study. VEGF concentration in tumors of GLV-1h164 only-treated animals was comparable to GLV-1h164+IR treated mice for the 7 and 14 day time point. At later time points, VEGF levels also decreased in all other groups when compared to control tumors, most prominent in mice treated with IR and GLV-1h68. Previous studies have shown that injection of GLV-1h68 into tumor-bearing mice decreased levels of tumoral VEGF-A (Weibel *et al.* submitted). Decreased VEGF concentrations at later time points in other groups could in part be attributed to glioma cell death, which is a major intratumoral source of VEGF. However, we could not detect an upregulation of VEGF in mice that received only IR as we would have expected from our cell culture data. Other

DISCUSSION

studies though, have found an upregulation of pro-angiogenic effectors including VEGF in the in vivo setting [109].

We then verified that targeting VEGF translated into a decreased tumor vessel number. Tumors were harvested 14 days post injection, embedded and 100 μm thick sections were stained for CD31 which serves as a marker for endothelial cells to analyze tumor vasculature. We quantitated vessel number by counting vessels in different areas of the tumor and several sections. We found that tumor vessel number decreased to 30% of vessel number found in control tumors in animals treated with GLV-164 and fractionated IR. We also observed a reduction of vessel number in animal treated with GLV-1h164 alone or IR alone to 70 and 60%, respectively. GLV-1h68 treatment, however, had no influence on vessel number which correlates with previous studies from our group that found GLV-1h68 does not infect tumor vasculature [110]. We propose the strong reduction in vessel number in the GLV-1h164 plus fractionated IR group is mainly due to increased replication of GLV-1h164 in irradiated xenografts producing early on high levels of GLAF-2 resulting in a drastic and early decrease VEGF. Persistent anti-angiogenic treatment ultimately results in degradation of tumor vasculature. Our experiments with endothelial cells have shown that blocking VEGF-induced stress response by a VEGF targeting single-chain antibody, GLAF-1, IR-induced cell death is increased. It is also likely that this effect plays a part in killing tumor vasculature we have observed in our studies. It was shown that the endothelium plays a critical role in IR mediated tumor destruction and studies have proposed that IR induced apoptosis is induced by endothelia cell death rather than dying tumor cells [39]. Thus targeting the tumor vascular component into treatment regimens instead of solely targeting cancer cells is an attractive therapeutic strategy. Here, we show that combining a VACV expressing a VEGF-targeting antibody with IR to increase viral replication and simultaneously enhancing efficacy of anti-angiogenic therapy as well as radiosensitizing the tumor vasculature by reversing VEGF mediated radioresistance.

Within this work, we have shown how focal tumor targeted IR can be incorporated with systemically delivered oncolytic VACV to increase viral replication and enhance tumor xenograft regression. We showed that IR can act as a sensitizer for tumor oncolysis by VACV. In an bilateral animal glioma model, we found that focal IR resulted in preferential oncolytic viral replication as measured by increased marker gene expression as well as viral titers and viral distribution within the irradiated tumor xenograft compared to non-irradiated tumor xenograft in the same animal. Furthermore, we could demonstrate that tumor control could be further improved by combining fractionated IR with a systemically delivered oncolytic VACV expressing an anti-VEGF antibody. Here, in addition to IR and viral-induced

DISCUSSION

tumor cell destruction we were able to efficiently target the tumor vasculature. This was achieved by enhanced viral replication translating in increased levels of GLAF-2 disrupting tumor vessels as well as the radiosensitization of tumor vasculature to IR by blocking VEGF.

Our preclinical results have implications in how focal radiotherapy can be combined with systemic oncolytic viral administration for locally advanced tumors with the potential, by using an anti-angiogenic VACV, to modulate the tumor micro-environment to further increase tumor radiation sensitivity.

6   References

1.   Harrison SC, Alberts B, Ehrenfeld E, Enquist L, Fineberg H, McKnight SL *et al.* **Discovery of antivirals against smallpox**. *Proceedings of the National Academy of Sciences of the United States of America* 2004;**101**:11178-11192.

2.   Plaut M, Tinkle SS. **Risks of smallpox vaccination: 200 years after Jenner**. *J Allergy Clin Immunol* 2003;**112**:683-685.

3.   Fenner F. **A successful eradication campaign. Global eradication of smallpox**. *Rev Infect Dis* 1982;**4**:916-930.

4.   Fenner F. **The global eradication of smallpox**. *The Medical journal of Australia* 1980;**1**:455-455.

5.   Baxby D. **Edward Jenner's Inquiry; a bicentenary analysis**. *Vaccine* 1999;**17**:301-307.

6.   Condit RC, Moussatche N, Traktman P. **In a nutshell: structure and assembly of the vaccinia virion**. *Adv Virus Res* 2006;**66**:31-124.

7.   Moss B. **Regulation of vaccinia virus transcription**. *Annu Rev Biochem* 1990;**59**:661-688.

8.   Roberts KL, Smith GL. **Vaccinia virus morphogenesis and dissemination**. *Trends Microbiol* 2008;**16**:472-479.

9.   Smith GL, Vanderplasschen A, Law M. **The formation and function of extracellular enveloped vaccinia virus**. *The Journal of general virology* 2002;**83**:2915-2931.

10.   Broyles SS. **Vaccinia virus transcription**. *The Journal of general virology* 2003;**84**:2293-2303.

11.   Hanahan D, Weinberg RA. **The hallmarks of cancer**. *Cell* 2000;**100**:57-70.

12.   Hanahan D, Weinberg RA. **Hallmarks of cancer: the next generation**. *Cell* 2011;**144**:646-674.

13.   Ferrara N. **VEGF and the quest for tumour angiogenesis factors**. *Nature reviews Cancer* 2002;**2**:795-803.

14.   Ide AG, Baker N.H., Warren S.L. **Vascularization of the Brown Pearce rabbitepithelioma transplant as seen in the transparent ear chamber**. *Am J Roentgenol* 1939;**42**:891–899

15.   Folkman J. **Tumor angiogenesis: therapeutic implications**. *The New England journal of medicine* 1971;**285**:1182-1186.

16.   Senger DR, Galli SJ, Dvorak AM, Perruzzi CA, Harvey VS, Dvorak HF. **Tumor cells secrete a vascular permeability factor that promotes accumulation of ascites fluid**. *Science* 1983;**219**:983-985.

17.   Ferrara N, Henzel WJ. **Pituitary follicular cells secrete a novel heparin-binding growth factor specific for vascular endothelial cells**. *Biochemical and biophysical research communications* 1989;**161**:851-858.

18.   Plouet J, Schilling J, Gospodarowicz D. **Isolation and characterization of a newly identified endothelial cell mitogen produced by AtT-20 cells**. *Embo J* 1989;**8**:3801-3806.

19.   Dvorak HF. **Vascular permeability factor/vascular endothelial growth factor: a critical cytokine in tumor angiogenesis and a potential target for diagnosis and therapy**. *Journal of clinical oncology : official journal of the American Society of Clinical Oncology* 2002;**20**:4368-4380.

20.   Safran M, Kaelin WG, Jr. **HIF hydroxylation and the mammalian oxygen-sensing pathway**. *The Journal of clinical investigation* 2003;**111**:779-783.

21.   Ferrara N, Kerbel RS. **Angiogenesis as a therapeutic target**. *Nature* 2005;**438**:967-974.

22.   Hurwitz H, Fehrenbacher L, Novotny W, Cartwright T, Hainsworth J, Heim W *et al*. **Bevacizumab plus irinotecan, fluorouracil, and leucovorin for metastatic colorectal cancer**. *The New England journal of medicine* 2004;**350**:2335-2342.

23.   Moeller BJ, Dreher MR, Rabbani ZN, Schroeder T, Cao Y, Li CY *et al*. **Pleiotropic effects of HIF-1 blockade on tumor radiosensitivity**. *Cancer Cell* 2005;**8**:99-110.

24.   Jain RK. **Normalizing tumor vasculature with anti-angiogenic therapy: a new paradigm for combination therapy**. *Nat med* 2001;**7**:987-989.

25.   Carmeliet P, Jain RK. **Principles and mechanisms of vessel normalization for cancer and other angiogenic diseases**. *Nat Rev Drug Discov* 2011;**10**:417-427.

26.   Goel S, Duda DG, Xu L, Munn LL, Boucher Y, Fukumura D *et al*. **Normalization of the vasculature for treatment of cancer and other diseases**. *Physiol Rev* 2011;**91**:1071-1121.

27.   Morgan WF, Sowa MB. **Effects of ionizing radiation in nonirradiated cells**. *Proceedings of the National Academy of Sciences of the United States of America* 2005;**102**:14127-14128.

28.   Hall EJ, Giaccia, A.: **Radiobiology for the Radiologist**: Lippincott Williams & Wilkins; 2006.

29.   Brown JM, Wilson WR. **Exploiting tumour hypoxia in cancer treatment**. *Nature reviews Cancer* 2004;**4**:437-447.

30.   DeVita V.T HS, Rosenberg S.A.: **Cancer, Principles and Practice of Oncology**, 7th Edition edn. Philadelphia: Lippincott Williams&Wilkins; 2005.

31.   Yuan J, Adamski R, Chen J. **Focus on histone variant H2AX: to be or not to be**. *FEBS Lett* 2010;**584**:3717-3724.

32.   Kass EM, Jasin M. **Collaboration and competition between DNA double-strand break repair pathways**. *FEBS Lett* 2010;**584**:3703-3708.

33.   Sinclair WK, Morton RA. **X-ray sensitivity during the cell generation cycle of cultured Chinese hamster cells**. *Radiation research* 1966;**29**:450-474.

34.   Dings RP, Loren M, Heun H, McNiel E, Griffioen AW, Mayo KH *et al*. **Scheduling of radiation with angiogenesis inhibitors anginex and Avastin improves therapeutic outcome via vessel normalization**. *Clin Cancer Res* 2007;**13**:3395-3402.

35.   Myers AL, Williams RF, Ng CY, Hartwich JE, Davidoff AM. **Bevacizumab-induced tumor vessel remodeling in rhabdomyosarcoma xenografts increases the effectiveness of adjuvant ionizing radiation**. *J Pediatr Surg* 2010;**45**:1080-1085.

REFERENCES

36. Gorski DH, Beckett MA, Jaskowiak NT, Calvin DP, Mauceri HJ, Salloum RM *et al*. **Blockage of the vascular endothelial growth factor stress response increases the antitumor effects of ionizing radiation**. *Cancer Res* 1999;**59**:3374-3378.

37. Sofia Vala I, Martins LR, Imaizumi N, Nunes RJ, Rino J, Kuonen F *et al*. **Low doses of ionizing radiation promote tumor growth and metastasis by enhancing angiogenesis**. *PLoS One* 2010;**5**:e11222.

38. Gupta VK, Jaskowiak NT, Beckett MA, Mauceri HJ, Grunstein J, Johnson RS *et al*. **Vascular endothelial growth factor enhances endothelial cell survival and tumor radioresistance**. *Cancer J* 2002;**8**:47-54.

39. Garcia-Barros M, Paris F, Cordon-Cardo C, Lyden D, Rafii S, Haimovitz-Friedman A *et al*. **Tumor response to radiotherapy regulated by endothelial cell apoptosis**. *Science* 2003;**300**:1155-1159.

40. Wachsberger P, Burd R, Dicker AP. **Tumor response to ionizing radiation combined with antiangiogenesis or vascular targeting agents: exploring mechanisms of interaction**. *Clin Cancer Res* 2003;**9**:1957-1971.

41. Stupp R, Roila F. **Malignant glioma: ESMO clinical recommendations for diagnosis, treatment and follow-up**. *Annals of oncology : official journal of the European Society for Medical Oncology / ESMO* 2009;**20 Suppl 4**:126-128.

42. Stupp R, Tonn JC, Brada M, Pentheroudakis G. **High-grade malignant glioma: ESMO Clinical Practice Guidelines for diagnosis, treatment and follow-up**. *Ann Oncol* 2010;**21 Suppl 5**:v190-193.

43. Apuzzo M: **Malignant Cerebral Glioma**, vol. 2; 1990.

44. Choucair AK, Levin VA, Gutin PH, Davis RL, Silver P, Edwards MS *et al*. **Development of multiple lesions during radiation therapy and chemotherapy in patients with gliomas**. *J Neurosurg* 1986;**65**:654-658.

45. Stupp R, Hegi ME, Mason WP, van den Bent MJ, Taphoorn MJ, Janzer RC *et al*. **Effects of radiotherapy with concomitant and adjuvant temozolomide versus radiotherapy alone on survival in glioblastoma in a randomised phase III study: 5-year analysis of the EORTC-NCIC trial**. *The lancet oncology* 2009;**10**:459-466.

46. Stupp R, Hegi ME, Gilbert MR, Chakravarti A. **Chemoradiotherapy in malignant glioma: standard of care and future directions**. *Journal of clinical oncology : official journal of the American Society of Clinical Oncology* 2007;**25**:4127-4136.

47. Leon SP, Folkerth RD, Black PM. **Microvessel density is a prognostic indicator for patients with astroglial brain tumors**. *Cancer* 1996;**77**:362-372.

48. Aghi M, Chiocca EA. **Contribution of bone marrow-derived cells to blood vessels in ischemic tissues and tumors**. *Molecular therapy : the journal of the American Society of Gene Therapy* 2005;**12**:994-1005.

49. Tate MC, Aghi MK. **Biology of angiogenesis and invasion in glioma**. *Neurotherapeutics : the journal of the American Society for Experimental NeuroTherapeutics* 2009;**6**:447-457.

50. Cea V, Sala C, Verpelli C. **Antiangiogenic therapy for glioma**. *J Signal Transduct* 2012;**2012**:483040.

51. Winkler F, Kozin SV, Tong RT, Chae SS, Booth MF, Garkavtsev I *et al*. **Kinetics of vascular normalization by VEGFR2 blockade governs brain tumor response to radiation: role of oxygenation, angiopoietin-1, and matrix metalloproteinases**. *Cancer Cell* 2004;**6**:553-563.

52.   Cohen MH, Shen YL, Keegan P, Pazdur R. **FDA drug approval summary: bevacizumab (Avastin) as treatment of recurrent glioblastoma multiforme**. *Oncologist* 2009;**14**:1131-1138.

53.   Chamberlain MC. **Treatment of glioblastoma with bevacizumab: has a new standard therapy been defined?** *CNS Drugs* 2011;**25**:815-818.

54.   Liu TC, Galanis E, Kirn D. **Clinical trial results with oncolytic virotherapy: a century of promise, a decade of progress**. *Nat Clin Pract Oncol* 2007;**4**:101-117.

55.   Chiocca EA. **Oncolytic viruses**. *Nat Rev Cancer* 2002;**2**:938-950.

56.   Parato KA, Senger D, Forsyth PA, Bell JC. **Recent progress in the battle between oncolytic viruses and tumours**. *Nature reviews Cancer* 2005;**5**:965-976.

57.   Breitbach CJ, Reid T, Burke J, Bell JC, Kirn DH. **Navigating the clinical development landscape for oncolytic viruses and other cancer therapeutics: no shortcuts on the road to approval**. *Cytokine & Growth Factor Reviews* 2010;**21**:85-89.

58.   Kirn DH, Thorne SH. **Targeted and armed oncolytic poxviruses: a novel multi-mechanistic therapeutic class for cancer**. *Nat Rev Cancer* 2009;**9**:64-71.

59.   Liu TC, Kirn D. **Systemic efficacy with oncolytic virus therapeutics: clinical proof-of-concept and future directions**. *Cancer Res* 2007;**67**:429-432.

60.   Chen NG SA. **Oncolytic vaccinia virus: a theranostic agent for cancer**. *Future Virol* 2010;**5**:21.

61.   Thorne SH, Bartlett DL, Kirn DH. **The use of oncolytic vaccinia viruses in the treatment of cancer: a new role for an old ally?** *Current gene therapy* 2005;**5**:429-443.

62.   Parato KA, Breitbach CJ, Le Boeuf F, Wang J, Storbeck C, Ilkow C *et al*. **The oncolytic poxvirus JX-594 selectively replicates in and destroys cancer cells driven by genetic pathways commonly activated in cancers**. *Molecular therapy : the journal of the American Society of Gene Therapy* 2012;**20**:749-758.

63.   Breitbach CJ, Burke J, Jonker D, Stephenson J, Haas AR, Chow LQ *et al*. **Intravenous delivery of a multi-mechanistic cancer-targeted oncolytic poxvirus in humans**. *Nature* 2011;**477**:99-102.

64.   Kim JH, Oh JY, Park BH, Lee DE, Kim JS, Park HE *et al*. **Systemic armed oncolytic and immunologic therapy for cancer with JX-594, a targeted poxvirus expressing GM-CSF**. *Molecular therapy : the journal of the American Society of Gene Therapy* 2006;**14**:361-370.

65.   Zhang Q, Yu YA, Wang E, Chen N, Danner RL, Munson PJ *et al*. **Eradication of Solid Human Breast Tumors in Nude Mice with an Intravenously Injected Light-Emitting Oncolytic Vaccinia Virus**. *Cancer Res* 2007;**67**:10038-10046.

66.   Zhang Q, Liang C, Yu YA, Chen N, Dandekar T, Szalay AA. **The highly attenuated oncolytic recombinant vaccinia virus GLV-1h68: comparative genomic features and the contribution of F14.5L inactivation**. *Mol Genet Genomics* 2009;**282**:417-435.

67.   Yu YA, Galanis C, Woo Y, Chen N, Zhang Q, Fong Y *et al*. **Regression of human pancreatic tumor xenografts in mice after a single systemic injection of recombinant vaccinia virus GLV-1h68**. *Mol Cancer Ther* 2009;**8**:141-151.

68.   He S, Li P, Chen CH, Bakst RL, Chernichenko N, Yu YA *et al*. **Effective oncolytic vaccinia therapy for human sarcomas**. *The Journal of surgical research* 2012;**175**:e53-60.

69.   Yu Z, Li S, Brader P, Chen N, Yu YA, Zhang Q *et al*. **Oncolytic vaccinia therapy of squamous cell carcinoma**. *Mol Cancer* 2009;**8**:45.

70.   Gentschev I, Donat U, Hofmann E, Weibel S, Adelfinger M, Raab V *et al*. **Regression of human prostate tumors and metastases in nude mice following treatment with the recombinant oncolytic vaccinia virus GLV-1h68**. *Journal of biomedicine & biotechnology* 2010;**2010**:489759.

71.   Kelly KJ, Woo Y, Brader P, Yu Z, Riedl C, Lin SF *et al*. **Novel oncolytic agent GLV-1h68 is effective against malignant pleural mesothelioma**. *Human gene therapy* 2008;**19**:774-782.

72.   Kelly E, Russell SJ. **History of oncolytic viruses: genesis to genetic engineering**. *Molecular therapy : the journal of the American Society of Gene Therapy* 2007;**15**:651-659.

73.   Zemp FJ, Corredor JC, Lun X, Muruve DA, Forsyth PA. **Oncolytic viruses as experimental treatments for malignant gliomas: Using a scourge to treat a devil**. *Cytokine Growth Factor Rev* 2010;**21**:103-117.

74.   Wollmann G, Ozduman K, van den Pol AN. **Oncolytic virus therapy for glioblastoma multiforme: concepts and candidates**. *Cancer J* 2012;**18**:69-81.

75.   Mohyeldin A, Chiocca EA. **Gene and viral therapy for glioblastoma: a review of clinical trials and future directions**. *Cancer J* 2012;**18**:82-88.

76.   Naik JD, Twelves CJ, Selby PJ, Vile RG, Chester JD. **Immune recruitment and therapeutic synergy: keys to optimizing oncolytic viral therapy?** *Clinical cancer research : an official journal of the American Association for Cancer Research* 2011;**17**:4214-4224.

77.   Senzer NN, Kaufman HL, Amatruda T, Nemunaitis M, Reid T, Daniels G *et al*. **Phase II clinical trial of a granulocyte-macrophage colony-stimulating factor-encoding, second-generation oncolytic herpesvirus in patients with unresectable metastatic melanoma**. *Journal of clinical oncology : official journal of the American Society of Clinical Oncology* 2009;**27**:5763-5771.

78.   Kaufman HL, Bines SD. **OPTIM trial: a Phase III trial of an oncolytic herpes virus encoding GM-CSF for unresectable stage III or IV melanoma**. *Future Oncol* 2010;**6**:941-949.

79.   Khuri FR, Nemunaitis J, Ganly I, Arseneau J, Tannock IF, Romel L *et al*. **a controlled trial of intratumoral ONYX-015, a selectively-replicating adenovirus, in combination with cisplatin and 5-fluorouracil in patients with recurrent head and neck cancer**. *Nature medicine* 2000;**6**:879-885.

80.   Advani SJ, Mezhir JJ, Roizman B, Weichselbaum RR. **ReVOLT: radiation-enhanced viral oncolytic therapy**. *Int J Radiat Oncol Biol Phys* 2006;**66**:637-646.

81.   Advani SJ, Sibley GS, Song PY, Hallahan DE, Kataoka Y, Roizman B *et al*. **Enhancement of replication of genetically engineered herpes simplex viruses by ionizing radiation: a new paradigm for destruction of therapeutically intractable tumors**. *Gene Ther* 1998;**5**:160-165.

82.   Bradley JD, Kataoka Y, Advani S, Chung SM, Arani RB, Gillespie GY *et al*. **Ionizing radiation improves survival in mice bearing intracranial high-grade gliomas injected with genetically modified herpes simplex virus**. *Clin Cancer Res* 1999;**5**:1517-1522.

83.   Liu C, Sarkaria JN, Petell CA, Paraskevakou G, Zollman PJ, Schroeder M *et al*. **Combination of measles virus virotherapy and radiation therapy has**

synergistic activity in the treatment of glioblastoma multiforme. *Clin Cancer Res* 2007;**13**:7155-7165.

84.   Geoerger B, Grill J, Opolon P, Morizet J, Aubert G, Lecluse Y *et al*. **Potentiation of radiation therapy by the oncolytic adenovirus dl1520 (ONYX-015) in human malignant glioma xenografts**. *British journal of cancer* 2003;**89**:577-584.

85.   Twigger K, Vidal L, White CL, De Bono JS, Bhide S, Coffey M *et al*. **Enhanced in vitro and in vivo cytotoxicity of combined reovirus and radiotherapy**. *Clin Cancer Res* 2008;**14**:912-923.

86.   Alajez NM, Mocanu JD, Shi W, Chia MC, Breitbach CJ, Hui AB *et al*. **Efficacy of systemically administered mutant vesicular stomatitis virus (VSVDelta51) combined with radiation for nasopharyngeal carcinoma**. *Clin Cancer Res* 2008;**14**:4891-4897.

87.   Adusumilli PS, Stiles BM, Chan MK, Chou TC, Wong RJ, Rusch VW *et al*. **Radiation therapy potentiates effective oncolytic viral therapy in the treatment of lung cancer**. *Ann Thorac Surg* 2005;**80**:409-416; discussion 416-407.

88.   Dilley J, Reddy S, Ko D, Nguyen N, Rojas G, Working P *et al*. **Oncolytic adenovirus CG7870 in combination with radiation demonstrates synergistic enhancements of antitumor efficacy without loss of specificity**. *Cancer Gene Ther* 2005;**12**:715-722.

89.   Gridley DS, Andres ML, Li J, Timiryasova T, Chen B, Fodor I. **Evaluation of radiation effects against C6 glioma in combination with vaccinia virus-p53 gene therapy**. *Int J Oncol* 1998;**13**:1093-1098.

90.   Timiryasova TM, Gridley DS, Chen B, Andres ML, Dutta-Roy R, Miller G *et al*. **Radiation enhances the anti-tumor effects of vaccinia-p53 gene therapy in glioma**. *Technol Cancer Res Treat* 2003;**2**:223-235.

91.   Wali A, Strayer DS. **Infection with vaccinia virus alters regulation of cell cycle progression**. *DNA Cell Biol* 1999;**18**:837-843.

92.   Biondo A, Pedersen JV, Karapanagiotou EM, Tunariu N, Mansfield D, Sassi S *et al*. **1258 POSTER Phase I Clinical Trial of a Genetically Modified Oncolytic Vaccinia Virus GL-ONC1 With Green Fluorescent Protein Imaging**. *Eur J Cancer* 2011;**47**:S162.

93.   Lun XQ, Jang JH, Tang N, Deng H, Head R, Bell JC *et al*. **Efficacy of systemically administered oncolytic vaccinia virotherapy for malignant gliomas is enhanced by combination therapy with rapamycin or cyclophosphamide**. *Clin Cancer Res* 2009;**15**:2777-2788.

94.   Portella G, Pacelli R, Libertini S, Cella L, Vecchio G, Salvatore M *et al*. **ONYX-015 enhances radiation-induced death of human anaplastic thyroid carcinoma cells**. *The Journal of clinical endocrinology and metabolism* 2003;**88**:5027-5032.

95.   Lamfers ML, Grill J, Dirven CM, Van Beusechem VW, Geoerger B, Van Den Berg J *et al*. **Potential of the conditionally replicative adenovirus Ad5-Delta24RGD in the treatment of malignant gliomas and its enhanced effect with radiotherapy**. *Cancer Research* 2002;**62**:5736-5742.

96.   Chen Y, DeWeese T, Dilley J, Zhang Y, Li Y, Ramesh N *et al*. **CV706, a prostate cancer-specific adenovirus variant, in combination with radiotherapy produces synergistic antitumor efficacy without increasing toxicity**. *Cancer Research* 2001;**61**:5453-5460.

97. Stanziale SF, Petrowsky H, Joe JK, Roberts GD, Zager JS, Gusani NJ *et al*. **Ionizing radiation potentiates the antitumor efficacy of oncolytic herpes simplex virus G207 by upregulating ribonucleotide reductase**. *Surgery* 2002;**132**:353-359.

98. Advani SJ, Buckel L, Chen NG, Scanderbeg DJ, Geissinger U, Zhang Q *et al*. **Preferential replication of systemically delivered oncolytic vaccinia virus in focally irradiated glioma xenografts**. *Clin Cancer Res* 2012;**18**:2579-2590.

99. Geiger GA, Fu W, Kao GD. **Temozolomide-mediated radiosensitization of human glioma cells in a zebrafish embryonic system**. *Cancer Research* 2008;**68**:3396-3404.

100. Lawrence TS, Blackstock AW, McGinn C. **The mechanism of action of radiosensitization of conventional chemotherapeutic agents**. *Semin Radiat Oncol* 2003;**13**:13-21.

101. Higi M, Schreiber D, Arndt D, Henning A, Schmitt G. **[Cisplatin as a radiosensitizer in the treatment of solid tumours--a clinical pilot study]**. *Strahlentherapie* 1982;**158**:616-619.

102. Burgos-Tiburcio A, Santos ES, Arango BA, Raez LE. **Development of targeted therapy for squamous cell carcinomas of the head and neck**. *Expert review of anticancer therapy* 2011;**11**:373-386.

103. Hamalukic M, Huelsenbeck J, Schad A, Wirtz S, Kaina B, Fritz G. **Rac1-regulated endothelial radiation response stimulates extravasation and metastasis that can be blocked by HMG-CoA reductase inhibitors**. *PLoS One* 2011;**6**:e26413.

104. Hadjipanayis CG, DeLuca NA. **Inhibition of DNA repair by a herpes simplex virus vector enhances the radiosensitivity of human glioblastoma cells**. *Cancer Res* 2005;**65**:5310-5316.

105. Frentzen A, Yu YA, Chen N, Zhang Q, Weibel S, Raab V *et al*. **Anti-VEGF single-chain antibody GLAF-1 encoded by oncolytic vaccinia virus significantly enhances antitumor therapy**. *Proc Natl Acad Sci U S A* 2009;**106**:12915-12920.

106. Jain RK, di Tomaso E, Duda DG, Loeffler JS, Sorensen AG, Batchelor TT. **Angiogenesis in brain tumours**. *Nat Rev Neurosci* 2007;**8**:610-622.

107. Park JS, Qiao L, Su ZZ, Hinman D, Willoughby K, McKinstry R *et al*. **Ionizing radiation modulates vascular endothelial growth factor (VEGF) expression through multiple mitogen activated protein kinase dependent pathways**. *Oncogene* 2001;**20**:3266-3280.

108. Brown CK, Khodarev NN, Yu J, Moo-Young T, Labay E, Darga TE *et al*. **Glioblastoma cells block radiation-induced programmed cell death of endothelial cells**. *FEBS Lett* 2004;**565**:167-170.

109. Koutsimpelas D, Brieger J, Kim DW, Stenzel M, Hast J, Mann WJ. **Proangiogenic effects of ionizing irradiation on squamous cell carcinoma of the hypopharynx**. *Auris Nasus Larynx* 2008;**35**:369-375.

110. Weibel S, Raab V, Yu YA, Worschech A, Wang E, Marincola FM *et al*. **Viral-mediated oncolysis is the most critical factor in the late-phase of the tumor regression process upon vaccinia virus infection**. *BMC Cancer* 2011;**11**:68.

7   Acknowledgement

First of all, I would like to thank Prof. Szalay for giving me the opportunity to carry out my work here at Genelux Corporation in San Diego and of course for the chance to work on such an interesting and exciting project. Also I would like to thank him for his continuous support and help. I am also very grateful for the stipend provided by Genelux Corporation.

Another big thank you is dedicated to Sunil, who was introducing me to the field of radiotherapy and was working with me on the project. I would like to thank him for the guidance and immense help throughout my PhD. Also I thank him for proof-reading my thesis.

Next I would like to thank all the members of Genelux Corporation for cordially welcoming me, the nice working atmosphere and all their help and support. I would like to thank Terry for all the work he is doing to provide us with cells, products and solutions to all kinds of different emergencies in the lab. Also, I thank Jason and Melody for their excellent technical assistance. Especially, I would like to thank Tony for always taking a big interest in my work and a lot of fruitful discussion. Also I appreciate the help of all other senior mentors, Qian, Rohit, Nanhai, Boris and especially Jochen, who I would like to thank for his active support and his friendship in and outside of the lab. I would like to thank Alexa for her great cooperation with the GLV-1h164 project and also her huge help in getting settled in San Diego. Also I'm thankful for Camha assistance with all kinds of different problems and for her caring for us foreign students.

A special thank you I would like to dedicate to Ricky, who was initially working with me on the radiation project. I am very grateful for everything she helped me out with, all our great trips and her friendship which extends far outside the lab.

I am also grateful for my fellow PhD students, past and present, in all our different labs, Micha, Jenny, Dana, Julie, Jackie, Duong, Desi, Ting, Marion and all the others for all their help, moral support and friendship. Especially, I would like to thank Klaas who was accompanying me for almost the last 10 years, throughout our studies at the University of Würzburg and here in San Diego, for all his support.

In Würzburg I would like to thank especially Prof. Grummt for his enormous help in putting my work to paper and his encouraging words.

ACKNOWLEDGMENT

8 Curriculum Vitae

Persönliche Daten:

Name:	Lisa Buckel
Geburtsdatum:	26.01.1984
Geburtsort:	Rothenburg ob der Tauber
Staatsangehörigkeit:	deutsch
Familienstand:	ledig
Religion:	evangelisch
Adresse:	Ackerweg 6
	91610 Insingen
	3937 Nobel Drive #140
	San Diego, CA 92122
	USA

Schulausbildung:

09/1989-07/1994	Grundschule Gebsattel Insingen, Gebsattel
09/1994-06/2003	Reichsstadt Gymnasium, Rothenburg ob der Tauber

Hochschulausbildung:

10/2003-10/2008	Biologiestudium an der Julius-Maximilians-Universität, Würzburg
Sommersemester 2007	Auslandssemester an der Universitat de Barcelona, Spanien
12/2008-10/2009	Diplomarbeit in der AG Szalay an der Julius-Maximilians-Universität, Würzburg

Promotionsstudium:	seit 01/2007 Promotionsstudium in der AG Szalay an der Julius-Maximilians-Universität, Würzburg und Genelux Corporation, San Diego, USA

9   Publications

Advani SJ*, Buckel L*, Chen NG, Scanderbeg DJ, Geissinger U, Zhang Q, Yu YA, Aguilar RJ, Mundt AJ, Szalay AA.
Preferential replication of systemically delivered oncolytic vaccinia virus in focally irradiated glioma xenografts.
Clin Cancer Res 2012 May 1;18(9):2579-90. Epub 2012 Feb 29.
* Authors contributed equally

Buckel L, Advani SJ, Frentzen A, Zhang Q, Yu YA, Chen NG, Ehrig K, Stritzker K, Mundt AJ, Szalay
Vaccinia virus expressed single-chain antibody against VEGF increases response to radiation by targeting the vascular component of the tumor
Clin Cancer Res (submitted)

Ehrig K, Chen NG, Stritzker J, Buckel L, Zhang Q, Szalay AA.
Growth inhibition of different human colorectal cancer xenografts after a single intravenous injection of oncolytic vaccinia virus GLV-1h68
J Transl Med (submitted)

Stritzker J, Kirscher L, Scadeng M, Deliolanis NC, Morscher S, Symvoulidis P, Schaefer K, Zhang Q, Buckel L, Hess M, Donat U, Bradley WG, Ntziachristos V, Szalay AA
Gene-Evoked Melanin Production as Novel Mediator of Theranostics
Proc Natl Acad Sci U S A (submitted)

Advani SJ, Buckel L, Scanderbeg D, Chen N, Zhang Q, Yu YA, Mundt AJ, Szalay AA.
Radiotargeting Systemically Administered Oncolytic Vaccinia Virus to Preferentially Replicate in Radiated Gliomas
2011 ASTRO's annual meeting Abstract #287 (Scientific session)

Advani SJ, Buckel L, Frentzen A, Scanderbeg D, Chen N, Zhang Q, Yu YA, Mundt AJ, Szalay AA
Oncolytic Vaccinia Virus Encoding an Anti-VEGF Antibody Improves the Efficacy of Fractionated Radiation in Lung Tumor Xenografts
2011 ASTRO's annual meeting Abstract #3102 (Poster)